Technische Universität München
Fachgebiet für Entwicklungsbiologie der Pflanzen

Molecular genetic analysis of *UNICORN*, a tumor suppressor gene required for planar development of integuments in *Arabidopsis thaliana*

BALAJI ENUGUTTI

Vollständiger Abdruck der von der Fakultät Wissenschaftszentrum Weihenstephan für Ernährung, Landnutzung und Umwelt der Technischen Universität München zur Erlangung des akademischen Grades eines

Doktors der Naturwissenschaften

genehmigten Dissertation.

Vorsitzender:	Univ.-Prof. Dr. R. Hückelhoven
Prüfer der Dissertation:	1. Univ.-Prof. Dr. K. Schneitz
	2. Univ.-Prof. Dr. C. Schwechheimer
	3. apl. Prof. Dr. R. A. Torres Ruiz

Die Dissertation wurde am 12.01.2012 bei der Technischen Universität München eingereicht und durch die Fakultät Wissenschaftszentrum Weihenstephan für Ernährung, Landnutzung und Umwelt am 10.04.2012 angenommen.

I. Table of Contents

III. Summary

The coordination of growth and differentiation is pivotal to organogenesis and the maintenance of tissue architecture. In animals and humans, it is well known that alterations in the genetic mechanisms underlying development and growth often result in spontaneous tumor formation and cancer {Berger et al., 2011}. Tumor suppressors include well-characterized AGC kinases {Pearce et al., 2010}, such as Warts and LATS {Justice et al., 1995; St John et al., 1999; Xu et al., 1995}. In plants, convincing evidence for similar tumor suppressors is presently absent**.** This raises the question how plants suppress neoplastic growth.

Here I present the evidence that *UNICORN* restricts neoplastic growth in several plant organs. Recessive mutations in *UCN* result in localized spontaneous ectopic growth in several tissues, including ovules, petals, and filaments as well as aberrant embryogenesis. Hyperproliferated cells that developed in abnormal size and shapes characterize the aberrant outgrowths. The *ucn-1* protuberances contain differentiated cells rather than callus. Given these effects on cell proliferation and cell differentiation I propose *UCN* to be a first bona-fide plant tumor suppressor.

I further showed that *UCN* encodes an active AGCVIII kinase and in a cell, it is broadly distributed including the nucleus. In addition, the combined genetic, biochemical and cell biological evidence is compatible with the notion that UCN suppresses tumor formation in ovules through the direct negative regulation of the KANADI transcription factor ATS. *UCN* acts in a context-dependent fashion as tumor development in other tissues, such as filaments and petals, still occurs in *ucn ats* double mutants. Thus, *UCN* appears to be a general tumor suppressor that interacts with additional, as yet to be identified factors.

The findings indicate that *UCN* is a tumor suppressor that functions by negatively regulating a transcriptional regulator involved in the control of growth and development. The data further show that molecular components involved in tumor suppression are related across plant and animal kingdoms and include distinct members of the AGC kinase family.

IV. Zusammenfassung

Die Koordinierung von Wachstum und Differenzierung ist entscheidend für die Organogenese und die Aufrechterhaltung der Gewebeaufbaus. Von Tieren und Menschen ist es bekannt, dass eine Veränderung der genetischen Mechanismen, die die Entwicklung und das Wachstum steuern, oft zu einer spontanen Ausbildung von Tumoren und Krebs führen {Berger et al., 2011}. Gut untersuchte AGC-Kinasen {Pearce et al., 2010} wie Warts und LATS gehören zu den Tumorsuppressoren {Justice et al., 1995; St John et al., 1999; Xu et al., 1995}. Hinweise über ähnliche Tumorsuppressoren in Pflanzen liegen derzeit nicht vor. Dies führt zu der Fragestellung, wie Pflanzen die Ausbildung von Neoplasien unterdrücken.

In dieser Arbeit zeige ich, dass *UNICORN* (*UCN*) die Ausbildung von Neoplasien in unterschiedlichen pflanzlichen Organen unterdrückt. Rezessive Mutationen in *UCN* führen zum einen zu lokalen, spontanen, ektopischen Wachstum in verschiedenen Geweben, wie z.B. den Samenanlagen, den Petale sowie den Filamenten der Stamina und zum anderen zu einer gestörten Embryogenese. Das abnorme Wachstum wird durch hyperproliferierende Zellen charakterisiert, welche eine abweichende Größe und Form aufweisen. Die Auswüchse in der *ucn-1*-Mutante bestehen nicht aus Kallus sondern aus differenziertem Gewebe. In Anbetracht der Wirkungsweise auf Zellvermehrung und Zelldifferenzierung handelt es sich bei *UCN* um den ersten beschriebenen pflanzlichen Tumorsuppresor.

Weiter zeige ich in der vorliegenden Arbeit, dass *UCN* für eine AGCVIII-Kinase kodiert, welche u.a. innerhalb des Zellkerns lokalisiert ist. Zusätzlich zeigen meine genetischen, biochemischen und zellbiologischen Arbeiten, dass UCN die Ausbildung von Tumoren direkt über die negative Regulierung des KANADI-Transkriptionsfaktors ATS steuert. Dieser Mechanismus ist auf die Samenanlagen beschränkt, da *ucn ats*-Doppelmutanten weiterhin Tumore in anderen Geweben aufweisen. Daher scheint es sich bei UCN um einen allgemeinen Tumorsuppressor zu handelt, welcher neben ATS mit anderen, noch zu identifizierenden Faktoren interagiert.

Diese Befunde weisen darauf hin, dass *UCN* die Ausbildung von Tumoren durch Repression eines Transkriptionregulators, welcher an der Regulierung von Wachstum und Entwicklung beteiligt ist, verhindert. Außerdem zeigen diese Ergebnisse, dass die molekularen Mechanismen der Tumorsuppression innerhalb des Reiches der Pflanzen und dem Tierreich miteinander verwandt sind und jeweils Mitglieder der AGC-Kinasefamilie beinhalten.

1. Introduction

Tissue morphogenesis in multi-cellular eukaryotes critically depends on the spatial and temporal coordination of growth and differentiation within tissue layers. Cells and groups of cells have to communicate to promote and restrict cell proliferation and growth as disturbances in such growth patterns frequently result in altered tissue architecture. The underlying signaling mechanisms are under intense investigation. In animals and humans, it is well established that genetic lesions in mechanisms regulating developmental processes and growth control frequently result in tumor formation and cancer {Visvader, 2011}.

1.1 Tumor - definition

In plants {Doonan and Sablowski, 2010} and animals {Weinberg, 2006} a tumor is commonly defined as a de novo generated excrescence or lump (neoplasm), caused by ectopic cellular proliferation, which is uncoordinated with that of the surrounding normal tissue. Animal tumors can be malignant or benign. Malignant tumors or cancers, such as colon or mamma carcinoma, consist of poorly or variably differentiated cells with high genomic instability. They are usually initiated by altered single stem cells or progenitor cells {Visvader, 2011}. Malignant tumors grow uncontrollably and invasively, and form metastases. By contrast, benign tumors, for example squamous cell papilloma or chondroma, slowly grow to a certain size, exhibit defined boundaries, and contain well-differentiated cells. They do not invade neighboring tissues and do not develop metastases {Weinberg, 2006}. There is no equivalent to malignant tumor in plants, as they do not develop cancer.

1.2 Animal tumor suppressors

In general, tumor or cancer development is a consequence of derailed growth control patterns due to mutations in the ‘accelerators’ of cell division and/ or ‘brakes’ on uncontrolled cell division. Cell division rate ‘accelerators’ are referred as ‘oncogenes’ that switch on in appropriate times and ‘brakes’ as ‘tumor suppressors’ that fail to work properly. Classical tumor suppressors include RETINOBLASTOMA (RB), p53 and

p16 {Sherr, 2004}. Cell signaling is mediated by phosphorylation events and involves protein kinases. Kinases that are often deregulated in animal and human cancers are able to initiate or alter signals that eventually lead to cell proliferation and transformation. The animal AGC kinase family includes several members known to play prominent and diverse roles in growth regulation {Pearce et al., 2010}. For example, the AGC kinase Warts/LATS is a core element of the Hippo signaling pathway, which is involved in tumor suppression {Bao et al., 2011; Halder and Johnson, 2011}. Mutations in the *warts*/*lats* gene result in overproliferation of imaginal discs of Drosophila {Justice et al., 1995; Xu et al., 1995} and tumor formation in mouse {St John et al., 1999}, while human cancers are frequently characterized by epigenetic silencing of the *LATS1* and *LATS2* promoters {Bao et al., 2011; Halder and Johnson, 2011}. By contrast, aberrant activation of the ACG kinase Akt/PKB has long been associated with human cancer {Vivanco and Sawyers, 2002} and recent results demonstrated its direct oncogenic role {Carpten et al., 2007}.

1.3 How do plants suppress aberrant growth?

While in animals and humans a large number of tumor suppressor genes keep in check ectopic growth {Berger et al., 2011} such genes remain to be identified in plants {Dodueva et al., 2007; Doonan and Sablowski, 2010}. Classic tumor suppressors {Haber and Harlow, 1997} i.e., recessive mutations in which result in tumor formation, are unknown in plants. Genome and genetic analyses indicate that plants contain functional orthologue counterparts of many mammalian tumor suppressors, but these genes do not seem to play a role in neoplastic growth suppression. For example, null-alleles of *RETINOBLASTOMA-RELATED (RBR),* the single Arabidopsis ortholog of the hallmark human tumor suppressor *Rb*, do not result in tumor formation {Ebel et al., 2004; Wachsman et al., 2011}. Even ectopic expression of many core cell cycle regulators failed to result in tumor formation {Doonan and Sablowski, 2010}. Thus, it remains unclear what mechanisms impose social control over cell proliferation that results in neoplastic growth suppression in plants.

1.4 Plant tumors

Plants seem to maintain tissue architecture more rigidly, as, for unknown reasons, they appear comparably robust to hereditary or spontaneous tumors and thus are considered to differ from animals in their control of tissue growth and maintenance of tissue architecture {Dodueva et al., 2007; Doonan and Sablowski, 2010}. Given the fact that the plant cells are fixed in a cell wall matrix makes them non motile and therefore metastases cannot occur. Although plants do not develop cancer, they are well capable to grow tumors. Nevertheless, the well-known occurrence of hereditary (so-called genetic tumors) and sporadic (due to somatic mutations) tumors in animals stands in marked contrast to most plants where tumor formation is usually associated with pathogenesis, disturbances in hormone homeostasis and complex genetics.

1.5 Origin of plant tumors

The tumor formation in plants can be caused by several factors. Most of known plant tumor biology relates to various forms of pathogen-induced tumorigenesis, for example through bacterial, fungal, or viral infections. However, tumors can also develop spontaneously, particularly in interspecific hybrids and some monogenic mutants.

1.5.1 Pathogen induced tumors

1.5.1.1 Bacterial induced tumors

Various plant pathogenic bacteria are able to induce ectopic aberrant growth on host plants. Some of the examples include *Agrobactrium* {Gelvin, 2003}, *Pseudomonas savastanoi* {Glickmann *et al.* 1998}, *Rhodococcus fascians* {Vandeputte *et al.* 2005} and *Pantoea agglomerata* {Chapulowicz *et al.* 2006}, which cause the formation of gall tumors with varied growth. The common feature of all tumor-inducing bacteria is the ability to regulate synthesis of cytokinin and auxin in the affected plant, which is determinated by their plasmid or chromosomal genes {Morris 1986}. Tumors induced by *Agrobacterium* are the most commonly studied exmple in plant tumor biology. Rhizobiaceae family bacterium, *Agrobacterium tumefaciens* induced tumors develop at the junction between root and stem called neck or crown; therefore, the name - crown

gall (Fig.1.1). Upon infection, *Agrobacterium tumefaciens* introduce and integrates the Ti plasmid that carries the genes for auxin and cytokinin biosynthesis. Thus, Agrobacterium induced crown galls are mediated by modifying plant endogenous auxin and cytokinin levels caused by the expression of agrobacterial Ti genes {Gelvin, 2003}.

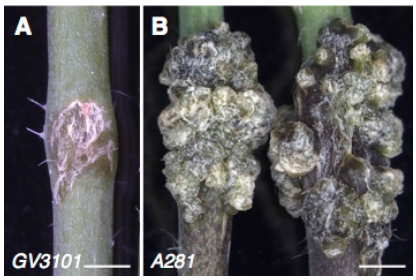

Fig.1.1. Agrobacterium induced tumors. (A). Arabidopsis stems infected with non-pathogenic *Agrobacterium* lab strain: *GV3101* do not induced any tumor formation. (B). The pathogenic strain *A281* caused tumor induction.

1.5.1.2 Fungal induced tumors

Few fungal species are capable to induce tumors on plants. Tumor formation in maize by the fungus *Ustilago maydis* caused by the transfer of fungal proteins to host cells {Brefort et al., 2009; Skibbe et al., 2010} and the stimulation of auxin synthesis and the expression of auxin-responsive genes in the plant {Doehlemann et al., 2008}. Additionally, it was shown that *Taphrina deformans* causes the formation of tumors on peach leaves {Tavares *et al.* 2004}, and *Dibotryon morbosum* forms black knot galls on the stems of *Rosaceae* plants {Fernando *et al.* 2005}.

1.5.1.3 Viral induced tumors

Some plant pathogenic viruses are also capable of inducing tumors. *Phytoreovirus* {Kudo et al., 1991; Streissle and Maramorosch, 1963} and *Gemini virus* {Nagar et al, 1995} are the some of the common tumor inducing viruses on plants. Gemini viruses seem to interfere with the central cell cycle machinery directly {Ascencio-Ibanez et al., 2008; Desvoyes et al., 2006; Doonan and Sablowski, 2010; Hanley-Bowdoin et al., 2004; Rojas et al., 2005}. This is interesting given that aberrant activity of several cell cycle regulator genes does not result in tumorigenesis in plants {Beemster et al., 2003; Doonan and Sablowski, 2010; Harashima and Schnittger, 2010}.

1.5.1.4 Other pathogen induced tumors

Apart from Bacteria, fungi, and viruses several protists (*Plasmodiophora brassica* Woronin) {Devoset al., 2005}, root-knot nematodes (*Meloidogyne*), cyst nematodes (Globodera and *Heterodera*) {Bird and Koltai 2000; de Meutter *et al.* 2003} and various insects such as flies, wasps and aphids {Armstrong, 1995} are shown to induce tumors on infected plants.

1.5.2 Genetic tumors

Genetic tumors develop spontaneously in the absence of pathogens or other exogenous causal agents, and their formation depends on the genetic makeup of the organism. Theoretically, genetic lesions that lead to loss-of-function or gain-of-function of key cell cycle regulatory genes or of signaling genes that are involved in the plant cell cycle regulation is supposed to alter the cell division rates and lead to uncontrolled cell proliferation and tumor formation. In fact, a good number of plant tumors induced by various agents show alterations in several genes acting at various levels of plant cell cycle control {Frank *et al.* 2002; Harrar *et al.* 2003; Lee *et al.* 2004} Surprisingly, aberrant activity of many cell cycle regulator genes does not result in neoplasia {Beemster et al., 2003; Doonan and Sablowski, 2010; Harashima and Schnittger, 2010}. Plants seem to be strikingly resistant to tumor formation compared to animals. However, plants do occasionally develop genetic tumors, mostly involving complex genetics.

1.5.2.1 Tumor development involving complex genetics

The phenomenon of spontaneous genetic tumors has been known for a century, mainly in classic literature {Ahuja, 1998}. Genetic tumors are known to occur, particularly in certain interspecies hybrids {Ahuja, 1998}. Classic examples include tumor formation in ovules of Datura {Blakeslee and Satina, 1947}, flowers of tobacco {Kostoff, 1939; Sharp and Gunckel, 1969}, or tomato leaves {Martin, 1966}. However, the underlying genetic basis of tumor formation is not well understood {Ahuja, 1998}.

1.5.2.2 Monogenic tumors

Genetic tumors can be caused by single-locus defects {Nuttall and Lyall, 1964}. Molecular genetic studies over the last 10-15 years exemplified few monogenic spontaneous tumor mutants. Recent examples include the leaf "knots" caused by dominant neomorphic alleles of maize *Knotted-1* (*Kn1*) resulting in ectopic *Kn1* expression {Freeling and Hake, 1985; Smith et al., 1992}, or the protrusions on Arabidopsis leaf petioles that relate to overdominant allele combinations at the *OUTGROWTH-ASSOCIATED KINASE* (*OAK*) locus {Smith et al., 2011}. The *tumorous shoot development* (*tsd*) mutants show callus formation in the apex, particularly under in vitro growth conditions {Frank et al., 2002}. Interestingly, *TSD1*/*KORRIGAN* (*KOR*) and *TSD2*/*QUASIMODO2* (*QUA2*) contribute to the biosynthesis of cellulose and pectin, suggesting a prominent role of the cell wall in the coordination of cellular growth in a tissue context {Krupkova and Schmülling, 2009; Krupkova et al., 2007; Mouille et al., 2007; Nicol et al., 1998}. In addition, an essential role for very-long-chain fatty acids (VLCFAs) in plant growth was discovered through the study of the pleiotropic *gurke* (*gk*)/*pasticcino* (*pas*)/*pepino* (*pep*) mutants. They exhibit aberrant development and ectopic cell proliferation, and the corresponding genes are involved in the biosynthesis of VLCFAs {Baud et al., 2004; Faure et al., 1998; Haberer et al., 2002; Roudier et al., 2010; Torres-Ruiz et al., 1996}.

Antagonistic regulatory interactions between abaxial (ab) identity specifying KANADI (KAN), YABBY and adaxial (ad) fate specifying HD-ZIPIII class of transcription factors function to maintain the ab/ad polarity in laminar structures. Plants with mutations in tissue patterning genes developed ectopic outgrowths on cotyledons and leaves. For example, compromise in abaxial identity specifying gene function in *kan1-2 kan2-1* double mutants causes abaxial outgrowths on rosette leaves {Eshed et al., 2001}. Double mutants of *arf3 (ett) arf4* also showed abaxial outgrowths on leaves similar to *kan1-2 kan2-1* double mutants {Pekker et al., 2005} suggesting a role in abaxial identity specification for *ARF3* and *ARF4*, the auxin response factor family of transcription factors (Remington et al., 2004; Ulmasov et al., 1999). Ectopic outgrowths were also seen on adaxial side of the leaf in *piggyback* (*pgy*) *asymmetric leaves1* (*as1)* double mutants due to dorso-ventral patterning disturabance. *PGY* family genes encode cytoplasmic large subunit ribosomal proteins {Pinon et al., 2008} and *AS1* encodes a

MYB-domain transcription factor that promotes adaxial identity in leaves {Xu et al., 2003}. In all these cases, the aberrant outgrowths have been addressed as ectopic leaf blades. Plants with mutations in *BLISTER*, a Pc-G histone methyltransferase *CURLY LEAF* (*CLF*) interactor that controls expression of polycomb-group target genes developed ectopic outgrowth of cells on cotyledons and leaves {Schatlowski et al, 2010} suggesting a role for epigenetic components in growth control.

1.5.3 Phytohormones in tumorigenesis

Phytohormones are known to play vital regulatory roles in the growth and development of plant. Among plant hormones, especially auxin and cytokinin excerts crucial role at various stages of plant development such as tissue differentiation and organogenesis by modulating cell division and differentiation. Alterations in auxin and cytokinin homeostasis sometimes lead to de-differentiation and tumor development in plants {Ahuja, 1998; Dodueva et al., 2007; Doonan and Sablowski, 2010}. Furthermore, the expression of several cell cycle regulators in plants is under phytohormonal control. For example, *Arabidopsis CDKA;1*{Chung and Parrish 1995} and alfalfa *CycA2;2*{Roudier *et al.* 2003} expression is induced by auxin. The *Arabidopsis CycD3;1* gene expression is upregulated by the cytokinins - zeatin and 6-benzylaminopurine (BAP) {Riou-Khamlichi *et al.* 1999}. Infact, in phytohormone mutants the expression of cell-cycle genes was shown to be altered {Sieberer et al., 2003}. For example, defects in *PROPORZ1* (*PRZ1*), encoding a putative component of a chromatin-remodeling complex showed increased expression levels of *CDKB1;1* and *E2Fc* genes and result in callus formation upon addition of auxin or cytokinin {Sieberer et al., 2003}. Thus, *PRZ1* highlights the importance of transcriptional control and hormone homeostasis in this process. In addition, Anand et al., showed that exogenous supplements of gibberellin promote agrobacterium induced tumor formation in moderately aged bean leaves {Anand et al., 1975} probably by regulating cell division rates. In summary, phytohormones induce tumor induction through interfering with cell cycle machinery.

In understanding the function of a gene and the protein it encodes, sometimes drastic changes - eliminating a gene product entirely or flooding cells with huge quantities of hyperactive protein may either result in functional compensation by redundant genes or embryo lethality. It is sometimes useful to make subtle changes in a gene expression or protein activity to uncover their role in developmental or physiological processes. Given the fact that ectopic expression of various cell cycle genes and loss-of-function mutations in animal tumor suppressor representative *RBR* did not result in tumor formation, focusing on signaling components may help in understanding the mechanism of neoplastic growth suppression in plants. Protein kinases are the prime molecules in orchestrating signaling transduction.

1.6 Arabidopsis AGC kinases

Although some members of animal and human AGC kinases were shown to act as oncogenes and tumor suppressors, similar functions exerted by plant AGC kinases is presently unknown. As pathogen induced tumors and some of the genetic tumors alters the phytohormone homeostasis and there by develop tumors, it is of great interest to understand the functions of plant AGC kinases as few of them were shown to involve in auxin transport signaling mechanism {Friml et al., 2004; Zourelidou et al., 2009}. However, so far defects in none of them result in tumor-like outgrowths on plants.

AGC kinases are Ser/Thr protein kinases that were named after the collective mammalian PKA, PKG and PKC kinases. There are thirty-nine AGC kinases in *Arabidopsis* that fall into six subfamilies {Bögre et al, 2003}. The subgroups are named as PDK1 subfamily, AGCVI, AGCVII, AGCVIIIa, AGCVIIIb and AGC other. The PDK1 subfamily has two highly conserved members and was shown to mediate *Piriformospora indica (P. indica)* induced growth promotion {Camehl et al, 2011}. AGCVI includes two p70 ribosomal S6 kinase (S6K) homologues and AGC- VII contains eight Arabidopsis genes that are related to the animal nuclear Dbf2-related kinase (NDR), which are involved various aspects of the cell division control and morphogenesis. AGC other subfamily has four members, and these genes are related to the animal SGK and to the fission yeast CEK1 and to the budding yeast Rim15 genes. The other member of this family is *incomplete root hair elongation* (*ire*) that was

implicated in regulating root hair growth and microtubule organization {Oyama et al, 2002}.

1.6.1 AGCVIII protein kinases in Arabidopsis

Plant AGCVIII kinases are discriminated by a change of the conserved DFG triplet to DFD in subdomain VII of the catalytic domain and a variably sized insertion (in the range of 36 to 90 amino acids) between subdomains VII and VIII. The Arabidopsis AGCVIII family has 23 members that include both AGCVIIIa and VIIIb clades {Galván-Ampudia and Offringa, 2007}. What is known about the functions of AGCVIII protein kinases? OXI1, is the only member of the AGC2 group studied so far in detail and was found to act downstream of active oxygen species and to participate in phospholipid-signaling in stress and developmental responses {Anthony et al., 2004; Petersen et al., 2009; Rentel et al., 2004}. OXI1 is for example activated by H_2O_2, both at the transcriptional and at the kinase activity levels. Activation of OXI1 kinase activity is also induced by phosphatidic acid (PA) through a direct interaction of OXI1 with 3' phosphoinositide-dependent kinase 1 (PDK1). OXI1 functions at least in part through activating the mitogen-activated protein kinases MAPK3 and MAPK6. In addition, *OXI1* is required for basal resistance to *Peronospora parasitica* and root hair growth, two processes that are under control of active oxygen species-dependent mechanisms as well. OXI1 and AGC2-2, homolog of OXI1 were recently shown to required for the beneficial interaction with *P. indica* {Camehl et al, 2011}. OXI1 appears to undergo develomentally regulated dynamic subcellular localisation during root hair development. Initially, an OX1:GFP reporter signal was detected in a cortical region in immature root hairs. During later stages of root hair growth, the reporter signal was observed beneath the tip of the root hair and eventually also in the nucleus.

Several members of the AGCVIII family are involved in the regulation of polar auxin transport {Robert and Offringa, 2008}. The plant hormone auxin is an essential regulator of several aspects of plant development, including embryo and root patterning, phyllotaxis, vascular differentiation, and several tropisms, such as phototropism and gravitropism. Auxin acts through auxin maxima and gradients that are set up by polar auxin transport via the developmental and environmental control of

the polar subcellular localisation of the plasma membrane localized PINFORMED (PIN) auxin efflux carriers {Tanaka et al., 2006}. Despite the fact that the control of the polarity (and activity) of PINs is at the center of auxin signaling very little is known about these processes. Interestingly, PINOID (PID) {Benjamins et al., 2001; Christensen et al., 2000}, a member of the AGC3 subclass, regulates targeting of PINFORMED 1 (PIN1) to the apical side of the plasma membrane in epidermal cells in the inflorescence meristem {Friml et al., 2004}. The subcellular polarity of PIN depends on differential PIN phosphorylation that is mediated by the antagonistic actions of PID and a PP2A phosphatase {Michniewicz et al., 2007}. The D6 protein kinases, four members of the AGC1 subclass, are localized at the plasma membrane in a polar fashion and often co-localize with PINs in root cells. However, they do not regulate PIN polarity but are implicated in the regulation of PIN activity {Zourelidou et al., 2009}. Additional AGCVIII protein kinases likely involved in auxin transport or auxin responses include the two blue-light receptors PHOT1 and PHOT2 {Christie et al., 1998; Sakai et al., 2001} and WAVY ROOT GROWTH 1 (WAG1) and WAG2, negative regulators of root waving {Santner and Watson, 2006}. Other AGCVIII kinases, however, may have functions not directly related to auxin. For example, AGC1-5 and AGC1-7 are required for the organization of the actin cytoskeleton and the polarized growth of pollen tubes {Zhang et al., 2009a}.

AGC kinases are often regulated by lipid signals, including phosphatidic acid (PA), that mediate their action through the activation of PDK1, itself an AGC kinase that associates with phospholipids via its pleckstrin homology domain (PH) {Testerink and Munnik, 2005; Mora et al., 2004}. PDK1 binds to AGC kinases that have a PDK1 interacting fragment (PIF), usually located at the very C terminus of the target kinase and share a conserved PDK1 phosphorylation site in the activation loop (or T-loop). Many plant AGCVIII kinases contain a PIF motif and examples that have been reported to be activated by PDK1 include OXI1 and PID among others {Anthony et al., 2004; Zegzouti et al., 2006a; Zegzouti et al., 2006b}.

1.7 Ovule integument: A model tissue for understanding laminar growth control and neoplastic growth suppression

Flowers are central to plant sexual reproduction in higher plants. Flowers comprise four types of organs in concentric whorls. The ovule, carrying the egg cell is the major female reproductive structure and is embedded in the central floral organ, the carpel. Apart from their exciting biology the ovules of *Arabidopsis thaliana* have also emerged as a prominent model system to study organogenesis at the genetic and molecular level {Chevalier et al., 2002; Colombo et al., 2008; Kelley and Gasser, 2009}. Ovule development in this species is well understood at the descriptive level {Robinson-Beers et al., 1992, Schneitz et al., 1995}. Along the proximal-distal (P-D) axis, three pattern elements can be recognized. At the distal end the nucellus eventually produces the haploid embryo sac containing the egg cell. Proximally, the funiculus connects the ovule to the placenta. The central chalaza is characterized by the initiation of the inner and outer integuments at its flanks.

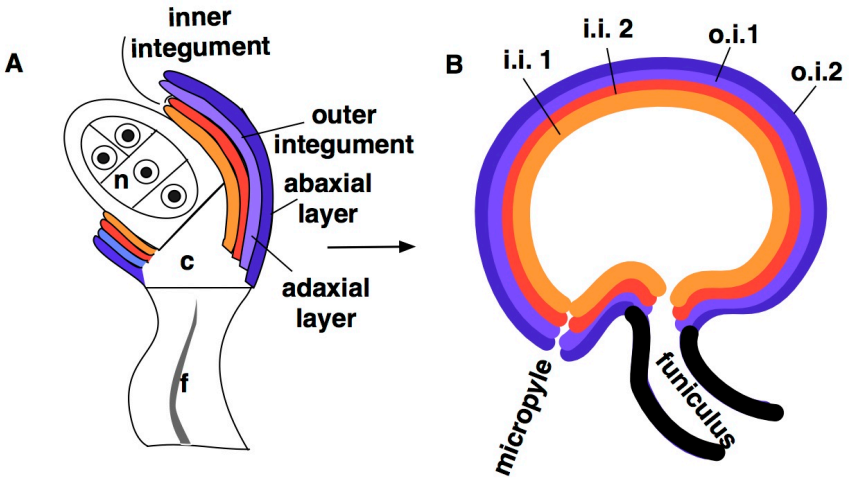

Figure 1.2. The development of ovule integuments in *Arabidopsis*. (A) Two inner and two outer integuments initiate from the flanks of the chalaza during early ovule development. The outer integument on the adaxial side of the ovule doesn't grow. **(B)** Ovule at stage of fertilization: Integuments have grown around nucellus, i.i.1: inner (adaxial) layer of inner integument, i.i.2: outer (abaxial) layer of inner integument, o.i.1: inner (adaxial) layer of outer integument, o.i.2: outer (abaxial) layer of outer integument. (n) nucellus, (c) chalaza, (f) funiculus.

Integuments are typically considered as lateral determinate tissues. They develop into laminar extensions that eventually envelop the nucellus and embryo sac. Their simple cellular architecture and stereotypic mode of development make Arabidopsis integuments a fitting model to study tissue morphogenesis. Integuments are of epidermal origin {Jenik and Irish, 2000; Schneitz et al., 1995} and upon integument initiation cells of the inner and outer integuments divide in a stereotypic anticlinal fashion resulting in the extension of two bi-layered sheets of regularly arranged cells {Schneitz et al., 1995; Truernit and Haseloff, 2008} (Fig.1.2). Thus, each integument is made of an inner or adaxial and an outer or abaxial cell layer.

A notable feature of integuments is the extension of the different cell layers through proliferative cell division. What mechanism keeps the cells dividing within the plane of the developing integument? A large number of genes affecting integument morphogenesis has been identified {Skinner et al., 2004}. They encode a range of different proteins, from receptor-like kinases (RLKs), such as STRUBBELIG {Chevalier et al., 2005} or ERECTA {Pillitteri et al., 2007}, to mitochondrial proteins {Hill et al., 2006; Skinner et al., 2001}. However, with the exception of the three RLK genes *ARABIDOPSIS CRINKLY4* (*ACR4*), *ABNORMAL LEAF SHAPE 2* (*ALE2*) {Gifford et al., 2003; Tanaka et al., 2007; Watanabe et al., 2004} and *STRUBBELIG* {Chevalier et al., 2005}, none of these genes has been implied to play a primary role in the maintenance of the sheet-like organization of the integumentary cell layers. Thus, the signaling mechanisms regulating a central aspect of stereotypic laminar integument growth are poorly understood. The regulated stereotypical cell division pattern is fundamental for proper tissue or organ growth. However, the mechanism that control stereotypical division patterns keeping check to neoplastic growth suppression in plants is unclear.

1.8 In this study

Here in this study, I provided first insight into longstanding fundamental question that how aberrant (neoplastic) growth suppression is achieved during laminar growth and per se during plant development. I showed that *UNICORN* (*UCN*) encodes a functional AGC kinase and regulates laminar growth in integuments by suppressing localized ectopic growth. I further demonstrated that the neoplastic growth suppression in ovule integuments is mediated by UCN by negative posttranscriptional regulation of a KANADI transcription factor ATS in the nucleus, possibly through differential phosphorylation.

2. Materials and Methods

2.1 Plant work, plant genetics

Arabidopsis thaliana (L.) Heynh. var. Landsberg (*erecta* mutant) (L*er*) and var. Columbia (Col-0) were used as wild-type strains. Dry seeds were sown on soil (Patzer Einheitserde, extra-gesiebt, Typ T, Patzer GmbH & Co. KG, Sinntal-Jossa, Germany) overlying perlite and stratified for 4 days at 4°C. Plants were either grown in a greenhouse under Philips SON-T Plus 400 Watt fluorescent bulbs on a long day cycle (16 hrs light) or in a growth chamber under Osram Lumilux Cool White L36W/840 bulbs under continuous light with approximately 120 µE/m^2/second at pot height. Plant trays were covered for 7-8 days to increase humidity and support equal germination. Transgenic seeds after surface sterilization and 1-4 days of stratification at 4° C were grown on respective antibiotic (Kanamycin: 50 µg/ml; Basta: 10 µg/ml Rifampicin: 10 µg/ml; Gentamycin: 25 µg/ml) containing sterile MS (Sigma) Agar (1%) plates. Bactyl (Ticarcillin and Clavulanic acid) at a concentration of 30 µg/ml was used to inhibit the agrobacterium growth while selecting the primary (T1) transformants. Flowers were staged according to {Smyth et al., 1990}. The *ucn-1* mutant was isolated previously in an ethane methyl sulfonate (EMS) mutagenesis {Schneitz et al., 1997} and outcrossed three times to L*er* prior to further analysis.

The EMS-induced mutants *ucn-7* to *ucn-9* (Supplementary Table 7.2) were identified in conjunction with the Seattle Arabidopsis TILLING facility (http://tilling.fhcrc.org/files/Welcome_to_ATP.html/) {Till et al., 2003}. Tilling was performed in a Col line that carries the fast-neutron-induced *er-105* mutation {Torii et al., 1996}. A 1.3 kb genomic fragment spanning the coding sequence of *UCN* was screened. The mutations in homozygous form were confirmed in M3 plants by sequencing. Mutant plants were outcrossed to Col *er-105*.

T-DNA insertion lines (Supplementary Table 7.2) were received from the SALK collection {Alonso et al., 2003} and the Syngenta Arabidopsis Insertion Library (SAIL) {Sessions et al., 2002} (*ucnl-1*, SAIL_238-A09, Col). The gene trap line GT931.DS5 (*ucnl-5*, L*er*) was obtained from the Cold Spring Harbor Lab Genetrap collection

(http://genetrap.cshl.org) {Martienssen, 1998; Sundaresan et al., 1995}. All lines were ordered through the Arabidopsis Biological Resource Center (ABRC, http://www.arabidopsis.org/abrc/index.jsp).

Plant transformation was done using the floral dip method {Clough and Bent, 1998} and *Agrobacterium tumefaciens* strain GV3101 {Koncz and Schell, 1986}. Transgenic T1 plants were selected on respective antibiotic containing MS agar plates and subsequently transferred to soil.

2.2 Double mutant analysis with various ovule mutants

The different mutants were described before: *ale2-1* {Tanaka et al., 2007}; *acr4-2* {Gifford et al., 2003}; *ats-3* {McAbee et al., 2006}; *ant-72F5* and *bel1-1460* {Schneitz et al., 1997}; *ino-2* {Schneitz et al., 1997; Villanueva et al., 1999}; *nzz-2* and *sub-1* {Chevalier et al., 2005; Schiefthaler et al., 1999}; *sup-5* {Gaiser et al., 1995}. At least 200 F2 progeny of a parental cross between *ucn-1* and the respective mutant were analyzed. Double mutants were identified by direct phenotypic inspection (plants showing an *ucn-1* floral phenotype and corresponding ovule aberrations) and occurred with expected frequencies for a Mendelian di-hybrid cross.

2.3 Recombinant DNA work

For DNA and RNA work standard molecular biology techniques were used {Sambrook et al., 1989}. PCR-fragments used for cloning were obtained using Phusion high-fidelity DNA polymerase (New England Biolabs, Frankfurt, Germany). Site-directed mutagenesis of plasmids was done using the QuickChange XL site-directed mutagenesis kit (Stratagene, La Jolla, USA) according to the manufacturer's recommendations. All PCR-based constructs were sequenced. Information regarding all primers used in this study is given in Supplemetary table 7.2.

2.4 Construction of various *UCN* and *ATS* reporter constructs

F23H24 and F11M15 binary BAC (BIBAC2) {Hamilton, 1997} constructs were generated by sub cloning the inserts released from pBeloBAC11 after NotI digestion. To generate the *UNICORN* (*UCN*), At1g51150 and At1g51160 genomic rescue

constructs, the entire genomic regions spanning till to the flanking genes (with the exception of *UCN* starting at the F23H24 breakpoint and ending at the predicted stop codon of At1g51160) were PCR amplified with the primers: UCN (gen KpnI)_F/ UCN(gen PstI)_R; At1g51150 (KpnI)_F/At1g51150 (BamHI)_R and At1g51160 (*Kpn*I)_F/At1g51160 (*Pst*I)_R, respectively, using L*er* genomic DNA as template. The restriction digested PCR products were cloned into *Kpn*I/ *Pst*I or *Kpn*I/ *Bam*HI digested pCAMBIA2300.

To generate fluorescence reporter constructs, *UCN* coding sequence including *3'UTR* was PCR amplified (UCN (SmaI)_F/ UCN (SmaI)_R), restriction digested and was cloned into pEGAD binary vector {Cutler et al., 2000} resulting in the *35S::EGFP:UCN-3'UTR* reporter construct. *pUCN::EGFP:UCN-3'UTR* reporter construct was made by replacing the 35S promoter in the above construct with 500 bp UCN promoter that was PCR amplified from L*e*r genomic DNA using P-UCN (StuI)_F/ P-UCN (AgeI)_R primers. For transient protoplast expression, pGY1:UCN-EGFP construct was generated by cloning the UCN coding sequence into pGY1:EGFP {Hoefle et al, 2011} (amplified using UCN(pGY1)_F/ UCN(pGY1)_F primers followed by *Xma*I digestion). *UCN* and *ATS* BiFC constructs were generated by PCR amplifying the *UCN* and *ATS* coding sequences (primers: UCN (BiFC_AscI)_F/ UCN (BiFC_XmaI)_R; ATS (BiFC_AscI)_F/ ATS (BiFC_XmaI)_R and cloneing into Asc/XmaI digested pUC-SPYCE and pUC-SPYNE vectors {Walter et al., 2004}.

2.5 Generation of recombinant protein constructs

All recombinant proteins are fusions of either a 6x-His/X-press (His) or a glutathione-S-transferase (GST) tag to the amino-terminus of full-length UCN and ATS. His:UCN construct was generated by PCR amplifying the coding sequence of *UCN* from wild-type L*er* genomic DNA using primers UCN(KpnI)_F/UCN(HindIII)_R and ligating the fragments into the *Kpn*I/*Hind*III-digested vector pRSET B (Invitrogen, Karlsruhe, Germany). GST:UCN and GST:UCN_{G165S} constructs were generated by PCR amplifying the coding sequence of *UCN* and *ucn-1* from wild-type L*er* and *ucn-1* genomic DNA respectively, using primers UCN (pGEX XmaI)_F/UCN(pGEX NotI)_R and cloning into the XmaI/NotI digested vector pGEX-6P-1 (GE Healthcare Europe, Munich, Germany). The GST:UCN_{K55E} variant was generated by first cloning

the PCR-amplified *UCN* coding region into pJET1.2 and subsequent site-directed mutagenesis of the lysine at position 55 to glutamic acid using primers UCN(K55E)_F and UCN(K55E)_R. The mutated and sequence verified insert was then subcloned into *Xma*I/*Not*I-digested pGEX-6P-1. GST:ATS was obtained by amplifying the ATS coding sequence from U84211 with primers ATS(pGEX_XmaI)_F/ATS(pGEX NotI)_R and cloning the fragment into pGEX-6P-1, digested with *Xma*I/*Not*I.

2.6 Expression and purification of recombinant proteins

The various constructs were transformed into *E. coli* BL21 (DE3) cells (Invitrogen, Karlsruhe, Germany) and grown to an OD_{600} of 0.6. Recombinant protein expression was then induced by 0.5 mM isopropyl-β-d-thiogalactoside (IPTG, FLUKA, Germany) for 4 hours at 37º C. Cells were pelleted and subjected to solubilisation and recombinant protein purification using the Protino® Ni-TED 2000 (Macherey-Nagel, Düren, Germany) and Protino® Glutathione Agarose 4B kits (GE Healthcare, Germany), respectively, according to the manufacturer's recommendations.

2.7 In vitro kinase assays

Kinase assays were done with 4 µg of purified fusion protein and in the absence or presence of 2 µg myelin basic protein (MBP) (Sigma-Aldrich, Munich, Germany). Proteins were incubated in 20 µl of 40 mM Hepes (pH 7.4), 40 mM $MgCl_2$, 10 µM ATP, and 10 µCi [γ-^{32}P]ATP (Hartmann Analytic GmbH, Germany). The reaction was stopped by adding 10 µl of 4x sample buffer (100 mM Tris pH 6.8, 20% glycerol and 4% SDS). The samples were boiled and analysed by SDS/PAGE. Coomassie blue-stained gels were washed dried and exposed to film.

2.8 Phospholipid binding assay

Glutathione *S-transferase* (GST) fusion protein of UCN, mouse SytA were expressed in *Escherichia coli* (BL-21) and purified. 25% of Phosphatidylserine and 75% of Phosphatidylcholine (Avanti Polar Lipids) were dissolved in chloroform and were dried by evaporation followed by vacuum drying for 2 h. Phospholipids were then resuspended in Buffer A (50mM HEPES/NaOH pH 6.8, 100mM NaCl, 4mM EGTA).

Micelles were made by sonicating phopsholipid mixture for 10 minutes in a water bath sonicator. The vesicles were pelleted down by centrifugation at 20,800 × g, 4 °C for 20 minutes. The pelleted vesicles were resuspended with 4 µg protein solution in respective buffer A (with or without Ca_2^+) and then incubated at 27 ° C for 40 minutes at 200 rpm shaking. The vesicles were pelleted down and washed three times with 500µl of corresponding buffer A. The pellets obtained by centrifugation at 20,800 × g for 10 min at 4 °C were dissolved in SDS sample buffer and resolved on 10% SDS-PAGE, followed by coomassie brilliant blue R-250 staining. The protein concentrations were determined with a Bio-Rad protein assay kit (Bio-Rad Laboratories, Hercules, CA, USA) using BSA as a reference. The free Ca_2^+ concentration was calculated using WEBMAXC program (http://www.stanford.edu/~cpatton/maxc.html,NISTdatabase).

2.9 Semi quantitative RT PCR expression analysis of *UCN* and *UCNL*

To survey *UCN* and *UCNL* expression in plants RNA from different organs was isolated using the NucleoSpin RNA II kit (Macherey-Nagel, Düren, Germany). First-strand cDNA was synthesized from 2 µg of total RNA using Moloney Murine Leukemia Virus (M-MuLV) reverse transcriptase (New England Biolabs, Frankfurt, Germany). PCR was performed using *Taq* DNA polymerase (New England Biolabs) and *UCN* and *UCNL*-specific primer pairs (UCN(RT)_F, UCN(RT)_R; UCNL(RT)_F, UCNL(RT)_R). Between 19 and 32 thermal cycles were tested. The *GAPC* gene was used as positive control {Shih et al., 1991}.

2.10 Quantitative real-time PCR

Tissue for quantitative real-time PCR was harvested from 25-day plants grown under long day conditions. Tissue was harvested in Eppendorf tubes pre-cooled on dry ice for 30 minutes and stored at -80°C. With minor changes, RNA extraction and quality control was performed as described previously {Box et al., 2011}. DNase treatment was performed using rDNase (Macherey-Nagel, Düren, Germany) according to the manufacturer's instructions. First-strand cDNA was synthesized from 1.0 µg of total RNA via reverse transcription, using the First Strand cDNA Synthesis Kit (Fermentas, St. Leon-Rot, Germany). Quantitative real-time PCR was performed on a Roche LightCycler480 using the iQ SYBR Green Supermix (Bio-Rad, Hercules, USA)

according to the manufacturer's recommendations. Using the ΔΔ-Ct method, all gene expression levels were normalized against *At5g25760*, *At4g33380* and *At2g28390* expression {Czechowski et al., 2005}. Expression levels are depicted as -fold changes compared to wild type expression in the respective tissues. Primer sequences used in this study are summarized in supporting Table 7.2.

2. 11 in situ hybridization

In situ hybridization with digoxigenin-labelled probes was done essentially as described earlier {Sieber et al., 2004}. A detailed protocol can be found at http://plantdev.bio.wzw.tum.de/index.php?id=69. The *INO* probe was described earlier {Sieber et al., 2004}. A 0.831 kb *ATS* antisense probe was obtained by PCR using a full-length cDNA clone (U8421, The Arabidopsis Biological Resource Center, ABRC) as template and the primer pair ATSas_831_F/ATSas_831_R. The sense control was obtained using primer pair ATSsense_831_F/ATSsense_831_R. Slides were viewed with an Olympus BX61 upright microscope using DIC optics.

2. 12 GUS histo-chemistry

For GUS staining all the tissues were collected in 90% acetone and processed according to Gross-Hardt et al., 2002. *pRJM65* was used as *pINO::GUS* reporter {Meister et al., 2002} and *WUS::GUS* reporter {Gross-Hardt et al., 2002} to monitor *WUS* spatial expression patterns.

2.13 Antibody generation and immunohistochemistry

Full-length recombinant HIS:UCN fusion protein purified from a SDS-PAGE gel was used to raise a polyclonal rabbit antiserum followed by IgG purification (Davids Biotechnologie, Regensburg, Germany). Mouse monoclonal anti α-tubulin antibody was obtained from Sigma. Goat anti-rabbit monoclonal antibody was coupled to Alexa-m488 (Invitrogen). Nuclei were stained with 1 mg/ml DAPI (Sigma). Antibody staining was performed as described {Völker et al., 2001} with the exception of 8 hours primary antibody incubation on the root tips of 5-day-old seedlings grown on MS agar (Sigma) medium supplemented with 1% sucrose.

2.14 Bimolecular Fluorescence Complementation (BiFC) assay

Four µg of each plasmid in desired combinations were transiently transfected into mesophyll protoplasts that were generated from two-week-old *Arabidopsis* leaves (Col) {Yoo et al., 2007}. The protoplast transfection was carried out according to {Yoo et al., 2007}. The plasmid pGY-1:mCherry {Hoefle et al, 2011} was used as transformation control.

2. 15 Cleared whole-mount preparations, light microscopic studies and artwork

Cleared whole-mount preparations of ovules were done according to {Torres-Ruiz and Jürgens, 1994}. Embryos were observed using Olympus BX61 upright microscope and DIC optics. An Olympus SZX12 stereomicroscope was used to analyze plants or various plant organs. Images for adjusted for color and contrast using Adobe Photoshop CS5 (Adobe, San Jose, CA, USA) software.

2.16 Scanning electron microscopy

Freshly opened flower buds were immersed in fixative (70% acetone, 2% glutaraldehyde, in H2O) and fixed overnight at room temperature. The tissue was washed 10 times in 70% acetone, rehydrated through an acetone series in a cacodylate buffer 50 mM sodium cacodylate (pH 7.0; # 20840, Fluka), postfixed in 2% osmium tetroxide (# 75632, Fluka) in cacodylate buffer for 2 hours at room temperature, washed twice in cacodylate buffer for 10 min and dehydrated through an acetone series: 20%, 40%, 60% and 70%. Subsequently, critical point drying was performed, the specimens were mounted on stubs and the ovules were dissected free. The samples were visualized using JEOL JSM-5900LV scanning electron microscope.

2.17 Confocal laser scanning microscopy (CLSM)

Preparation and analysis of samples for confocal laser scanning microscopy was done essentially as described {Clark et al., 1993; Sieburth and Meyerowitz, 1997}. Confocal laser scanning microscopy using fixed and propidium iodide-stained specimen was performed with an Olympus FV1000 setup using an inverted IX81 stand and FluoView software (FV10-ASW version 01.04.00.09) (Olympus Europa GmbH, Hamburg, Germany). After excitation at 488 nm with a multi-line argon laser, propidium iodide fluorescence (580-630 nm slit width) and autofluorescence (500-530 nm slit width) was detected. One-way scan images (scan rate 12.5 µs/pixel, 512x512 pixels, Kahlman frame, average of four scans) were obtained using an Olympus 40x objective (UApo/340 40x/1.35 Oil Iris). BiFC images were acquired using 40x objective (PLAPO/40x WLSM/0.9 water). Excitation and emission wavelengths were as follows: YFP: 514 nm excitation, 527 nm emission; chlorophyll autofluorescence, 470 nm excitation, 680 nm emission; mCherry: 587 nm excitation, 610 nm emission. Images of UCN/ATS BiFC assay were obtained by sequential scanning. Images of immunolocalized UCN in roots were taken Slides were analyzed using a 40x objective (UApo/340 40x/1.35 Oil Iris) and sequential scanning was performed to eliminate interference of lasers while acquiring the images. Excitation and emission wavelengths were as follows: Alexa Fluor™, 495 nm excitation, 519 nm emission; DAPI, 358 nm excitation, 461 nm emission.

2.18 Bioinformatic analysis and comparative homology modeling

Sequence searches were performed using the BLAST algorithm {Altschul et al., 1990} and domain searches were done using the PFAM database {Finn et al., 2008}. The NLS sequence was predicted using http://nls-mapper.iab.keio.ac.jp/cgi-bin/NLS_Mapper_form.cgi. NES motifs were predicted using (http://www.cbs.dtu.dk/services/NetNES/. The sequence alignment for the unrooted Neighbor-Joining tree of the plant AGCVIII protein kinase family was generated by aligning the protein sequences of previously defined AGCVIII members {Galván-Ampudia and Offringa, 2007} with Clustal W {Thompson et al., 1994} at the European Bioinformatics Institute website {Larkin et al., 2007} (http://www.ebi.ac.uk/tools/clustalw2) using standard parameters. The phylogram was

constructed using the MEGA4 software (http://www.megasoftware.net){Tamura et al., 2007}. Comparative homology modeling of the UCN kinase domain was achieved by using the SWISS MODEL workspace in automated mode {Arnold et al., 2006}. The algorithm identified the structure of cAMP-dependent protein kinase {Knighton et al., 1993} as template (protein database file 1apmE). Sequence identity was 28% with an E-value of 0.00e-1. The model was saved as protein data bank (.pdb) file and molecular graphics images were produced using the UCSF Chimera package {Pettersen et al., 2004}. Quality assessment of the model was done using ANOLEA {Melo and Feytmans, 1998}, QMEAN {Benkert et al., 2009} and DFire {Zhou and Zhou, 2002} using the structure assessment tools of the Swiss-Model workspace website.

3. Results

To address neoplastic growth control in plants I took advantage of the regular "laminar" and stereotypic growth pattern of ovule integuments {Schneitz et al., 1995; Truernit and Haseloff, 2008}. The *ucn-1* mutant is used as a molecular tool to understand neoplastic growth suppression as they develop tumor-like outgrowths on ovule integuments and other floral organs (see below).

3.1 Phenotypic characterization of *unicorn-1* (*ucn-1*) mutant

3.1.1 *UCN* is a monogenic recessive locus

The EMS-induced *unicorn* allele (*ucn-1*) was originally identified on the basis of mutant plants carrying ovules with a cone-shaped protuberance emanating from the outer integument {Schneitz et al., 1997} (Fig. 3.1.1, E-H). Genetic analysis revealed the *ucn-1* allele to be recessive as no mutant phenotype was observed in more than 100 heterozygous F1 siblings from a parental cross between *ucn-1* and L*er*. Furthermore, in F2 population *ucn-1* segregated in a Mendelian fashion (total plants scored: 136; wild type: 101, *ucn-1*: 35; X^2=0.03, P=0.84) confirming it as a single nuclear recessive mutation.

3.1.2 *UCN* is required for the control of cell division patterns during integument development

Upon ovule integument initiation, cells of the Arabidopsis inner and outer integuments divide in a stereotypic anticlinal fashion (relative to integument surface) resulting in two bi-layered sheets of regularly arranged cells {Schneitz et al., 1995; Truernit and Haseloff, 2008} (Fig. 3.1.1, A-D). Ovules of *ucn-1* plants showed "spontaneous" localized tumor-like outgrowths caused by aberrant hyperproliferation of cells. These protuberances are also characterized by aberrant changes in cell size and shape. Notably two types of cone-like protrusions were observed. Instances of the prominent protrusion class usually, but not always, emanated from a gynobasal region of the outer integument. To determine the first onset of developmental defects, both the wild-type

and *ucn-1* ovules were analysed at sequential developmental series (Fig. 3.1.1, A-H) (Ovule stages according to {Schneitz et al., 1995}). Aberrations were first detected at around ovule stage 2-IV/V, shortly after both integuments have been initiated. In scanning electron micrographs, a small bulge encompassing about one or two cells were initially visible in the outer integument (Fig. 3.1.1, E). Cellular analysis using confocal microscopy revealed that this bulge was likely due to "out-of-plane" (i.e., periclinal, relative to the surface of the outer integument) cell division events in one or a few cells of the adaxial (anterior/dorsal) cell layer of the outer integument. At later stages the protrusions often contained aberrantly sized cells of both layers of the outer integument. Overall, however, the protrusion cells of the abaxial (posterior) cell layer of the outer integument continued to undergo relatively organized cell divisions, since the single cell layer structure was maintained. By contrast, the protrusion cells of the adaxial layer of the outer integument filled up the interior of the cone. Protrusion size was variable but growth usually stopped after the cone extended out from the outer integument by about 3-6 epidermal cell diameters (as in mid-optical sections). Usually one protrusion developed but occasionally up to four protrusions could be observed (Fig. 3.1.1, F).

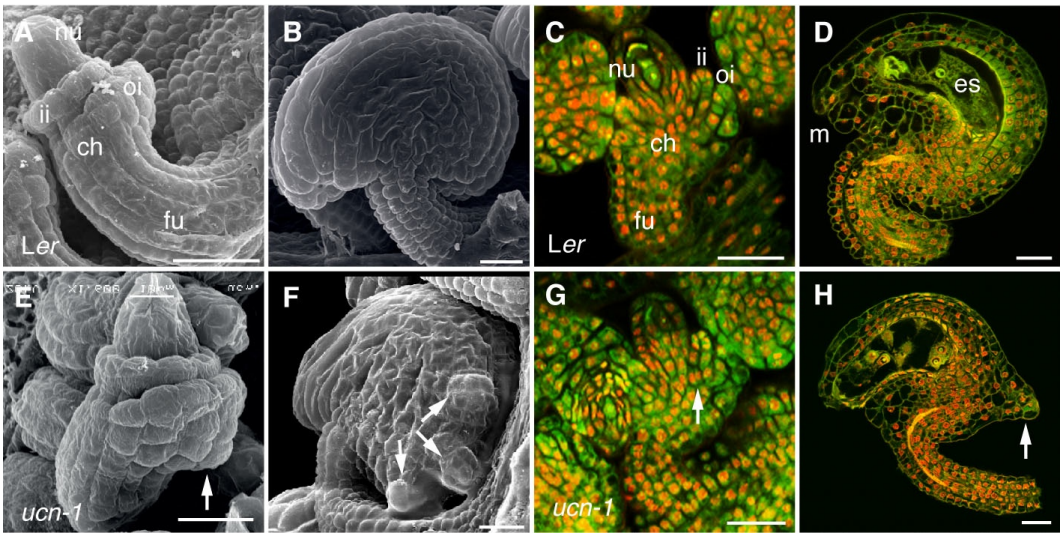

Figure 3.1.1. Neoplastic growth in *ucn-1* ovules. (A, B) Scanning electron micrographs (SEMs) of wild-type ovules. (A) Stage 2-IV. ii, inner integument; oi, outer integument. (B) Stage 4. (C, D) Confocal micrographs of wild-type ovules. (C) Stage 2-IV. (D) Stage 4-I. (E-H) Ovules of *ucn-1*. Similar series as in (A-D). (E) Early protrusion formation (arrow). (F) Protrusions (arrows). (G) Irregular cell division (arrow). Scale bars: 20 µm.

The second type of protrusion included cells of the inner integument (Fig. 3.1.1, G). These bumps were usually quite small and caused by one or possibly two cells of either the abaxial or, and less frequently, the adaxial cell layer of the inner integument undergoing one or two abnormal periclinal cell divisions. The small bump seemed to "push" toward the outer integument as judged by the formation of small cavities between the two integuments and a slight bulging out of the outer integument. Both the inner and outer integument protrusion types occurred independently from each other. The second type could also be present in the absence of the outer integument as it was still visible in ovules of *ucn-1 ino-2* double mutants lacking the outer integument (Fig. 3.1.4, B, see section 3.1.5). Once formed, protrusions persisted and could also be seen in *ucn-1* seeds.

In summary, the protrusions of *ucn-1* ovules seem to be largely based on a locally restricted disorganization of cell divisions in the inner and/or outer integuments. Increase in protrusion size was due to aberrant cell proliferation, cell size and morphology. Excrescences grew to considerable size in proportion to overall organ dimension. In addition, formation of protrusions on the inner integument does not depend on the presence of an outer integument.

3.1.3 Differentiated cells rather than callus contributes to *ucn-1* tumor-like outgrowths

The morphological analysis presented above indicated that the outer integument protrusions of *ucn-1* ovules are characterized by locally disorganized cellular morphogenesis, which contrasts with the regular behavior observed in cells of the wild-type outer integument. To test if cells of the *ucn-1* protrusions maintain outer integument identity, I analyzed the expression of *INNER NO OUTER (INO)* gene in *ucn-1* ovules. *INO* is a YABBY transcription factor that specifically expresses in the abaxial cell layer of the outer integument {Balasubramanian and Schneitz, 2002; Villanueva et al., 1999}.

To this end, a well-established *INO::GUS* reporter (pRJM65) {Meister et al., 2002} was crossed into *ucn-1*. Reporter activity was found in the protrusions of the *ucn-1* outer integuments from the time of their inception onwards (Fig. 3.1.2, C). The outer integument protrusion exhibited normal spatial expression of the abaxial cell fate

marker gene *INNER NO OUTER* (*INO*) indicating that cells contributing to the *ucn-1* integument protrusions exhibited at least partial outer integument identity and do not represent callus (Fig. 3.1.2, D).

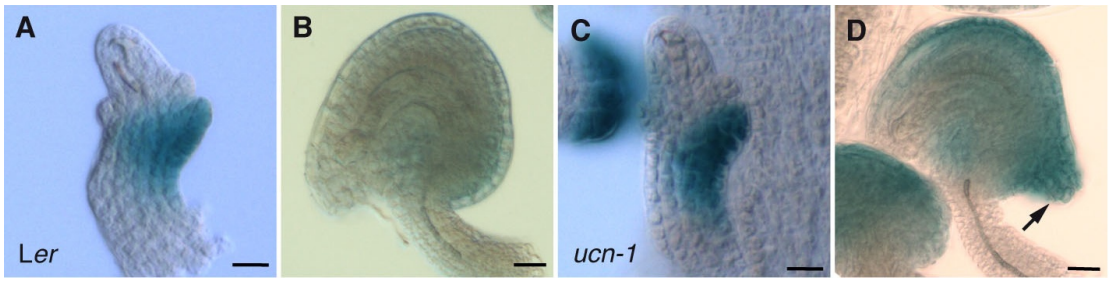

Figure 3.1.2. Differentiating cells contribute to *ucn-1* ovule protrusions. (A-D) Expression of the outer integument marker: *pINO::GUS* reporter (pRJM65). (A) Stage 2-III wild-type ovule. Signal is detectable in the outer integument. (B) Stage 3-VI/4-I wild-type ovule. (C, D) *ucn-1*. ovules of comparable stages as in (A, B) are depicted. The signal appears stronger in *ucn-1* ovules and is present in the protrusion (arrow). Scale bars: 30 µm.

3.1.4 *UCN* is a negative regulator of *INO* expression

Compared to wild type the *INO::GUS* reporter showed a slightly enhanced expression in *ucn-1* ovules. Interestingly, however, while *INO::GUS* reporter expression became undetectable at around stage 3-II ovule in wild type, it could still be observed in the outer integument and the protrusions of *ucn-1* ovules until at least early stage 4. This difference in expression pattern between wild type and *ucn-1* suggests that *UCN* is a negative regulator of *INO* expression. To obtain independent confirmation on the *INO* misexpression in *ucn-1* ovules, we analyzed endogenous *INO* expression by in situ hybridization and quantitative real-time PCR (qRT-PCR). The in situ hybridization results corroborated the normal spatial expression domain of *INO* in young ovules of *ucn-1* mutants (Fig. 3.1.3 C, D) and the qRT-PCR analysis revealed a more than two-fold increase in *INO* expression levels in stage 8 to 11 *ucn-1* flowers but not in older flowers (Fig. 3.1.3, E). The results suggest that *UCN* is a negative regulator of *INO* expression during pre-fertilization ovule development. The result also implies that *INO* expression levels are fine-tuned during integument development. The data further indicate that the *pINO::GUS* reporter lacks regulatory elements that control later *INO* expression levels.

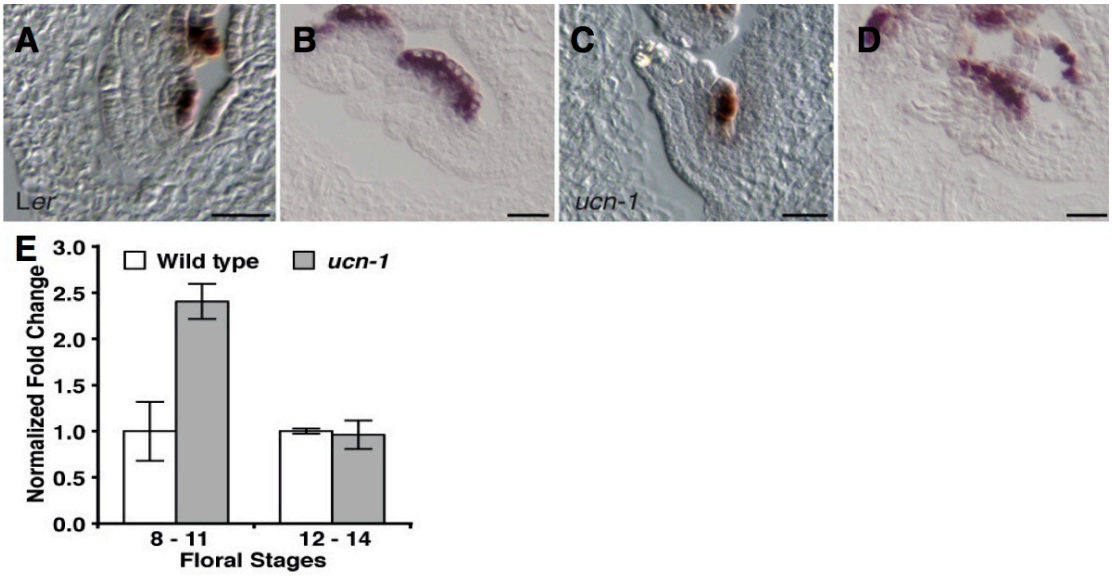

Figure 3.1.3. *UCN* acts as a negative regulator of *INO* expression. In situ hybridization on sectioned ovules using an *INO* probe. (A-D). Early stage 2-III and late stage 2-IV ovules, respectively. (**(**A, B) Wild type. *INO* expression is restricted to the abaxial cell layer in the outer integument. (C, D) *ucn-1*. Normal spatial expression domain of *INO*. (E). qRT-PCR measurements of floral *INO* mRNA levels. Note the increased expression level of *INO* at floral stages 8-11. This indicates that *UCN* is a direct or indirect negative regulator of *INO* expression. Scale bars: 20 µm.

3.1.5 Ectopic *INO* expression is not sufficient for *ucn-1* ovule protrusions

Ectopic *INO* expression observed in the *ucn-1* ovules suggests the possibility that this enhanced expression of *INO* could results in or contribute to the *ucn-1* tumor-like outgrowths. As the homozygous *ucn-1 ino-2* double mutants still formed protrusions on the inner integument (Fig. 3.1.4, B), *INO* activity seems not an essential requirement for tumor formation in *ucn-1* mutants. However, one cannot rule out ectopic *INO* contribution to outer integument protrusions.

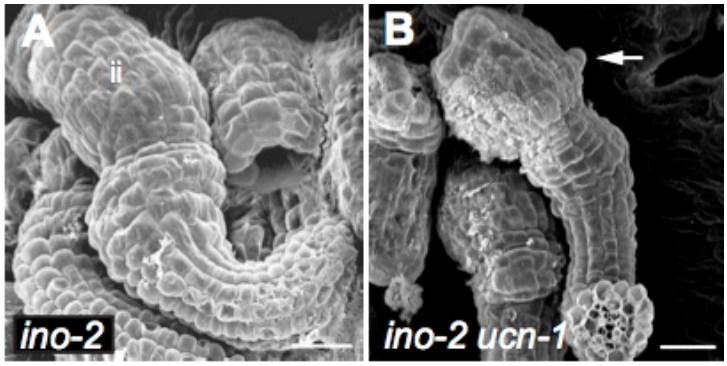

Figure 3.1.4. Elevated *INO* expression levels (Figure 3.3) are not principally required for *ucn-1* protrusion formation. SEMs of stage 4 ovules. (A) *ino-2* ovule. No outer integument. (B) *ino-2 ucn-1*. The inner integument still carries a protrusion (arrow). This implies that *ucn-1* protrusions can occur in the absence of functional *INO*. Scale bars: 20 µm.

3.1.6 *ucn-1* integument-like outgrowths are not due to *WUSCHEL* (*WUS*) misexpression

The homeodomain transcription factor *WUS* plays a central role in early ovule development. *WUS* is expressed in the nucellus during ovule stages 1 to 2 but appears to regulate patterning of the chalaza and formation of integuments in a non-cell-autonomous fashion {Gross-Hardt et al., 2002; Sieber et al., 2004}. Plants with a defect in *WUS* fail to form a regular chalaza and do not carry integuments. By contrast, ectopic expression of *WUS* in the chalaza results in the formation of small outer-integument-like protrusions at the flanks of the chalaza {Gross-Hardt et al., 2002}. In addition, it was shown that altered levels of *YAB1* expression results in deregulation of meristem patterning genes such *WUS* and *CLV3* {Goldshmidt et al., 2008}. As shown in (Fig. 3.1.4,E) the YABBY family gene *INO* is upregulated in *ucn-1* ovules. Thus, I set out to test if the *ucn-1* integument protrusions relate to ectopic *WUS* expression in *ucn-1* ovules. However, a *WUS::GUS* reporter, previously shown to recapitulate *WUS* expression in ovules {Gross-Hardt et al., 2002}, showed normal nucellar expression in *ucn-1* ovules (Fig. 3.1.4). The result was corroborated by in situ hybridization using a *WUS* probe.

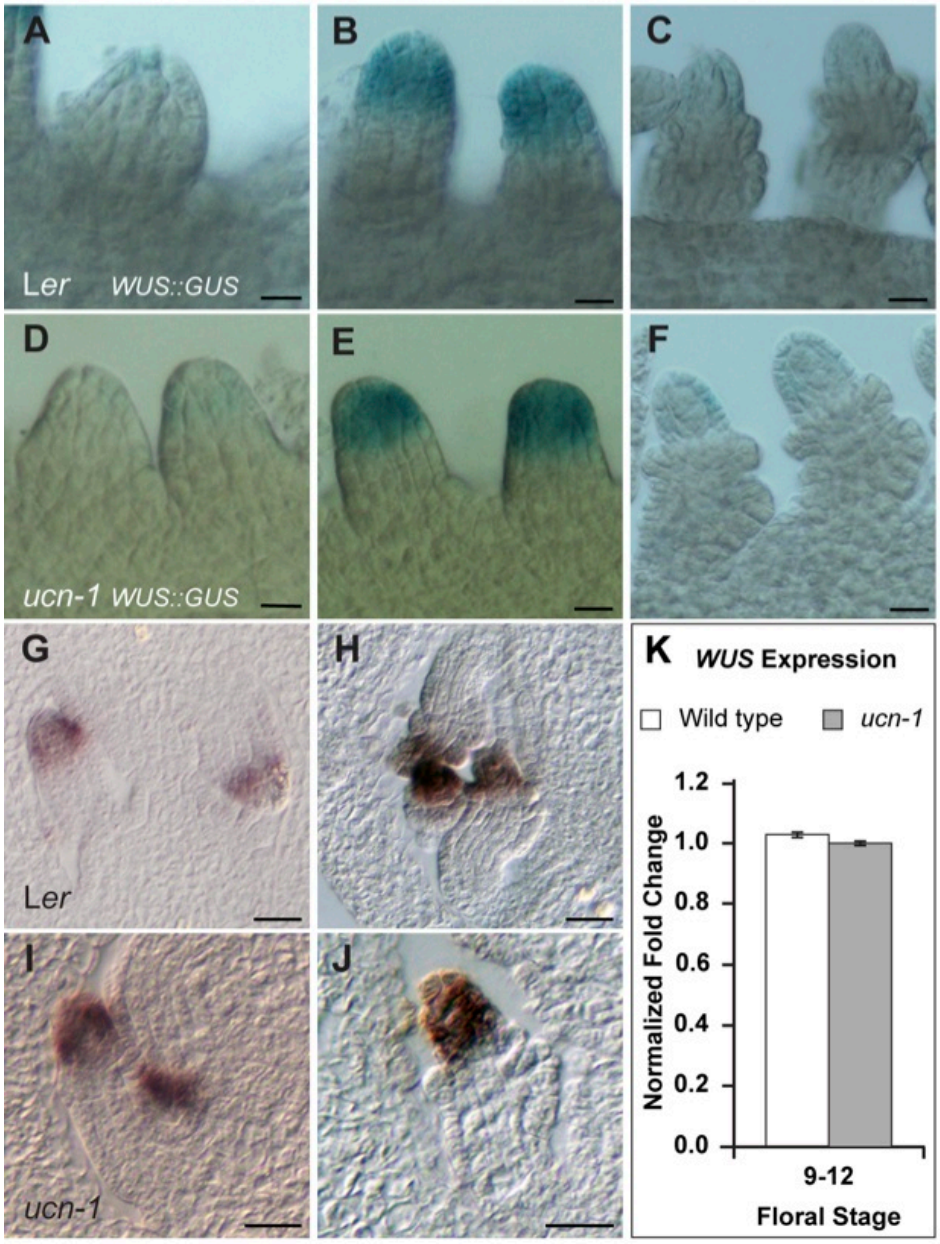

Figure 3.1.5. *WUS* expression patterns in *ucn-1* ovules. (A-F). *WUS::GUS* expression. (A-C) Stage 1-2 wildtype ovules expressing *WUS::GUS* expression exclusively in the nucellus. (D-F). Similar stage *ucn-1* ovules as in (A-C) showing no deviation of *WUS* from wild type ovules. (G-J). in situ hybridization with antisense *WUS* probe. (G-H) Wild-type and (I-J) ucn-1 ovules showing similar endogenous *WUS* expression. (K) q-RT expression analysis of *WUS* in stage 9-12 wt. and *ucn-1* ovules. Note no change in expression levels. Scale bars: (A-F): 30 µm, (G-J): 20 µm.

In addition, assessing *WUS* expression levels in *ucn-1* flowers by qRT-PCR did not reveal noticeable changes compared to wild type (Fig. 3.1.5, K). The data therefore

suggest that *UCN* does not regulate *WUS* expression in ovules and that *ucn-1* protrusions on integuments are not due to ectopic *WUS* transcript levels.

3.1.7 Adaxial-abaxial tissue polarity is maintained in *ucn-1* mutant

Establishment of adaxial-abaxial polarity is a fundamental prerequisite to achieve laminar tissue architecture of lateral organs. Perturbances in this developmental process can either result in development of various degrees of radially symmetrical lateral organs or ectopic outgrowths {Eshed et al., 2001; Kumaran et al, 2002}. To address whether *ucn-1* excrescences were a result of disturbances in polarity establishment, adaxial-abaxial polarity marker expression pattern was analysed in *ucn-1* ovule integuments by in situ hybridization. Abaxial cell fate marker gene *INNER NO OUTER* (*INO*) exhibited normal spatial expression in the *ucn-1* outer integument protrusion from very early inception of integuments (Fig. 3.1.3, A-D).

ABERRANT TESTA SHAPE (*ATS*) encodes a putative transcription factor of the plant-specific KANADI family {McAbee et al., 2006}. Members of this gene family are involved in the specification of abaxial cell identity in lateral organs, likely acting upstream of *YABBY* genes, such as *FILAMENTOUS FLOWER* (*FIL*) {Emery et al., 2003; Eshed et al., 2004; Izhaki and Bowman, 2007; Kerstetter et al., 2001}. In wild-type ovules *ATS* expression was found at the boundary between the two initiating integuments, for a short time at the abaxial side of the inner integument and the adaxial side of the outer integument, and eventually becomes restricted to the abaxial cells of the inner integument {McAbee et al., 2006}. *ATS* expression also showed no deviation from wild type in *ucn-1* mutants (Fig. 3.4.4, A-B). Thus, given the normal spatial *ATS* and *INO* expression in *ucn* ovules, *UCN* is unlikely to affect adaxial-abaxial tissue polarity of the integuments.

3.1.8 *UCN* suppresses aberrant growth in floral organs

Further inspection of *ucn-1* plants revealed that apart from ovules other floral organs were also affected. Petals of stage 13 *ucn-1* flowers were often wrinkled and showed serrated margins (Fig. 3.1.6, D) (floral stages according to {Smyth et al., 1990}). The flowers were characterized by protruding gynoecia, possibly because the sepals are

forced open by the misfolded petals. In addition, petal margins carried tissue outgrowths, particularly at the base and the distal tip of the petals (Fig. 3.1.6, D). The *ucn-1* stamen filaments also showed protrusions of variable size (Fig. 3.1.6, B). The results indicate that *UCN* is required to maintain normal growth patterns in petal and filaments. Interestingly, these tissues are composed of epidermal cells, similar to the integuments, indicating that *UCN* may be important for the regulation of epidermal growth patterns in some floral organs.

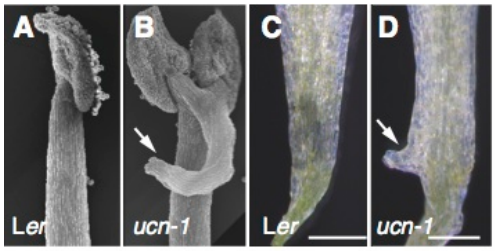

Figure 3.1.6. Neoplastic growth in *ucn-1* floral orgsans. (A-D) Floral defects (stage 13). (A, B) SEMs of stamens. (B) Protrusion on *ucn-1* filament (arrow), (C, D) Petals. (D) *ucn-1* petal with protrusion (arrow). protrusion (arrow). Scale bars: in (A, B) 50 μm; in (C-D) 0.5 mm.

3.1.9 *UCN* mediates growth control in embryo development

The gynoecia of *ucn-1* appeared normal and produced a slightly smaller than normal number of ovules (60.8 ± 1.2 SD per carpel in wild-type vs 57.2 ± 1.3 SD in *ucn-1*, 1 carpel per plant, 10 plants per genotype total). After fertilization, however, siliques developed to shorter length compared to wild type (Fig. 3.1.7, A) and showed a clear reduction in seed number. To investigate the reduction in fertility in more detail I analyzed embryo development in developing seeds of *ucn-1* mutants. Interestingly, in about twenty five percent of young *ucn-1* seeds (43/175 ovules isolated from stage 13/14 flowers) several distinct defects in embryo development were observed (Fig. 3.1.7, C-D**,** Table 3.1.1). Three classes of defective embryos were discernable. In one class eight ovules showed an arrested one-cell proembryo and a normally developed suspensor (Fig. 3.1.7, D). Occasionally aberrant cell divisions occurred in the distal cell of the suspensor, the future hypophysis, and the progenitor cell of the root. In the other class twenty-one ovules showed defective embryos exhibiting an overproliferation of cells and either a reduced or no suspensor (Fig. 3.1.6, C), indicating a general deregulation of growth. Finally, in the third class, no embryo could be detected in fourteen ovules. In addition, I also detected protrusions on petioles of cotyledons (Fig. 3.1.7, E-F).

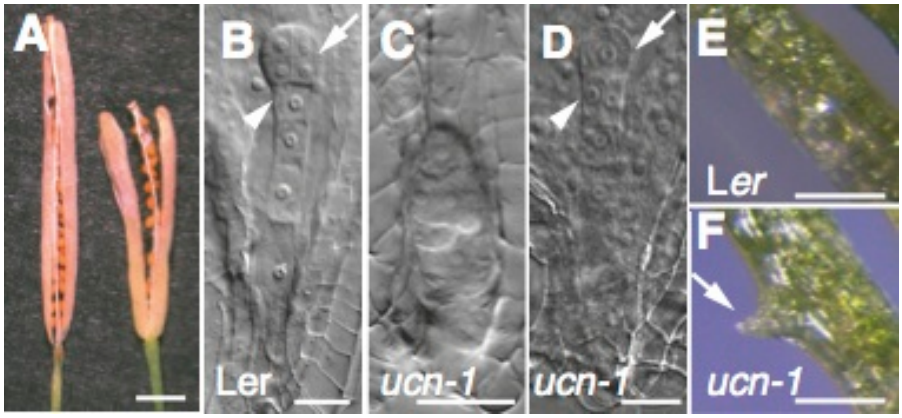

Figure 3.1.7. Growth aberration in *ucn-1* embryo and neoplastic growth on cotyledons.
(A). Wild type and ucn-1 siliques. Note *ucn-1* silique is short. (B-D). Embryo defects in fertilized ovules (stage 13 to 14 flowers). (B). Wild-type embryo with the future hypophysis (arrowhead) and the 8-nuclear proembryo (arrow). (C-D). *ucn-1* embryo. (C). Embryo-like tissue with irregular cell proliferation. (D). embryo with regularly proliferated suspensor but single cell pro-embryo. Scale bars in (A, E-F) 0.5 mm; in (B-D) 20 μm.

Taken together the results indicate that *UCN* not only mediates aberrant growth suppression in ovules but also in petals and filaments. In addition, *UCN* appears to play a role in the regulation of growth patterns in the developing early embryo indicating that *UCN* function as a general growth regulator.

Genotype	Embryos scored	Embryos arrested at one cell pro-embryo	Irregularly proliferated embryos with reduced suspensor	No embryo
Wt	175	0	0	0
ucn-1-/-	175	8	21	14
ucn-2-/- ucnl-5 +/-	175	5	15	18

Table 3.1.1. Classes of embryo phenotypes in *ucn-1* and *ucn-2 ucnl-5* double mutants, related to Figure 3.1.7 and Figure 3.2.8.

3.1.10 Core cell cycle genes are mis-regulated in *ucn-1* mutant

Mis-regulation of cell cycle genes, which may result in aberrant cell division patterns, unscheduled proliferation may lead to neoplasia development {Malumbres and Barbacid, 2001}. To test if cell cycle regulation was affected in the *ucn-1* mutant, Charlotte Kirchhelle assayed the expression of several core cell cycle genes in petals. Indeed, *UCN* influences the cell cycle as we found complex changes in their expression levels (Fig. 3.8). The results suggest that impaired activity of *UCN* function may alter cell division patterns through direct or indirect disruption of specific cell cycle regulator gene expression (Fig. 3.1.8).

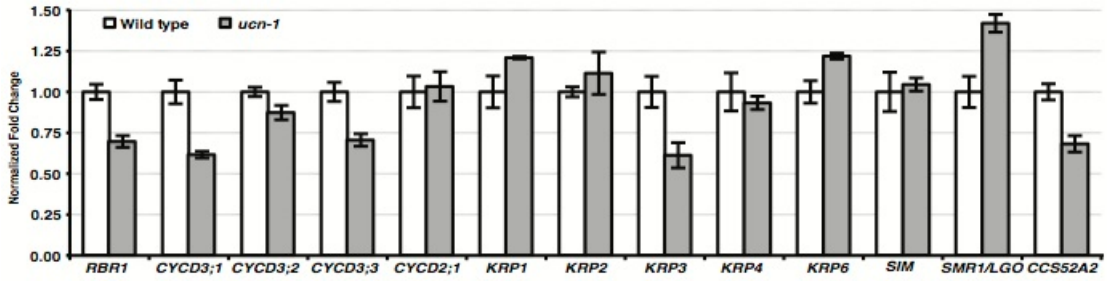

Figure 3.1.8. Comparison of core cell cycle gene expression levels between wild-type and *ucn-1* petals by qRT-PCR. Petals from stage 10 to 12 flowers were used. Cell cycle genes were selected according to Menges et al., 2005. Note a complex mis-regulation of many core cell cycle genes.

3.2 Positional cloning and molecular characterization of *UCN*

3.2.1 Mapping of *UNICORN (UCN)*

Using three separate *ucn-1* (Ler)/Col F2 mapping populations *ucn-1* was initially genetically linked to a single region on the lower arm of chromosome 1 between markers CIW1 and F13011. Further fine mapping placed *ucn-1* in a 129.2 kb interval between two self-generated CAPS markers in At1g51040 and At1g51380 (Fig. 3.2.1) (3480 chromosomes scored). No additional Ler/Col polymorphisms could be identified in this region even after sequencing a total of 18 kb of *ucn-1* genomic DNA scattered throughout the interval. This finding was supported by a recent study indicating that this 129 kb interval is devoid of Ler/Col polymorphisms {Clark et al., 2007}. Lack of

putative polymorphisms in the above 129.2 kb genomic region hampered the marker generation to further narrow down the *ucn-1* interval.

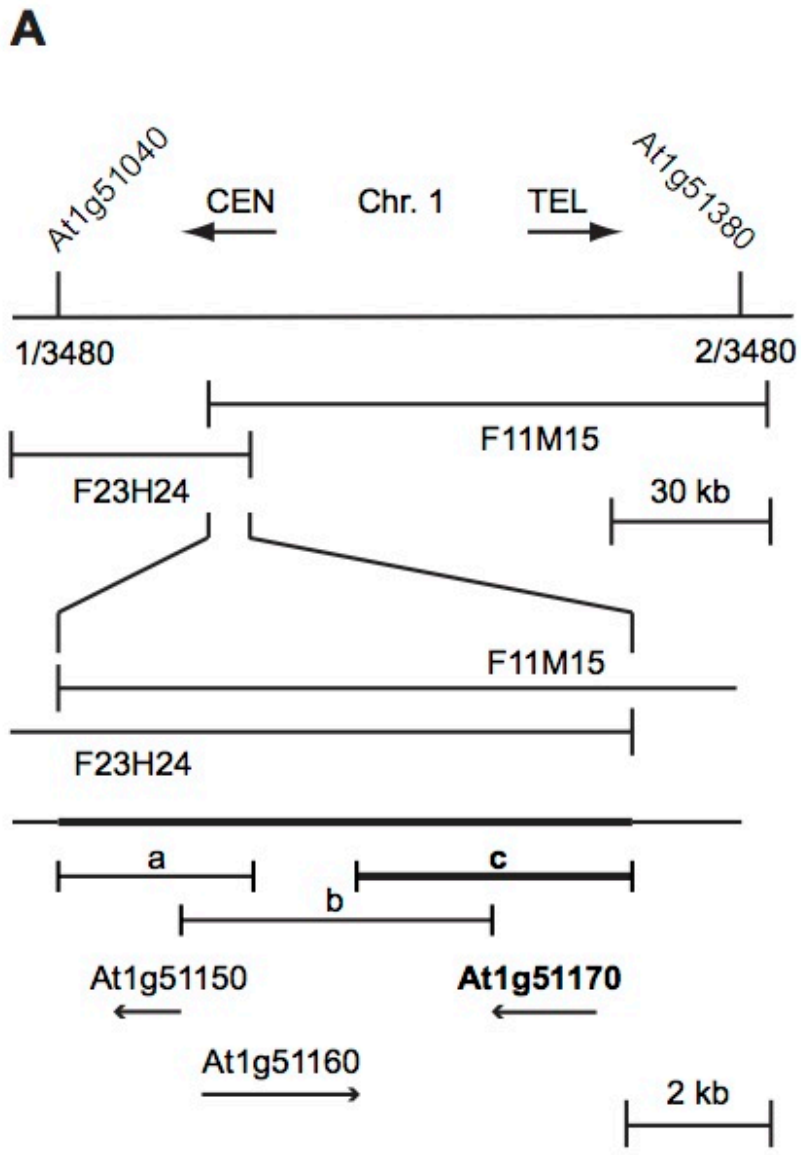

Figure 3.2.1. Positional cloning of *UCN*. The upper panel represents the genomic interval between the two closest genetic markers. The recombination frequency for each marker is given. The extent of two genomic BAC clones is outlined as well. Both BAC clones could rescue the *ucn* phenotype. The lower panel focuses on the overlap of the two rescuing BAC clones (indicated by the bold horizontal line). The three candidate genes within this region, and their orientation, are indicated by the extent and the orientation of the arrows. The a/b and c genomic clones used in further *ucn* rescue experiments are outlined. The c genomic clone, indicated by the bold horizontal line, rescued the *ucn* phenotype. Abbreviations: Chr., chromosome; CEN, centromere; TEL, telomere.

3.2.2 Cloning and complementation analysis of *UCN*

Two partially overlapping genomic BACs covered the *ucn-1* interval. The two BACs, F23H24 and F11M15 span 45.3 kb and 105.8 kb, respectively, and share an 7.9 kb overlap. The two BAC inserts were sub-cloned independently into the binary-BAC vector (BIBAC2) {Hamilton, 1997} after releasing the inserts from pBeloBAC11 by *Not*I digestions. Insert ends were verified by sequencing and the two constructs were transformed into *ucn-1* plants. Full integration was verified by testing that the transgenic plants exhibited proper GUS expression driven by a GUS reporter gene located next to the left T-DNA border. Corresponding transgenic *ucn-1* plants (T1 generation) were scored for floral and ovule phenotypes. Both BAC constructs were able to rescue the *ucn-1* mutant phenotype (data not shown). The result indicated that UCN resides on the 7.9 kb overlap region. This interval contains three annotated genes (Fig. 3.2.1). To identify the *ucn-1* mutation I sequenced the 7.9 kb using genomic DNA from *ucn-1*, Ler and Col and found a single G to A transition at position 18958015 in *ucn-1* only. The mutation resides within the coding sequence of At1g51170.

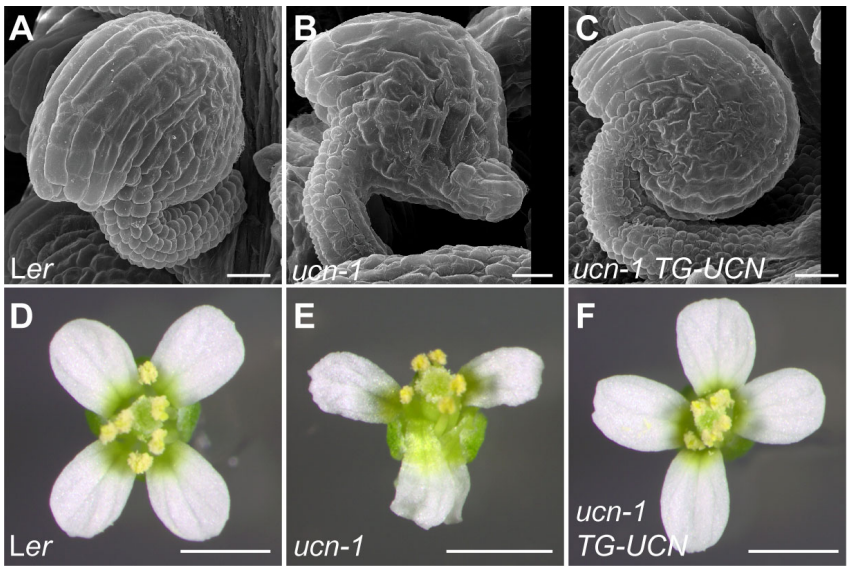

Figure 3.2.2. Genomic rescue of *ucn-1*. (A, D) Wild type ovule and flower. (B, E) *ucn-1* ovule and flower. (C, F) Note that a *ucn-1* plant carrying a 3.8 kb genomic *UCN* DNA construct (*TG-UCN*) (c-construct described in Fig. 3.2.1) shows apparently normal ovules and flowers. Scale bars: (A-C) 20 µm, (D-F) 0.5 mm.

To corroborate the identification of *UCN,* I cloned 3.8 kb of genomic L*er* DNA spanning At1g51170 (starting at the F23H24 breakpoint and ending at the predicted stop codon of At1g51160) into the binary vector pCAMBIA 2300. In addition, two 4.4 and 2.7 kb genomic constructs spanning At1g51160 and At1g51150 respectively were PCR amplified and cloned into pCAMBIA 2300. Plants homozygous for *ucn-1* were independently transformed with these three genomic rescue constructs. Only the construct harboring 3.8 kb of At1g51170 genomic DNA was able to rescue the *ucn-1* mutant phenotype (> 100 T1 lines) demonstrating complementation (Fig. 3.2.2). Comparable constructs spanning At1g51150 and At1g51160 failed to complement the *ucn-1* phenotype (not shown). Thus, I conclude that At1g51170 is *UCN*.

3.2.3 *UCN* encodes an AGCVIII class protein kinase

Results from the map-based cloning, isolation of multiple mutant alleles (section 3.2.4, Supplementary table Table 7.1), and genomic rescue experiments (Fig. 3.2.2) unambiguously confirmed that At1g51170 is *UCN*.

Searches across sequence databases and public cDNA repositories suggest *UCN* to be intronless and to encode a transcript spanning 1435 bp with a 5' untranslated region of 53 bp, an open reading frame of 1215 bp and a 3' untranslated region of 167 bp. Sequence analysis indicates that *UCN* encodes a member of the plant-specific AGCVIII family of protein serine-threonine kinases {Bögre et al., 2003; Galván-Ampudia and Offringa, 2007; Zhang and McCormick, 2009b}. AGC kinases were named after the mamalian cAMP-dependent protein kinase (PKA), cGMP-dependent protein kinase G (PKG), and phospholipid-dependent protein kinase C (PKC).

UCN falls into the AGC2-subclass of the plant AGCVIII kinase family that in turn consists of two distantly related sub-clades with two members each {Galván-Ampudia and Offringa, 2007} (Fig. 3.2.3). The closest homologue of UCN (also known as AGC2-3) is AGC2-4/At3g20830. AGC2-4 resides in a region of recent segmental genome duplication (http://wolfe.gen.tcd.ie/athal/all_results). UCN and AGC2-4 share 73 percent identity at the amino acid level and thus AGC2-4 was renamed to UNICORN-LIKE (UCNL). UCN and UCNL share only 37-41 percent identity at the amino acid level with the other two members of the AGC2 class. So far only one other

member of the AGC2 group, AGC2-1/OXIDATIVE SIGNAL INDUCIBLE 1 (OXI1), belonging to the sister group of UCN, has been functionally analyzed {Anthony et al., 2004; Forzani et al., 2011; Rentel et al., 2004}.

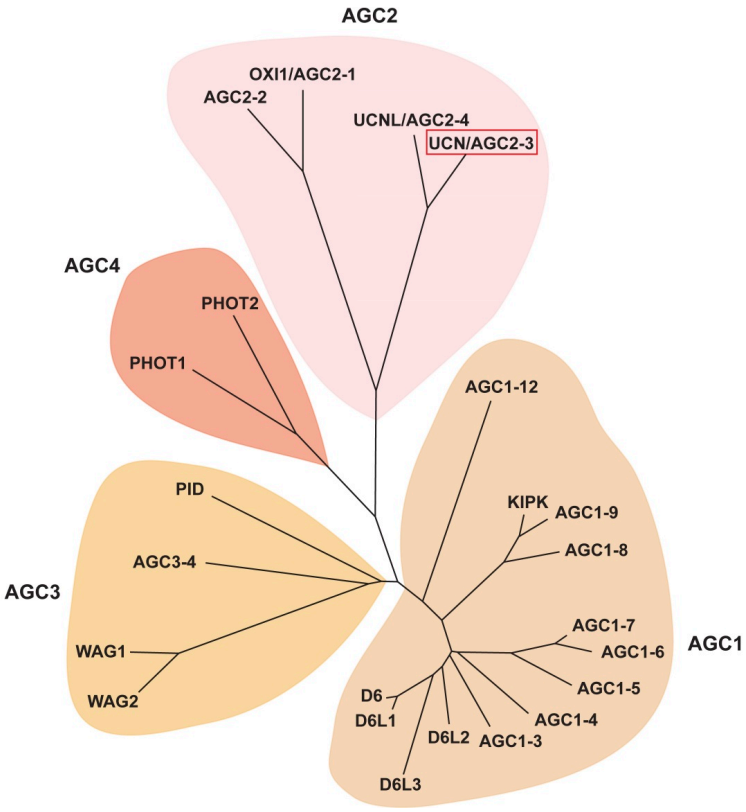

Figure 3.2.3. Unrooted neighbor-joining-based phylogram of all Arabidopsis AGC VIII kinases. Based on previous work {Bögre et al., 2003; Galván-Ampudia and Offringa, 2007}.

3.2.4 Identification of additional alleles in *UCN*

UCN is still transcribed in *ucn-1* plants (Fig. 3.2.7, see section 3.2.7) leaving the possibility that a defective UCN_{G165S} protein is present in *ucn-1* mutants. The mutant protein may either be inactive and biochemically inert or still interfere with *UCN*-dependent processes in a dominant-negative fashion. In the latter case, one would expect *ucn-1* to be dominant; genetic analysis, however, indicated *ucn-1* to be recessive. Moreover, expression of *ucn-1* genomic construct in wild type L*er* plants did not result in *ucn-1* phenocopy. Thus, I screened public T-DNA repositories to get additional alleles in the *UCN* locus. Five additional T-DNA insertions in At1g51170 were identified from the SALK-collection {Alonso et al., 2003} (Fig. 3.2.4, A;

Supplementary table 7.1) and the insertion sites were analyzed by sequencing. SALK_056694 (*ucn-3*) is located 95 bp upstream of the first ATG, SALK_084708 (*ucn-5*) and SALK_084711 (*ucn-4*) are situated in the 5' untranslated region 22 bp and 34 bp upstream of the first ATG, respectively. These lines still exhibit detectable *UCN* expression by RT-PCR (not shown). SALK_002381 (*ucn-2*) is a complex insertion located within the coding sequence 629 bp downstream of the first ATG. This mutant has the principal capacity to synthesize the first 209 residues; the breakpoint resides between kinase subdomains VII and VIII followed by an undeterminable sequence coming from the T-DNA insertion. Expression of a wild-type length *UCN* transcript in this line could not be detected by RT-PCR but primers annealing to the *UCN* region 5' to the T-DNA insertion site amplify a fragment. This result leaves the possibility of a truncated protein in *ucn-2* mutant. SALK_143744 (*ucn-6*) is located in the 3' untranslated region at position 1293 downstream of the first ATG. *UCN* expression was still detectable in this line by RT-PCR (not shown). None of the five homozygous lines showed a mutant phenotype (not shown).

As none of the homozygous T-DNA insertion lines in *UCN* locus differ remarkably from wild type, TILLING (Targeting Induced Local Lesions in Genomes) {McCallum et al., 2000} was carried out with the help of the Seattle Arabidopsis TILLING facility (http://tilling.fhcrc.org/files/Welcome_to_ATP.html/) {Till et al., 2003} in the coding sequence of the UCN locus to identify additional alleles. Three EMS-induced sequence-confirmed homozygous *ucn* alleles exhibiting the *ucn* phenotype (*ucn-7*, *ucn-8*, *ucn-9*) (Fig. 3.2.4, B; Supplementary table 7.1) were isolated. The *ucn-7* mutation (S42F) changes a non-conserved residue while *ucn-8* (G270E) alters an amino acid that is strictly conserved among the plant AGCVIII kinases. Finally, the *ucn-9* mutation (D320N) affects a position that normally either carries an aspartic or glutamic acid (with the exception of AGC3-4 that also carries an asparagine at this position). The *ucn-1* mutant shows the strongest phenotype with *ucn-9*, *ucn-8* and *ucn-7* exhibiting consecutively weaker phenotypes.

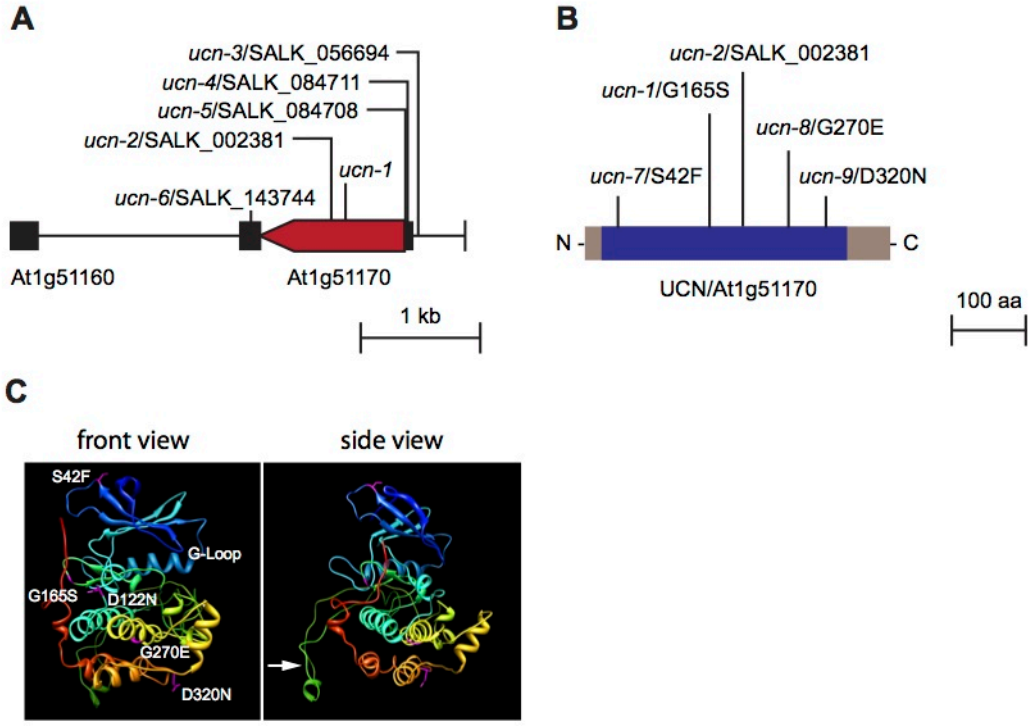

Fig. 3.2.4. Molecular characterization of *UCN* (A). Genomic map of *UCN* highlighting the position of several T-DNA insertion sites. Black boxes mark the 5' and 3' UTRs, respectively. The arrow indicates the extent and the orientation of the open reading frame. In u*cn-2* the insertion results in a predicted shorter protein, which deviates beginning at L209 from the UCN sequence and carries an undetermined number of aberrant residues. (B). Position of *ucn-1,ucn-2 and* TILLING alleles with in the protein. (C). Location of *ucn* lesions in the UCN protein, 3D structure based on Homology modeling.

3.2.5 Molecular characterization of *UCNL*

As the available *UCN* T-DNA insertion lines did not show any phenotype similar to *ucn-1,* and given that *UCNL* is the immediate homologue, I hypothesized functional redundancy between the two genes. Hence, to test this possibility, I analyzed by sequencing the insertion sites of five T-DNA lines within the *UCNL* locus (Fig. 3.2.5; Supplementary table 7.1). Bioinformatic comparisons including the analysis of public cDNA-repositories suggest *UCNL* to be intronless with a 1298 bp transcript with a 5' untranslated region of 10 bp, a coding sequence of 1227 bp and a 3' untranslated region of 61 bp. T-DNA line SAIL_238_A09 (*ucnl-1*) from the SAIL collection {Sessions et al., 2002} is situated in the promoter region 125 bp upstream of the first ATG.

GT931.DS5 (*ucnl-2*) from the Cold Spring Harbor Lab Genetrap collection (http://genetrap.cshl.edu) locates to the predicted 5' untranslated region 5 bp upstream of the first ATG. SALK_117406 (*ucnl-3*) is situated in the coding sequence 5 bp downstream of first ATG and SALK_066654 (*ucnl-4*) resides 32 bp downstream of the first ATG. In all these lines *UCNL* expression could still be detected by RT-PCR. SALK_024621 (*ucnl-5*) localizes 345 bp downstream of the first ATG and may produce a mutant UCNL protein with 115 regular residues followed by 10 aberrant residues (RILWCKQIDA*). Expression of a wild-type length *UCNL* transcript in this line could not be detected by RT-PCR but primers annealing to the UCN region 5' to the T-DNA insertion site amplify a fragment. None of the five T-DNA insertion lines showed a detectable mutant phenotype (not shown).

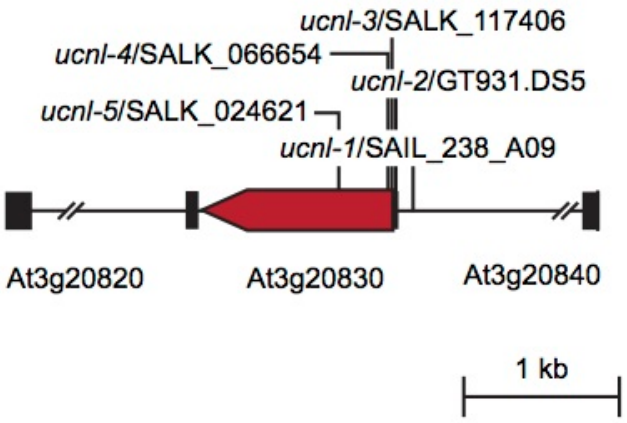

Fig. 3.2.5. Molecular characterization of *UCNL*. Genomic map of *UCNL* depicting the position of different T-DNA insertion sites. Black boxes mark 5' and 3' UTRs, respectively. The arrow indicates the extent and the orientation of the open reading frame. In *ucnl-3* the insertion results in a predicted three residues protein (M1-DA*) with the aspartate and the alanine being aberrant residues. In *ucnl-5* the insertion results in a predicted short protein at L116 followed by ten aberrant residues and a stop (L115-RILWCKQIDA*). In *ucnl-4* the insertion resides at S10 followed by an undermined number of aberrant residues.

3.2.6 *UCN* and *UCNL* are expressed in various plant organs

As *ucn-1* phenotype is mostly restricted to floral organs and embryos, I was curious to know whether *UCN* and *UCNL* gene expression is restricted to only those organs. Expression of *UCN* and *UCNL* in different organs of the plant was analyzed by semi quantitative RT-PCR. I found that both *UCN* and *UCNL* are expressed in all the plant organs (from root to fruit) examined albeit *UCNL* in lesser amounts compared to *UCN*

(Fig. 3.2.6). *UCN* and *UCNL* expression profiles suggest a broader role for the two genes than revealed by *ucn-1* phenotype.

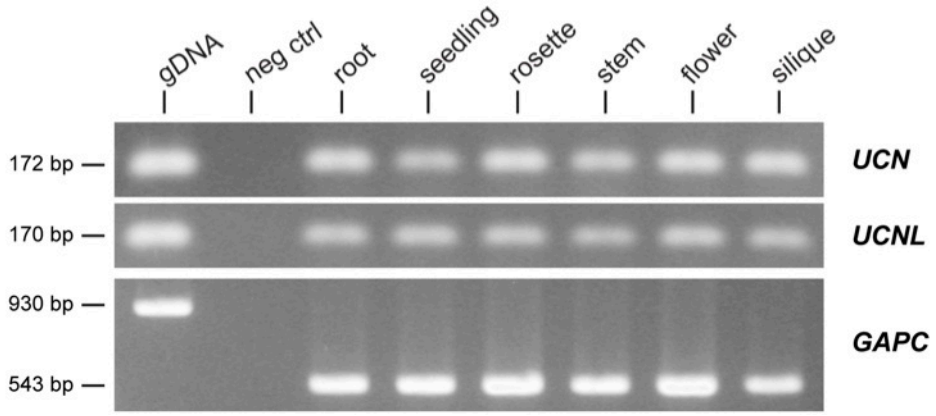

Figure 3.2.6 Tissue distribution of *UCN* and *UCNL* expression as revealed by semi-quantitative reverse transcription PCR. The result obtained after 26 cycles for all tested genes is shown. *GAPC* served as control {Shih et al., 1991, Gene, 104, 133-138}. Root: 10-day seedling, seedling: 10-day seedlings, rosette leaves: 19-day plant, stem: 24-day plant, flowers: whole flowers from a 24-day plant, silique: all green siliques of a 24-day plant. In the negative control a template was omitted from the PCR-reaction.

3.2.7 *UCN* and *UCNL* are expressed in developing flowers

To determine the spatial expression pattern of *UCN* and *UCNL* during flower and ovule development in situ hybridization was carried out. Despite several attempts detection of *UCN* expression in developing flowers by in situ hybridization was unsuccessful, indicating that *UCN* is expressed at very low levels. However, quantitative real-time PCR (qRT-PCR) revealed *UCN* expression at floral stages 8 to 11 (Fig. 3.2.7), which encompasses the period when the *ucn-1* phenotype becomes first apparent. Similarly, *UCNL* expression was detected, albeit at lower levels corroborating the semi quantitative RT-PCR results. The results also showed that *UCN* is normally transcribed in stage 8-11 *ucn-1* flowers but slightly higher in later stages. The increase in *UCN* transcript levels in the later stages of *ucn-1* flowers suggests that *UCN* expression is under its own negative feed back control at later floral stages.

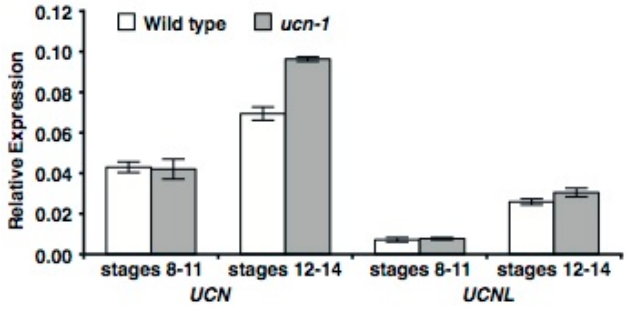

Figure 3.2.7. *UCN* and *UCNL* expression profile in flowers. A qRT-PCR-based comparison of floral *UCN* and *UCNL* mRNA levels, respectively, in wild type and *ucn-1*.

3.2.8 *UCN* and *UCNL* share redundant functions

The high homology between the *UCN* and *UCNL* genes, their similar expression patterns, and the absence of phenotype in individual full-length RNA nulls suggest redundant roles for these genes in growth control.

The T-DNA insertion in *ucn-2* resides within the open reading frame and *ucn-2* mutants may generate a mutant protein consisting of the first 209 residues followed by 10 arbitrary amino acids (Supplementary table 7.1). Since the truncation resides in the middle of the kinase domain it is to be expected that plants homozygous for this mutation are devoid of UCN activity. In the case of *ucn-2* (full length RNA null) one could reason that *UCNL* would provide redundant activity and thus rescue *ucn-2* mutant. Where as, the *ucnl-5* mutant carried an insertion in the *UCNL* open reading frame and was predicted to carry a short protein of 115 amino acids followed by 10 aberrant residues (Supplementary table 7.1). Such a short protein lacks most of the kinase domain and thus *ucnl-5* is predicted to be a null-allele. The absence of a mutant phenotype of *ucnl-5* mutants could be explained by redundant activity provided by *UCN*.

I therefore constructed double mutants of *ucn* and *ucnl,* using two different allelic combinations (*ucn-2 ucnl-5* and *ucn-1 ucnl-5).* Upon selfing of a *ucn-2*/*ucn-2 ucnl-5*/+ plant a total of 136 F1 plants were genotyped using T-DNA insertion site-specific primer pairs. Of those 136 F1 progeny 87 plants were heterozygous for *ucnl-5* while 49 plants carried the wild-type *UCNL* allele. This ratio indicated that *ucn-2 ucnl-5* double mutants were embryo lethal with full penetrance. To test this assumption, I looked at young developing seeds produced by selfing of a *ucn-2*/*ucn-2 ucnl-5*/+ plant. Of 175 scored ovules 38 exhibited embryo aberrations strongly resembling the embryo defects observed in *ucn-1* plants (Fig. 3.2.8; Fig. 3.1.7; Table 3.1.1**)**. While 5 embryos showed

the one-cell proembryo arrest and the aberrant cell divisions in the prospective hypophysis and 15 embryos showed the reduced suspensor and over-proliferation of cells. In 18 ovules no embryo could be detected. These results corroborate the notion that complete absence of functional *UCN* and *UCNL* activity leads to fully penetrant embryo lethality. Interestingly, homozygous *ucn-1* plants show the null phenotype with a reduced penetrance of about 25 percent raising the possibility that UCN and UCNL are members of a multi-protein complex.

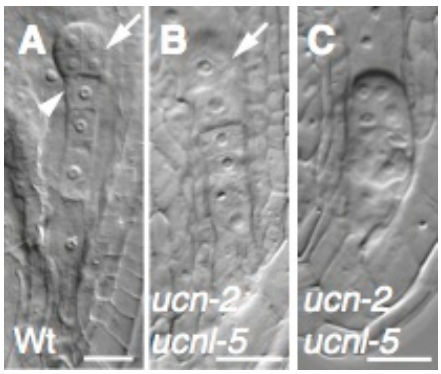

Figure 3.2.8. UCN and UCNL double mutant analysis. Embryo defects in fertilized ovules (stage 13 to 14 flowers). (A) Wild-type embryo with the future hypophysis (arrowhead) and the 8-nuclear proembryo (arrow). (B, C) *ucn-2*/*ucn-2 ucnl-5*/- embroys. (B). Arrested proembryo. (C) A mutant embryo in a ovule from a selfed *ucn-2*/*ucn-2 ucnl-5*/+ parent. Similar phenotype to *ucn-1* embryos. Scale bars: 20 μm.

Surprisingly, the double homozygous *ucn-1 ucnl-5* mutant still showed *ucn-1* phenotype. However, unlike *ucn-2* allele, in *ucn-1* full-length *ucn-1* RNA is made. *ucn-1* is partially functional with respect to embryogenesis. Taken together the data suggests that the functional redundancy between *UCN* and *UCNL* exist. The data further indicates that the compensation mechanism between *UCN* and *UCNL* works only when the respective full-length transcript message is completely absent.

3.3 Biochemical and cell biological characterization of the UCN protein

3.3.1 Functional domains and motifs in UCN

The kinase domain of the UCN protein features all the hallmarks of a regular protein kinase {Hanks and Quinn, 1991}. Alterations include the change of the conserved DFG triplet to DFD in subdomain VII of the catalytic domain and an insertion (about 63 amino acids in the case of UCN) between kinase subdomains VII and VIII in the activation loop, referred to as the T-loop extension, and is typical for plant AGCVIII kinases**.** Until to date, the T-loop extension of only three Arabidopsis AGCVIII kinases has been studied and demonstrated to contain cellular localization signals such as

nuclear localization signal (NLS) and lipid binding properties {Zegzouti et al, 2006; Ek-Ramos et al, 2010}. Here I show that the UCN T-loop extension also has predicted bipartite (206KKSLRIFRQKKKKTKSARVNPITRRR^{231}) and monopartite (^{213}RQKKKKTK^{220}) nuclear localization signals (NLS) (http://nls-mapper.iab.keio.ac.jp/cgi-bin/NLS_Mapper_form.cgi). The above stretch of basic amino acids could also serve as an anchor in phospholipid binding. UCN also has two potential nuclear export signals (NES) (L-X$_{(2,3)}$-[LIVFM]-X$_{(2,3)}$-L-X-[LI]) (http://www.cbs.dtu.dk/services/NetNES/) at the beginning (^{19}LDRLKVLKL^{27}) and the end (^{309}LTDLIRRLLV^{318}) of the kinase domain. The hydrophobic/PIF motif (FXXF) predicted to bind PDK1 {Zegzouti et al, 2006b} is present at its very c-terminus (Fig. 3.3.1) and UCN exhibits a consensus PDK1 phosphorylation motif in its catalytic loop with S242 being the candidate residue for phosphorylation.

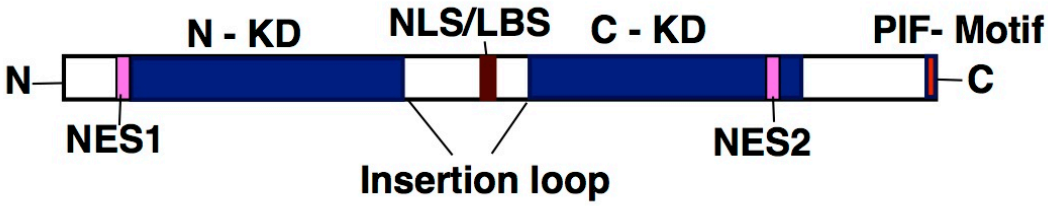

Figure 3.3.1. Functional domains and motifs in UCN. Ser/ Thr Kinase UCN has the standard kindase dmain (Blue) interspaced by 66 aa insertion loop. Insertion loop has a streach of basic amino acids that are predicted to be Nuclear localization signal (NLS) and Lipid binding sites (LBS) represented in brown colour. Note the two predicted Nuclear export signals (NES) (Pink) and PIF motif at the C-terminus of the protein that facilitates the interaction with PDK1 kinase.

3.3.2 UCN is a functional kinase

In vitro kinase assays, using a bacterially produced recombinant N-terminal translational fusion of either glutathione S-transferase to UCN (GST:UCN) or 6X His tag to UCN (His:UCN) revealed that UCN is a functional kinase that auto-phosphorylates and trans-phosphorylates the general substrate myelin basic protein (MBP) (Fig. 3.3.2). However GST:UCN$_{G165S}$ (ucn-1) recombinant protein didnot show any detectable phosphorylation activity both at auto and substrate phosphorylation levels suggesting *ucn-1* is a loss-of-function mutation. A highly conserved lysine in kinase subdomain II that interacts directly with ATP is required for catalytic activity

among the protein kinases. Mutation of this residue leads to a classical "kinase-dead" mutant {Hanks et al., 1988; Kamps et al., 1984}. The equivalent conserved lysine residue in UCN (K55) is mutated to alanine to yield artificially generated UCN_{KD} variant that served as a negative control in this study.

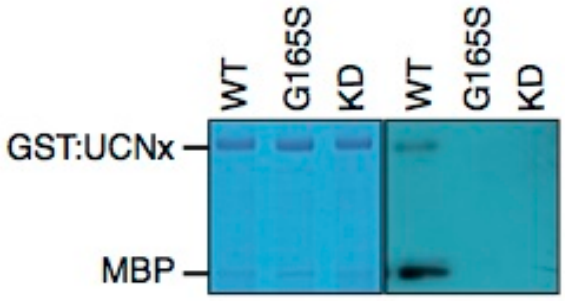

Figure 3.3.2. UCN is an active AGC kinase. In vitro kinase assay with purified GST:UCN fusion proteins. Left panels: coomassie blue gel. Right panels: corresponding autoradiographs. GST:UCNx denotes different GST:UCN variants indicated on top. Note the autophosphorylation and transphosphorylation of myelin basic protein (MBP). GST:UCN_{KD} (K55E mutation, negative control).

3.3.3 UCN undergoes trans auto-phosphorylation

To examine whether UCN auto-phosphorylation is achieved through intra or inter molecular interaction I performed in vitro kinase assay with the purified recombinant UCN, ucn-1 and UCN_{KD} variant proteins. Co-incubation of GST:UCN with either of the kinase inactive His:ucn-1 or His:UCN_{KD} recombinant protein resulted in the phosphorylation of ucn-1 and UCN_{KD} versions **(**Fig. 3.3.3**)**. The result demonstrates that UCN undergoes auto-phosphorylation in an intermolecular manner. However, this result does not rule out intramolecular phosphorylation of UCN.

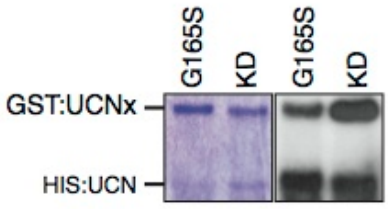

Figure 3.3.3. Trans-autophosphorylation of UCN. In vitro kinase assay with purified HIS:UCN fusion protein. Left panels: coomassie blue gel. Right panels: corresponding autoradiographs. GST:UCNx denotes different GST:UCN variants indicated on top. Note the auto-phosphorylation and trans-phosphorylation of unfunctional GST:UCN_{G165S} or GST:UCN_{KD} (showed in Figure 3.3.2) by HIS:UCN.

3.3.4 UCN forms homo-dimers in plant cells

The in vitro auto-phosphorylation kinase assay results raised the possibility that UCN forms homo-oligomers leading to intermolecular auto-phosphorylation as an event essential for activation. Therefore, I investigated whether UCN undergoes homo oligomerization in plant cells using bimolecular fluorescence complementation (BiFC) analysis (Fig 3.3.5, A-D**,** see section 3.3.5). The results indicate that full-length UCN can form homodimers in a plant cell, confirming the results from the in vitro kinase assays. Co-transfecting 4 µg or 10 mg of empty pUC-SPYNE/SPYCE plasmids did not result in signal (not shown).

3.3.5 UCN localizes to nucleus, cytoplasm and likely to plasma membrane

To get insight into cellular localization of UCN, I used various approaches. Firstly, stable transgenic plants were generated carrying an *EGFP:UCN* reporter gene under the control of the 500 bp of promoter sequence that was shown to be sufficient to rescue *ucn-1* phenotype (Fig. 3.2.2). The *ucn-1* plants carrying this reporter (*UCN::UCN:GFP, ucn-1*) exhibited a wild-type phenotype indicating that the EGFP:UCN fusion protein is biologically functional (data not shown). Analysis of the *UCN::EGFP:UCN* reporter in meristematic zone root cells revealed possible plasma membrane, a broad cytoplasmic and nuclear distribution of the UCN (Fig. 3.3.4). Reporter signal, however, could only be detected in the root although transgene expression could be detected by RT-PCR in flowers as well (not shown). This result indicates that UCN expression is subject to intricate regulation.

Next, I generated constructs encoding N-terminal and C-terminal translational fusions of full-length *UCN* to green fluorescent protein (*GFP:UCN, UCN:GFP*) driven by the 35S promoter. These reporter constructs were transfected into Arabidopsis leaf mesophyll protoplasts. In both cases cytoplasmic, nuclear and plasma membrane localization of the reporter was detected (Fig 3.3.4 E-G) similar to the signals observed in transgenic *UCN::EGFP:UCN* plants. Surprisingly, however western blot studies of either stably transformed *UCN::EGFP:UCN* plants or transiently transfected *35S::GFP:UCN/ 35S::UCN:GFP* protoplasts showed degradation bands of the

transgenic protein (blots probed with anti-GFP antibody) (not shown). The immunoblot result suggests that the nuclear and cytoplasmic localization signal observed for the two constructs above could be due to passive diffusion of cleaved free EGFP.

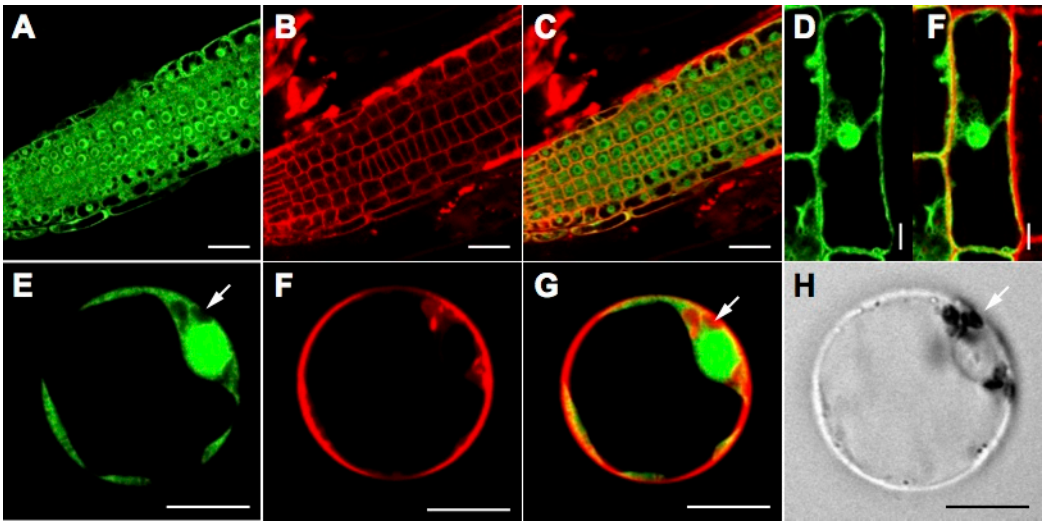

Figure. 3.3.4. Cellular localization of EGFP tagged UCN. (A-F). Root meristematic zone of *UCN::EGFP:UCN:3'UTR* stable transgenics. (A). EGFP-UCN, note the nuclear, cytoplasmic localization. (B). FM4-64, plasma membrane dye. (C). merge (A+B). (D). Single root cell showing EGFP-UCN signal. (E-F). Transiently transfected protoplasts expressing UCN-EGFP. (E). UCN-EGFP signal. Note the cytoplasmic and nuclear signal. (F). FM4-64 DYE fluorescence (G). merge, (E+F). (H). Bright filed view of the protoplast.

In order to assess the sub-cellular localization of UCN more accurately, I performed bimolecular fluorescence complementation (BiFC) analysis. Co-expression of the N-terminal half of YFP fused to UCN (nYFP-UCN) and the C-terminal half of YFP fused to UCN (cYFP-UCN) and vice versa in *Arabidopsis* mesophyll protoplasts resulted in fluorescence predominantly in the nuclei and cytoplasm (Fig. 3.3.5, A-D). No fluorescence was detected between co-transformed empty vectors pSPYNE/ pSPYCE, and between either nYFP-UCN/ pSPYCE, pSPYNE/ cYFP-UCN, confirming the specificity of the interaction.

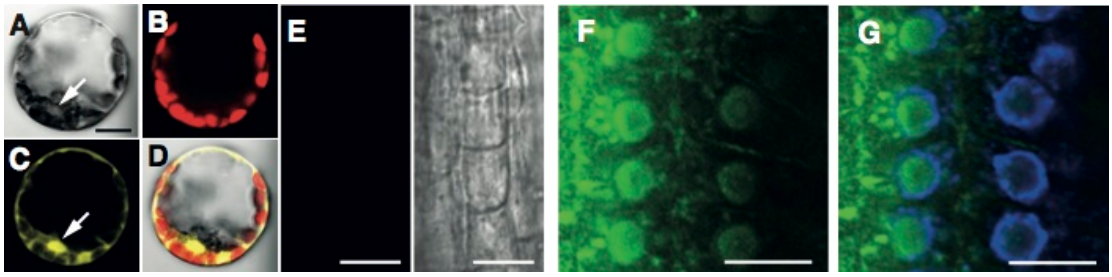

Figure 3.3.5. UCN homodimerization and Immunolocalization. (A-D). BiFC-visualization of UCN dimerization. Different views of a protoplast co-transfected with *pSPYNE:UCN* and *pSPYCE:UCN* plasmids. (A) Bright-field view. (B) Chloroplast autofluorescence (red signal). (C) YFP channel (yellow signal). Arrow indicates nucleus. (D) Merge. Co-transfecting 4 µg or 10 µg of empty pUC-SPYNE/SPYCE plasmids did not result in signal (not shown). (E-G) Immunolocalization of UCN in whole-mount roots of 6 day-old seedlings. (E) Pre-immune serum (left), bright-field view (right). (F) Anti-UCN antibody. (G) plus DAPI. Scale bars: (A-D), 30 µm; (E-G), 10 µm.

Finally, direct detection of endogenous UCN protein using an anti-UCN antiserum revealed expression in the epidermis and cortex of the proliferation zone above the root meristem. Cells exhibited signal in the nucleus, cytoplasm and likely at the plasma membrane (Fig. 3.3.5, F-G). Similar studies using floral tissue were unsuccessful. Taken together, the data indicate that UCN shows a broad subcellular distribution and may function in different cellular compartments.

3.3.6 UCN binds to phospholipids

The immunolocalization data suggest a broad subcellular localization of UCN, including its presence at plasma membrane. However, UCN does not carry recognizable transmembrane, GPI-anchor domains, a potential myristoylation and palmitoylation sites. This raises the possibility that the recruitment of UCN to the plsmamembrane can be achieved either by direct phospholipid binding or membrane protein interaction. Thus, I tested whether UCN has any propensity for phospholipids using a centrifugation method described by Fernandez-Chacon et al {Fernandez-Chacon et al, 2001}. Mouse Synaptotagmin1 (mSYT1) was used as positive control. The mSYT1 protein is a C_2 domain containing protein that binds to phospholipids in Ca^{2+}-dependent manner and trigger neurotransmitter release {Shin et al, 2003}. The recombinant GST-UCN and GST-mSYT were incubated with liposomes (25%

phosphotidylserine, 75% phosphotidylcholine) in the presence and absence of free 100 µM Ca2+. After isolation, liposome-bound proteins were resolved using 12% SDS-PAGE and visualized by coomassie blue staining. As does the positive control mSYT1, UCN also showed binding capacity to phospholipids (Fig. 3.3.6). However, in case of UCN, addition of Ca2+ amounts did not have any influence on phospholipid binding. Taken together the data suggest that UCN can directly bind to phospholipids and this lipid interaction could facilitate the UCN recruitment to the plasma membrane.

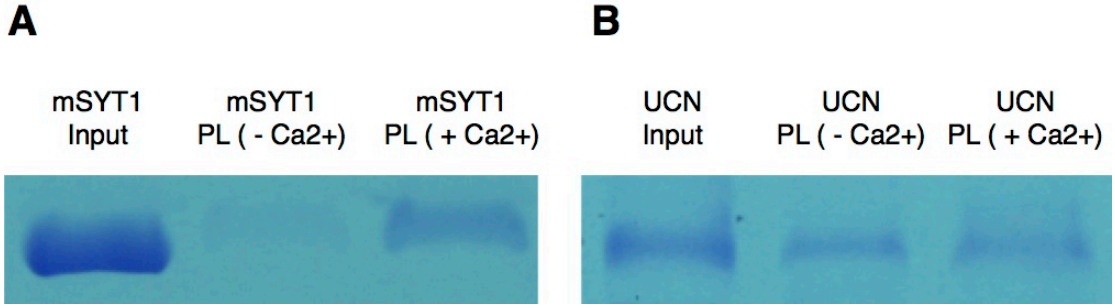

Figure 3.3.6. UCN phospholipid binding assay. (A). Recombinant Mouse SYMAPTOTAGMIN 1 (GST-mSYT1, positive control) binds to Phopholipids in the presence of 100 µM Ca^{2+}. (B). GST-UCN binds to phospholipids irrespective of CA^{2+}. PL: Phospholipids.

3.4 Mechanism of *UCN*-mediated neoplastic growth suppression

The phenotypic analysis of *ucn-1* mutant plants and *ucn ucnl* double mutants indicated that *UCN* and *UCNL* act as an aberrant growth suppressors in ovule, floral organ and embryo development. To address the molecular basis of *UCN*-mediated neoplastic growth suppression, I combined *ucn-1* mutant with several ovule integument mutants. Suppression of *ucn* phenotype in the respective gene mutant background and understanding the mode of interaction might shed light on the long-standing fundamental question that how plants suppress neoplastic growth.

3.4.1 *UCN* acts independently of many known ovule development pathways

Recent years have witnessed the isolation of a number of genes with roles in early ovule patterning and morphogenesis and the development of a genetic network regulating ovule development {Chevalier et al., 2002; Colombo et al., 2008; Kelley and Gasser, 2009}. To place *UCN* in the context of this known ovule genetic network, and to

understand the *UCN*-mediated neoplastic growth suppression, I combined *ucn-1* with a number of mutants and analyzed the ovules of the double-mutant plants.

3.4.1.1 *AINTEGUMENTA* and *INO* acts earlier than *UCN* in integument development

AINTEGUMENTA (*ANT*) encodes an AP2-class transcription factor and is expressed in dividing cells in plant primordial. *INO* is expressed in abaxial cells of the young outer integument and encodes a putative YABBY transcription factor thought to regulate abaxial identity in the outer integument {Balasubramanian and Schneitz, 2000; Villanueva et al., 1999}. Mutations in *ANT* and *INO* result in the failure to initiate both integuments or just the outer integument, respectively {Baker et al., 1997; Klucher et al., 1996; Schneitz et al., 1997; Villanueva et al., 1999}. As *ucn-1* ovules have integument-like outgrowths, it is quite interesting to know the effect of integument regulators *ANT* and *INO* on *ucn-1* integument outgrowths. Thus, I generated double mutants: *ant-72F5 ucn-1* and *ino-2 ucn-1* and found *ant-72F5, ino-2* to be epistatic to *ucn-1* (Fig. 3.4.1, C-D). The result indicates that *ANT* acts earlier than *UCN* in integument development. However, in the other floral organs *ant* is acting additive to *ucn-1* as both ant and *ucn* the mutant phenotypes were noticeable.

3.4.1.2 *UCN* acts independent of *BELL1*, *NOZZLE*, *SUPERMAN* and *STRUBBELIG*

BELL1 (*BEL1*), *NOZZLE/SPOROCYTELESS (NZZ/SPL)* and *SUPERMAN* (*SUP*) encode different types of transcription factors involved in various steps of chalazal pattern formation and early integument development {Gaiser et al., 1995; Reiser et al., 1995; Robinson-Beers et al., 1992; Sakai et al., 1995; Schiefthaler et al., 1999; Schneitz et al., 1997; Yang et al., 1999}. *STRUBBELIG/SCRAMBLED* (*SUB*/*SCM*) encodes a receptor-like kinase (RLK) regulating inter-cell-layer signaling in ovules {Chevalier et al., 2005; Kwak et al., 2005}. I tested the genetic interactions between *ucn* and mutants carrying defects in the above genes but in all instances the double mutant phenotypes were additives suggesting that *UCN* acts independently of those genes (Fig. 3.4.1, E-L) in integument development.

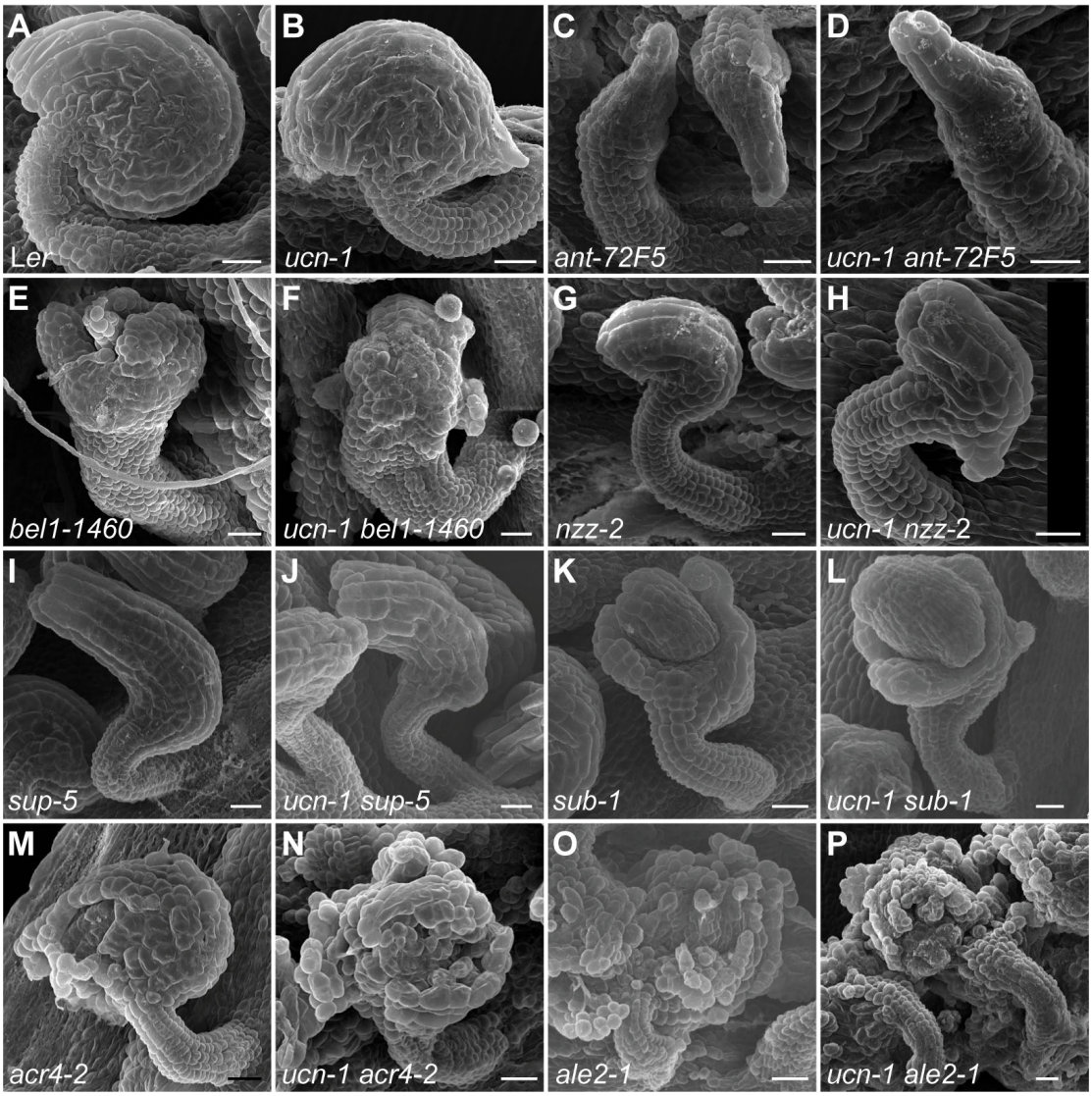

Figure 3.4.1. Analysis of ovule phenotypes of various double mutants. Scanning electron micrographs of early stage 4 ovules are depicted. (A, B) Ler and *ucn-1* controls. (C, D) *ucn-1 ant-72F5* analysis. (D) Note the absence of integuments and epistasis of *ant-72F5*. (E, F) *ucn-1 bel1-1460* analysis. (E) The *bel1* ovules are characterized by aberrant outgrowths in place of normal integuments. (F) Note the presence of *ucn-1* like protrusions on *bel1*-like outgrowths. (G, H) *ucn-1 nzz-2* analysis. (H) Note the occurrence of an *ucn-1*-like outgrowth on a *nzz-like* outer integument. (I, J) *ucn-1 sup-5* analysis. (J) An *ucn-1*-like protrusion is seen on a *sup-5*-like outer integument. (K, L) *ucn-1 sub-1* analysis. (L) Note the presence of *ucn-1*-like protrusions on the *sub-1*-like outer integument. (M, N) *ucn-1 acr4-2* analysis. (M) There is aberrant integument development in *acr4-2* ovules which includes the formation of protrusions. (N) Perhaps slightly more exaggerated integument development in *ucn-1 acr4-2* ovules suggested by an increased number of protrusions. (O, P) *ucn-1 ale2-1* analysis. *ucn-1 ale2-1* and *ucn-1 acr4-2* ovules share a very similar phenotype (compare (P) with (N)). Scale bars: 20 µm.

3.4.1.3 *UCN* is not part of the *ACR4*/*ALE2* epidermal cell-signaling pathway

Arabidopsis integuments are of epidermal origin {Jenik and Irish, 2000; Schneitz et al., 1995} and the results obtained so far indicate that *UCN*-signaling is important for the regulation of growth patterns in floral epidermal tissues. Specification and organized development of epidermal cells in several organs, including ovules, is known to be under the control of a signaling mechanism that includes the action of two receptor-like kinases: ACR4, the Arabidopsis homolog of maize CRINKLY4 (CR4) and ABNORMAL LEAF SHAPE 2 (ALE2) {Becraft et al., 1996; Gifford et al., 2003; Gifford et al., 2005; Tanaka et al., 2002; Watanabe et al., 2004}. To test if UCN contributes to signaling by these two RLKs I generated and analyzed the ovules of *ucn-1 acr4-2* and *ucn-1 ale2-1* double mutants (Fig. 3.4.1, M-P). Ovules of both double mutants showed an additive or possibly slightly enhanced phenotype (abnormal integument cell pattering) indicating that *UCN* and *ACR4*/*ALE2* function in different signaling pathways during ovule development.

3.4.2 *UCN* suppresses neoplastic growth in ovules through post-transcriptional negative regulation of *ATS*

3.4.2.1 The localized neoplastic growth in *ucn-1* integuments depends on functional *ATS*

Defects in plants lacking KANADI transcription factor *ATS* activity are specific to ovules {Léon-Kloosterziel et al., 1994; McAbee et al., 2006}. In *ats* mutants both integuments are initiated but the number of cells between the two integuments is reduced. Eventually, the two integuments fuse, thus giving the appearance of a single integument.

In order to test how *UCN* relates to *ATS, ucn-1 ats-3* double mutants were generated. Very interestingly, ovules of the double mutants showed *ats*-like integuments that did not develop *ucn*-like protrusions (Fig. 3.4.2, Table 3.4.1). This result demonstrates that *ats* is epistatic to *ucn*. The result further strongly suggests that *UCN* and *ATS* act in the same pathway in the regulation of integument growth patterns. Finally, the genetic studies indicate that *UCN* is a negative regulator of *ATS*.

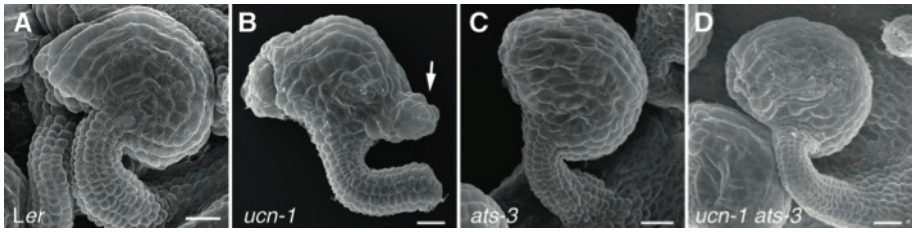

Figure 3.4.2. *ats-3* is acts epistatic to *ucn-1*. (A-E) SEMs of early stage 4 ovules. (A) Wild type. (B) *ucn-1*. (C) *ats-3*. (D) *ucn-1 ats-3*. Note absence of protrusions. Scale bars : 20 µm.

3.4.2.2 Ectopically elevated levels of ATS expression is associated with a *ucn*-like phenocopy in ovules

If *UCN* negatively regulates, ectopic expression of *ATS* may result in an *ucn-1* phenocopy. To test this prediction, I made use of a recently identified activation tagging line - *sk21-D*. The *sk21-D* line was identified in a screen set to isolate mutants with a defect in proanthocyanidin patterns in seed coats. The mutant effect was shown to be due to the ectopic expression of *ATS* {Gao et al., 2010}.

To test if ectopic *ATS* expression affects ovule development prior to seed coat formation I analyzed developing ovules of *sk21-D* homozygous plants. I discovered that indeed 112/245 ovules also carried an *ucn-like* protrusion (Fig. 3.4.3, Table 3.4.1). Each affected ovule carried only a single protrusion rather than multiple ones as sometimes-observed in *ucn-1.* The finding indicates that abnormal negative regulation of *ATS* transcription is associated with neoplastic growth in ovules. The spatial *ATS* expression domain in young ovules of *sk21- D* plants appeared essentially normal in in situ hybridization experiments (Fig. 3.4.3, E-F). Generally, the signal was slightly stronger when compared to wild type. In contrast to the normal spatial *ATS* expression domain, and in accordance with the stronger in situ hybridization signal, qRT-PCR analysis revealed that *sk21-D* flowers of stage 8 to 11 exhibited an approximately 45-fold increase in *ATS* expression levels (Fig. 3.4.3, G).

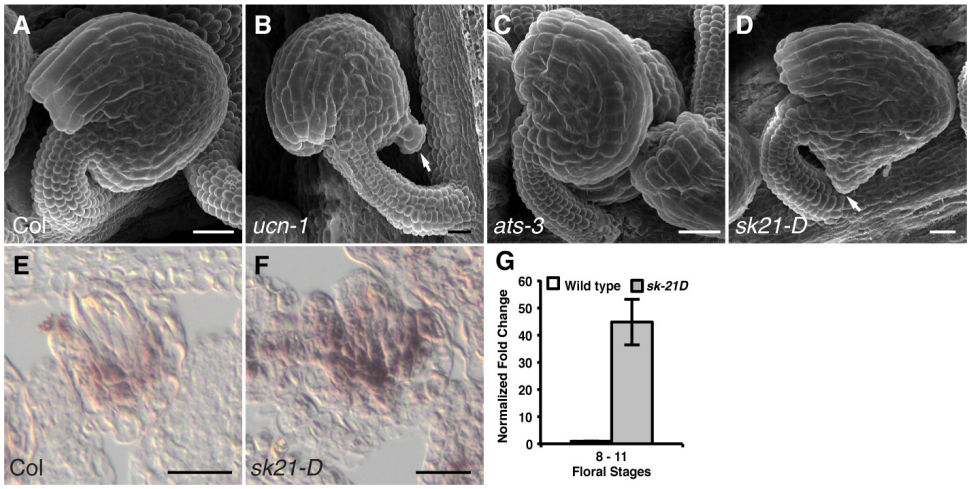

Figure 3.4.3. Analysis of the activation-tagged *ATS* line *sk21-D*. (**A** to **D**) Scanning electron micrographs of early stage 4 ovules. (A) Wild type. (B) *ucn-1*. (C) *ats-3*. (D) *sk21-D*. Note the presence of a *ucn*-like protrusion as in (B) (arrow). (**E** to **F**) Spatial *ATS* expression analyzed by in situ hybridization on sectioned ovules. Stage 2-IV wild-type and *sk21-D* ovules, respectively. *ATS* expression appears normal in *sk21-D*. (**G**) Floral *ATS* mRNA levels in wild type and *sk21-D*. Measured by qRT-PCR. Note the high level of *ATS* expression at floral stages 8 to 11 in *sk21-D*. Scale bars: (A-F) 20 µm. (Molecular characterization of the T-DNA insertion site has been reported by Gao et al., 2010).

Genotype	No. of Ovules analyzed	No. of Ovules with *ucn-1* like protrusions	Percentage of ovules with a protrusion
Wt	600	0	0
ucn-1	600	552	92
sk21-D	245	112	46
ats-3	600	0	0
ucn-1 ats-3	600	74	12

Table 3.4.1. Quantification of *ucn*-like ovule phenotype in *ucn-1*, *sk21-D*, and *ucn-1 ats-3* double mutants

Taken together, the results indicate that strong upregulation of *ATS* mRNA levels, in their normal spatial expression domain, is associated with *ucn-like* neoplastic growth in ovules. These data also emphasize the importance of proper negative regulation of *ATS.* The epistasis of *ats* in a *ucn ats* double mutant (Fig. 3.4.2; Fig.3.4.3) strongly

suggests that *UCN* is a negative regulator of *ATS.*

3.4.2.3 *UCN* may not regulate *ATS* expression in ovules

To test if *UCN* regulates *ATS* transcription, we investigated *ATS* expression in *ucn-1* mutants by in situ hybridization experiment. The results revealed that spatial *ATS* expression was normal in *ucn-1* ovules. Quantitative RT-PCR (qRT-PCR) experiments showed that *ATS* expression levels were increased by only 15-20% in *ucn-1* flowers (Fig. 3.4.4, C). These results suggest that *UCN* may play a minor role *ATS* expression control, if any at all.

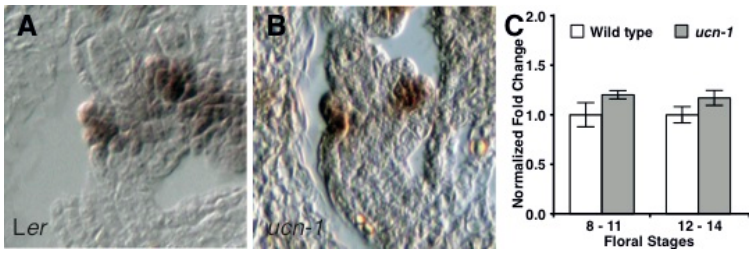

Figure. 3.4.4. ATS expression pattern in *ucn-1* Ovule. Spatial *ATS* expression analyzed by in situ hybridization on sectioned ovules. (I, J) Stage 2-III wild-type and *ucn-1* ovules, respectively. No changes observed. (K, L) Stage 2-V wild-type and *ucn-1* ovules, respectively. *ATS* expression is mainly observed in the inner integument. No changes observed. (M) Floral *ATS* mRNA levels measured by qRT-PCR. No significant changes observed. Scale bars: 20 µm

3.4.2.4 ATS is a phosphorylation target of UCN

How does *UCN* regulate *ATS? ATS* expression was essentially unaltered in *ucn-1* (Fig. 3.4.5) indicating that *UCN* regulates *ATS* post-transcriptionally. To test whether ATS is a phosphorylation substrate of UCN, I performed an in vitro kinase assay by co-incubating recombinant GST-UCN and GST-ATS proteins. Phosphorylation signal corresponding to the ATS protein band on the coomassie gel was observed on the autoradiograph. No phosphorylation was seen when ATS was co-incubated with ucn-1 and UCN_{KD} recombinant proteins. Taken together, the data demonstrate that ATS is a direct phosphorylation target of UCN.

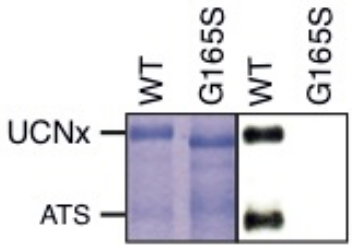

Figure 3.4.5. ATS is a direct phosphorylation target of UCN. In vitro kinase assay using purified GST:UCN and GST:ATS fusion proteins. Left panel: coomassie blue gel. Right panel: corresponding autoradiograph. UCNx denotes different GST:UCN variants indicated on top.

3.4.2.5 UCN and ATS interact in the nucleus by forming heterodimers

To determine whether UCN and ATS interact physically in planta, I employed a BiFC assay. Co-expression of the N-terminal half of YFP fused to UCN (nYFP-UCN) and the C-terminal half of YFP fused to ATS (cYFP-ATS) and vice versa in *Arabidopsis* mesophyll protoplasts resulted in fluorescence in the nuclei. No fluorescence was detected between co-transformed empty vectors pSPYNE/ pSPYNE, and between either nYFP-UCN/ pSPYCE, pSPYN/ cYFP-ATS, confirming the specificity of the interaction. The results from this assay indicate that the two proteins interact in nuclei of plant cells (Fig. 3.4.6). Thus, UCN may directly repress ATS in the nucleus, possibly through differential phosphorylation.

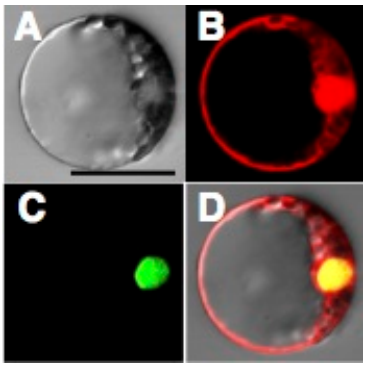

Figure 3.4.6. BiFC assay of UCN/ATS interaction. Different views of a protoplast co-transfected with *pSPYNE:ATS*, *pSPYCE:UCN*, and *pGY-1:mCherry* plasmids. (O) Bright-field view. (P) Signal distribution of free mCherry. Arrow highlights nucleus. (Q) YFP signal distribution indicating UCN/ATS interaction. (R) Merge. Co-transfecting 4 µg or 10 µg of empty pUC-SPYNE/SPYCE plasmids did not result in signal (not shown). Scale bars: 30 µm.

In summary, plants homozygous for recessive mutations in the *UNICORN* (*UCN*) locus show spontaneous, local disorganized growth of differentiated tissue in ovules, stamens, petals, and embryos. Cloning and molecular characterization reveals that *UCN* encodes a functional kinase of the plant-specific AGCVIII class. Biochemical, immunological and cell-biological data indicate that UCN forms a dimer and localizes to the nucleus, cytoplasm and plasma membrane. The genetic, biochemical and cell biological data suggests that UCN suppresses neoplastic growth in ovules by repressing the KANADI transcription factor ATS.

4. Discussion

Tissue morphogenesis depends on the coordination of cellular behavior. Dysfunction of growth control can result in tumorigenesis {Weinberg, 2006}. In animals, lesions in central growth control genes frequently result in tumor formation and cancer. In animals among many growth regulators, AGC kinase family includes several members known to play prominent and diverse roles in these processes {Pearce et al., 2010}.

Plants have evolved robust mechanisms that maintain organized tissue growth {Dodueva et al., 2007; Doonan and Sablowski, 2010}. Although plants do not develop cancer, they are nevertheless able to grow tumors. However, tumorigenesis in plants is mainly associated with pathogenesis and alterations in phytohormone homeostasis. For example, *Agrobacterium tumefaciens* induces crown gall tumors by introducing bacterial genes into the host genome that modify, amongst others, auxin and cytokinin levels {Gelvin, 2003}. Genetic tumors are rare; however, they do occur, particularly in certain interspecies hybrids {Ahuja, 1998}. Classic examples include tumor formation in ovules of Datura {Blakeslee and Satina, 1947} or flowers of tobacco {Kostoff, 1939; Sharp and Gunckel, 1969}. More recently, tumor formation has been described as a result of genetic overdominance caused by incompatible allele combinations {Smith et al., 2011}. However, classic tumor suppressors {Haber and Harlow, 1997} are presently unknown. This raises the question how plants suppress neoplastic growth.

4.1.1 *UCN* suppresses neoplastic growth

In this thesis work, I showed that *UCN* restrains aberrant growth in several plant organs that includes ovule integuments, petals, anther filaments and embryos. Occasionally protrusions on petioles of cotyledons were detected (Fig. 3.1.7, E-F), which superficially resembled leaf petiole outgrowths caused by allelic incompatibilities at the *OAK* locus {Smith et al., 2011}.

Plants homozygous for recessive *ucn* mutations carry spontaneous localized outward-oriented ectopic outgrowths characterized by cells with abnormal cell division planes that hyperproliferate and develop in abnormal size and shapes. Laminar growth results with juxtaposition of adaxial/abaxial domains and through proliferative cell division.

Despite the aberrant cell division plane in *ucn-1* mutants the newly formed cells maintain their identity (thus they are a result of proliferative cell division rather than formative cell division) (Fig. 3.1.2).

The mechanistic outcome of cell division planes in *ucn-1* are different from the maize *tangled-1* mutant that shows abnormally oriented cell divisions, yet develops a normal leaf with regular cell layers, nonetheless with roughened texture {Smith et al., 1996}. Further, the *ucn-1* outgrowths are distinct from the patchy wart-like excrescences in *warty* mutants of maize that were due to excessively enlarged epidermal cells {Hunter et al., 2011; Reynolds et al., 1998} or the epidermal cell swellings observed in plants with a defect in the *NEK6* locus {Motose et al., 2008}. Thus, alteration of normal cell division can therefore affect either local and global morphogenesis or rates of cell division at different levels. The phenotypic outcome of genetic mutations that disrupt cell division will depend on the nature of the lesion, particularly on whether it acts downstream of pattern formation or prevents its implementation.

Disturabances in plant hormone (such as auxin and cytokinin) homeostasis led to tumor development {Gelvin, 2003}. One clue to the mechanistic action of UCN lies in the observation that *ucn*-1 protrusions form spontaneously. For example, neither the aberrant cell division, nor the formation of ectopic outgrowths requires the addition of exogenous plant hormones or growth regulators. This is in contrast to genetic mutation in in *PROPORZ1* (*PRZ1*) which results callus-like tissue formation upon exogenous addition of auxin or cytokinin {Sieberer et al., 2003}. However, disturbances in endogenous auxin and cytokinin levels remain plausible in *ucn-1* mutant. The auxin and cytokinin reporter analysis in *ucn-1* tumors is underway. Given the unique effects on cell proliferation and cell differentiation I propose *UCN* to be a novel plant growth regulator.

4.1.2 *ucn-1* ectopic outgrowths do not represent callus

It is well established that differentiated plant cells will be reprogrammed to form callus upon phytohormone treatment {Salisbury and Ross, 1985}. However, *ucn-1* developed spontaneous tumors. The outer integument gene reporter *INO::GUS* expression in the *ucn-1* outer integument protuberances suggests that the outer integument protrusion

consisted of differentiated cells rather than callus (Fig. 3.1.2). Benign tumors in animals constitute differentiated cells and grow to definite size {Weinberg, 2006}. The *ucn-1* protrusions share interesting similarities with animal benign tumors, as they are spontaneous localized outgrowths containing differentiated cells.

4.1.3 *UCN* does not regulate *WUS* expression in ovules

Misexpression of *WUS* in the chalaza resulted in the formation of a single inner integument and multiple outer integument-like structures that express outer integument marker *INO* {Gross-Hardt et al., 2002; Sieber et al., 2004}. This raises the possibility that *ucn-1* protrusions are a result of *WUS* misexpression. However, no deviation in *WUS* expression could be detected. This finding does not support the *WUS* involvement in *ucn-1*integument outgrowths. Furthermore, ectopic expression of *WUS* always does not result in ectopic outer integument primordia. For example, in the *bel1* mutant *WUS* misexpression in chalaza did not result in multiple integument formation {Brambilla et al., 2007}. However, one cannot exclude the possibility that *UCN* may control *WUS* signaling components that act downstream of WUS, which cooperate with outer integument identity gene. Alternatively, a mere increase in cell division in *ucn-1* ovule is not the morphogenetic trigger of incipient integument primordium initiation but rather of a tumor-like outgrowth. The *ucn-1 ino-2* double mutants further support the notion that *ucn-1* protrusions are not outer integument primordia as the protrusions still develop on inner integument.

4.1.4 *UCN* is a negative regulator of *INO* expression and ectopic *INO* expression is not sufficient for *ucn-1* ovule protrusions

INO is an ovule specific gene and encodes a putative transcription factor belonging to the YABBY family {Schneitz et al., 1997; Villanueva et al., 1999}. *INO* expression is restricted to abaxial layer of the outer integument. In recent years evidence accumulated that proper control of the onset of *INNER NO OUTER* (*INO*) expression is important for the development of the outer integument and interestingly also for proximal-distal (P-D) patterning of the main ovule axis. YABBY initially known to regulate abaxial polarity now recognized to play a broader role in leaf development including leaf blade expansion downstream of KAN {Sarojam et al., 2010}.

INO expression is subject to a positive autoregulatory feedback loop {Meister et al., 2002; Villanueva et al., 1999}. The timing of the initiation of this feedback loop is negatively regulated by the *NOZZLE* (*NZZ*) gene {Balasubramanian and Schneitz, 2000; Balasubramanian and Schneitz, 2002}. NZZ likely performs this task by directly binding to the INO protein, thereby inhibiting the autoregulatory loop {Sieber et al., 2004}. The temporal control of this feedback loop appears to be central to patterning the main P-D axis as well, as precocious expression of *INO* results in major P-D defects, such as the absence of a functional nucellus and hyperplasy of the funiculus. This finding also implies that *INO* can function in a non-cell-autonomous fashion.

A variety of other factors have been identified that regulate *INO* expression. For example, several Zn-finger and so-called BPC proteins were found to bind to an enhancer element of the *INO* promoter in yeast one-hybrid and in vitro binding assays {Meister et al., 2004}. In addition, genetic evidence indicates that *BELL1* (*BEL1*) and *AINTEGUMENTA* (*ANT*) are positive regulators of *INO* expression {Balasubramanian and Schneitz, 2002}. Furthermore, several factors are known to delimit the *INO* expression domain. Mutations in *superman* (*sup*) result in asymmetric growth of the outer integument {Gaiser et al., 1995; Schneitz et al., 1997}. This phenotype is accompanied by ectopic expression of *INO* {Meister et al., 2002; Balasubramanian and Schneitz, 2002}. A *sup* phenocopy and a corresponding ectopic expression of *INO* can also be detected in *ats nzz* double mutants {Balasubramanian and Schneitz 2002; Balasubramanian and Schneitz, 2000}. These results indicate that SUP (a Zn-finger transcription factor {Sakai et al., 1995}), ATS (a KANADI-type transcription factor {McAbee et al., 2006}), and NZZ all restrict the spatial expression domain of *INO* by repressing *INO* in adaxial domains of the ovule.

So far, the genetic factors discussed above appear to regulate early aspects of either the spatial or the temporal expression of *INO*. Interestingly, *INO* expression is transient and disappears from the ovule during later stages of its development {Villanueva et al., 1999; Balasubramanian and Schneitz, 2002; Balasubramanian and Schneitz, 2000}. Nothing is known about this late control of *INO* expression.

Here, we presented the evidence that this repression of *INO* is mediated and maintained by *UCN.* In *ucn-1* ovules, *INO* expression is maintained throughout the ovule development starting from outer integument inception. Furthermore, there is two-fold increase in *INO* transcript levels in *ucn-1* mutants. The result also implies that *UCN* acts as a negative regulator of *INO* expression during pre-fertilization ovule development. It remains to be investigated that how UCN regulates *INO* expression during integument development.

4.1.5 UCN modulates expression of cell cycle genes

Losing control over cell division seems to be an important step in the progression of tumor development and misregulation of cell-cycle events might contribute to neoplasia {Malumbres and Barbacid, 2001}. In *Arabidopsis,* either loss or gain-of-function activities in core cell cycle genes do not result in tumor development {Doerner et al, 1996; Doonan and Sablowski, 2010}. However, recessive mutation in *ucn-1* allele presented in this study showed spontaneous tumor-like outgrowths on *Arabidopsis* ovules and floral organs. UCN may be able to modulate the cell cycle gene expression, as it is evident from the qRT-PCR analaysis (Fig. 3.1.8). A complex misregulation of cell cycle regulators is observed in *ucn-1* petals compared to wild type. Lats1, a tumor suppressor in mice encodes an AGC kinase {St John et al., 1999} that directly binds and negatively regulates Cdk1 {Tao et al, 1999}. These results indicate that UCN could act as a modulator of cell cycle gene expression and that its functional aberration might lead to aberrant proliferation. Understanding the molecular mechanisms that allow cells to enter the cell cycle will provide important clues as to the determinants of normal versus abnormal proliferation in multicellular organisms. However, how exactly *UCN* affects core cell cycle gene expression remains to be investigated.

4.2.1 Positional cloning of *UCN* and complementation analysis

The gene responsible for the *ucn-1* phenotype is mapped by positional cloning strategy. Three distinct lines of evidence indicate that the defect is caused by a mutation in the predicted gene At1g51170. First, comparison of the *ucn-1* allele with the wild-type sequence revealed single base-pair change (G to A) within the coding sequence of At1g51170 locus. Second, homozygous *ucn-1* mutant plants can be fully complemented using two BACs that span the At1g51170 locus and a genomic fragment containing only this predicted gene. Third, multiple mutant alleles isolated within the UCN locus showed similar phenotypes to *ucn-1*.

4.2.2 *UCN* encodes an AGCVIII class protein kinase

UCN is predicted to be a S/T kinase that belongs to AGCVIII class protein kinase {Bögre et al., 2003; Galván-Ampudia and Offringa, 2007}. AGC kinases were named after the mamalian cAMP-dependent protein kinase (PKA), cGMP-dependent protein kinase G (PKG), and phospholipid-dependent protein kinase C (PKC) involved in receptor-mediated growth factor signal transduction. Plant AGCVIII kinases are discriminated by a change of the conserved DFG triplet to DFD in subdomain VII of the catalytic domain and a variably sized insertion (in the range of 36 to 90 amino acids) between subdomains VII and VIII. The sequence similarity of UCN with animal AGC kinases indicates that *UCN* may play an important role in some common pathway as animal AGC kinases, possibly in neoplastic growth regulation {Pearce et al., 2010}. The *ucn-1* mutant phenotype is consistent with the above notion.

4.2.3 Structure-function revelations of *ucn* and *ucnl* mutant alleles

The *ucn-1* caused by a missense mutation in the kinase subdomain VIb, replacing one of the highly conserved glycine by a serine. *ucn-1* plants still produce *UCN* transcripts and it is likely that the ucn-1 protein retains some biological function in vivo. One obvious question is what the *ucn-1* null allele is like. After screening the public T-DNA libraries for the insertion lines in *UCN* locus resulted in five alleles - *ucn-2, ucn-3, ucn-4, ucn-5* and *ucn-6*. None of the homozygous *ucn-3/4/5/6* differed from the wild type plant is explained by the observation that *UCN* transcripts were still detectable in these

mutants indicating that *UCN* function is present in these lines. A potential null allele *ucn-2* was identified as it cause protein truncation and undetectable full-length RNA transcript but 5' half till the insertion site. Surprisingly, *ucn-2*, despite being a potential RNA null allele hasn't showed *ucn-1* phenotype. *ucn- 1* shows a stronger phenotype than full-length RNA null allele *ucn-2.* Since *ucn-1* is not dominant, it might not be interfering with the wild-type allele. Instead, *ucn-1* may act as recessive interfering allele by interfering with functionally redundant *UCN* homolog, *UCNL*. This would explain why the *ucn-1* shows a more severe phenotype than the null allele. If this scenario is true, further reduction of *ucn-1* transcript in *ucn-1* plants may remove the interfering effect of *ucn-1* and ameliorate the *ucn-1* phenotype. There is increasing evidence for such recessive interfering alleles in the *Arabidopsis* literature. For example, *clavata1* null alleles show a weak phenotype whereas many *clv1* missense mutations lead to a strong phenotype {Diévart et al., 2003}. It was reasoned that missense *clv1* alleles interfere with redundantly acting receptors, such as CLV2/CORYNE (CRN) and BAM1/2 {Bleckmann et al., 2010; Deyoung and Clark, 2008; DeYoung et al., 2006; Guo et al., 2010; Müller et al., 2008}. Truncated *ettin* (*ett*) alleles also show stronger phenotype than the full-length *ett* null alleles {Pekker et al., 2005}. Recently, Sijacic et al (Sijacic et al, 2011) showed that *tso* missense allele series function as recessive interfering alleles and show strong phenotype to nonsense *tso* null alleles class.

The EMS induced TILLING alleles *ucn-7/8/9* showed similar phenotype as *ucn-1.* The *ucn-7* mutation may affect a potential phosphorylation site. The serine mutated in the *ucn-7* allele was identified as an autophosphorylation site (unpublished data) indicating that phosphorylation on this residue might modulate the UCN activity. While the effects of *ucn-8* and *ucn-9* are presently unclear, but they may distort the overall conformation of the protein. The *ucn-9* mutant shows the similar phenotype with *ucn-1*, *ucn-8* and *ucn-7* exhibiting consecutively weaker phenotypes. *ucn-7/8/9* allelles may also behave like *ucn-1*.

UCN homologue, *UCNL* is a result of recent segmental genome duplication (http://wolfe.gen.tcd.ie/athal/all_results) and share 73% identity at amino acid level. Absence of phenotype in *UCN* null allele prompted me to analyze the T-DNA insertion lines for *UCNL* locus. Five T-DNA lines *ucnl-1, ucnl-2, ucnl-3/4/5* were scored from

SAIL, the Cold Spring Harbor Lab Gene trap and SALK collections respectively. None of the homozygous lines showed any phenotype. Absence of phenotype in the lines *ucnl-1/2/3/4* is explained by the observation that *UCNL* transcripts were still detectable in these mutants indicating that *UCNL* function is present in these lines. *ucnl-5*, could be a null allele as the full-length RNA transcript is undetectable. The 5' transcript upto the T-DNA insertion site can still be translated and result in a truncated protein that is devoid of kinase activity. However, like *ucn-2*, *ucnl-5* did not display any phenotype suggesting a functional redundancy between the *UCN* and *UCNL*.

4.2.4 *UCN* and *UCNL* function redundantly in the regulation of growth patterns in embryo and floral organ development

The sequence similarity found between *UCN* and *UCNL* genes, the overlapping expression patterns by semi quantitative RT- PCR and absence of phenotypes in full-length RNA nulls indicated that they have overlapping or partially redundant functions. Thus, it is likely that inactivating both genes will be required to see a loss-of-function phenotype. To test directly if *UCN* and *UCNL* can substitute for lack of each other's function, I generated two classes of double mutants: *ucn-2 ucnl-5* and *ucn-1 ucnl-5.*

In the case of *ucn-2 ucnl-5* double mutant fully penetrant embryo lethality was observed that is similar to *ucn-1* embryo phenotype. The data implies that either *ucn-1* is not a complete loss-of-function allele. Alternatively, UCNL might have additional growth regulatory function in embryos. In the latter case, in *ucn-1 ucnl-5* double mutants complete embryo lethality is expected. However, *ucn-1 ucnl-5* still exhibited *ucn-1* phenotype with only 25% embryo lethality and neoplasia on floral organs. The data suggests that *ucn-1* is not a complete loss-of-function allele. However, the data suggest the overlapping functions for *UCN* and *UCNL* in growth control in flowers and embryos. For example, such functional redundancy was shown to operate between the *SLEEPY* and *SNEEZY* genes that are involved in gibberellin signaling {Strader et al, 2004}.

4.2.5 Expression profile of *UCN* and *UCNL*

Semi quantitative RT-PCR based expression analysis of *UCN* and *UCNL* demonstrated a ubiquitous expression and broader functions for both the genes. The overlapping expression patterns of *UCN* and *UCNL* support a redundant function and that is in line with the absence of phenotypes in full-length RNA nulls. Spatial expression pattern detection in flowers by in situ hybridization was unsuccessful due to low expression levels. However, in flowers the *UCN* and *UCNL* transcripts are detectable by qRT-PCR at a stage that matches the time period when *ucn-1* phenotype is apparent. Compared to *UCN* expression levels *UCNL* is expressed at slightly reduced levels. As mentioned in section 4.2.4, *UCNL* is a result of recent gene duplication event. The difference in gene expression levels between UCN and UCNL and functional redundancy is further supported by the fact that expression reduction after gene duplication, a special type of sub-functionalization, facilitates the long-term maintenance of duplicate genes and their functional redundancy {Qian et al, 2010}.

4.3.1 UCN show both auto and substrate phosphorylation activities

Radioactive in vitro kinase assay using recombinant UCN protein showed auto-phosphorylation and substrate phosphorylation of MBP, a general kinase substrate confirming UCN as a functional kinase. Phosphorylation regulates a plethora of cellular proteins, including the function of the protein kinases themselves {Toker and Newton, 2000}. The auto-phosphorylation reactions can be intramolecular or intermolecular. Intermolecular auto-phosphorylation appears to regulate many protein kinases {Cooper and MacAuley, 1988}. In this study, I showed that UCN also undergoes intermolecular auto-phosphorylation as a functional UCN phosphorylated kinase inactive ucn-1 and classical kinase dead version of UCN_{K55A}. This result further implies that ucn-1 can still interact with atleast some partners.

4.3.2 *ucn-1* is an inactive kinase

The recessive nature of the *ucn-1* mutation and the complementation experiments indicate that *ucn-1* is a loss of function mutation. The *ucn-1* mutation results in the substitution of a glycine at position 165 for a serine (G165S). The G165 is strictly

conserved throughout all plant AGC kinases (data not shown) implying an important role for this glycine. Its specific function, however, is not known but the G165S substitution is likely to result in an inactive kinase. Furthermore, comparative homology modeling indicates that G165 is located at a position that may be important for protein-protein interactions (Fig. 3.2.4, C). The presence of an additional serine may also affect the phosphorylation pattern in the mutant protein and therefore interfere with the binding of interaction partners. Alternatively, the G165S mutation may simply result in an improperly folded and thus defective protein. In line with the above predictions, I could not detect in vitro kinase activity for ucn-1 protein using a mutant GST:UCN_{G165S} recombinant protein (Fig. 3.3.2).

4.3.3 UCN forms homodimers and localizes to nucleus, cytoplasm and likely plasmamembrane

UCN sub-cellular distribution predictions using bioinformatics tools suggested chloroplast localization. Previous work analyzing a translational fusion of the N-terminal 93 residues of At1g51170/UCN to red fluorescent protein ($At1g51170_{1-93}$:RFP) in transiently transfected protoplasts suggested a chloroplast localization for UCN{Schliebner et al., 2008}. However, this localization could not be confirmed by in vitro chloroplast import studies (Schliebner and Leister, personal communication). Furthermore, UCN was not included in two recent chloroplast proteome reference tables {Baginsky and Gruissem, 2009; Yu et al., 2008} that were built in part on several recent large-scale phosphoproteomic studies {Lohrig et al., 2009; Reiland et al., 2009; Sugiyama et al., 2008}. In addition, *ucn-1* mutants did not deviate from wild type in a chlorophyll fluorescence assay (Schliebner and Leister, personal communication). Finally, a chloroplast localization of UCN is difficult to reconcile with the *ucn-1* phenotype as for example L1-derived tissue, such as Arabidopsis integuments, filaments, and the epidermal layer of the petal blade {Jenik and Irish, 2000}, are devoid of chloroplasts. I therefore reinvestigated the subcellular localization of UCN.

BiFC assay and immunolocalization studies using anti-UCN antibody revealed a broad localization pattern to UCN. The UCN distribution is mainly seen in the nucleus, cytoplasm and possibly at the plasma membrane. Indeed, UCN carries a bi-partite nuclear localization signal and nuclear export signals. Other members of AGC kinases across the plant species were shown to localize to nucleus. For example, GFP:AGC2-1

reporter of OXI1 kinase, a sister member of the UCN clade showed a developmentally regulated dynamic cellular localization patterns, confining to nucleus and cell periphery {Anthony et al, 2004}. Recently it was shown that Tomato AGC kinase Adi3 Contains an N-terminal Nuclear Export Signal (NES) and a Nuclear Localization Signal in the T-loop extension and that Adi3 nuclear localization is required for its cell death suppression (CDS) activity {Ek- Ramos et al, 2010}. The cluster of basic amino acids that serves as a nuclear localization signal could also be implicated in phospholipid binding at the cell membrane and with in the cell milieu (see section 4.2.10). Presence of both NLS and NES suggests the shuttling of UCN between nucleus and cytoplasm on a developmental context. BiFC results indicate that full-length UCN can form homodimers in a plant cell confirming results from the in vitro kinase assays. Other AGC kinases such as ROCK2 were shown to homodimerize in solution {Couzens et al., 2009}. The broad subcellular distribution of UCN suggests that it may function in different cellular compartments. Thus, it will be interesting in future to dissect the nuclear, cell membrane and cytosolic functions of UCN by expressing a nuclear/membrane targeted or cytoplasmic retention UCN constructs in *ucn-1* mutants and scoring for phenotypic rescue.

4.3.4 UCN binds to phospholipids

Immuno-localization (with **α**-UCN antibody) and BiFC studies suggested plasma membrane localization to UCN in addition to broad cytoplasmic and nuclear distribution (Fig. 3.3.5). However, bioinformatic analysis revealed the absence of transmembrane domain, myristoylation, palmitoylation and GPI-anchor protein modifications in UCN that facilitates cell membrane localization. Recruitment of cytosolic proteins to membranes is governed by a combination of protein- membrane protein and/or protein-lipid interactions {Fischer et al., 2009}. Certain domains - notably some PH, FYVE, PX and C1, C2 domains associate with membranes that contain specific lipids. Several AGC kinases uses a PtdIns (3,4,5) P3 /PtdIns (3,4) P2 - binding PH domain to dock to the plasma membrane {Pearce et al., 2010}. For example, AtPDK1 specifically binds to Phophatidic acid and stimulates OXI1, another member in UCN sister clade {Anthony et al., 2004}. UCN is a member of the AGC kinase family and does not carry a PH domain. Nevertheless, it was shown that additional membrane-targeting signals, such as a cluster of basic amino acids could participate in

electrostatic interactions with acidic phospholipids and thereby associate proteins with the cell membrane {van dev Bogaart et al, 2011}. UCN possesses a stretch of basic amino acids (^{213}RQKKKKTK^{220}) within the insertion loop between the kinase sub domains VII and VIII. The same stretch of basic residues is also predicted to act as nuclear localization signal. Thus, it is possible that UCN membrane association is achieved through the stretch of basic residues in the insertion loop as the UCN binds to artificially made micelles (Fig. 3.3.6). Yet this does not exclude an additional protein–protein interactions mediating UCN membrane localization. PINOID, another member of the plant AGCVIII kinases was previously shown to bind directly to biologically active lipids using protein-lipid overlay experiment {Zegzouti et al, 2006b}. The phospholipid binding activity of UCN and recruitment to the plasma membrane suggest the possibility of UCN activation at plasmamembrane. For many members of AGC kinases localization to cell membrane has been identified as an important step in kinase activation {Peterson and Schreiber, 1999}.

Moreover, many components of lipid signaling have been identified from plants, but little is known about the in vivo mechanisms of lipid signaling and growth control. Typically, AGC kinases are components of lipid-signaling pathways {Pearce et al., 2010}. Thus, in future studies it will be interesting to explore if UCN is connected to lipid signaling.

4.4 *UCN* mediates neoplastic growth suppression

4.4.1 *UCN* acts independently of many known ovule development pathways

The integument mutants that were studied so far affected either integument initiation or growth. However, none of those genes are implied in the direct control of ‘planar’ periclinal cell division (cell division oriented relative to integument surface). In this thesis, I showed for the first time that UCN controls periclinal cell division and localized deregulation of cell proliferation in integument development. To address the molecular basis of *UCN*-mediated neoplastic growth suppression and to understand the position of UCN in the known ovule genetic network, I generated an array of double mutants with varied gene mutants involved in integument genesis and growth.

Defects in AP2 domain transcription factor *ANT* and YABBY transcription factor *INO* function result in arrest of both and outer integument biogenesis respectively Baker et al., 1997; Klucher et al., 1996; Schneitz et al., 1997; Villanueva et al., 1999}. Gain-of-function *ANT* in Arabidopsis transgenic plants increase*s* cell numbers and overall organ size. Surprisingly, the wounded or senesced-surfaces of *35S::ANT* plant organs developed spontaneous neoplasia without the exogenous phytohormone application {Krizek, 1999; Mizukami and Fisher, 2000}. The *ucn-1* mutants develop spontaneous local tumor-like outgrowths. In homozygous *ant-72F5 ucn-1* double mutants, petals and stamen filaments still showed ectopic outgrowths confirming that *ucn-1* neoplastic growths are not due to ectopic expression of *ANT* and that *UCN* and *ANT* act independently. However, the ovules of *ucn-1 ant-72F5* double mutant exhibited *ant* phenotype. Concerning outer integument, in *ucn-1 ino-2*, as the both the mutant phenotypes are evident it seems that they are acting additively. However, the epistasis of *ant* and *ino* in *ucn-1 ant* and *ucn-1 ino* double mutant can be explained by the fact that *ANT and INO* simply act prior to *UCN* in integument development. Thus, taken together *UCN* acts in a different pathway to *ANT* and *INO*.

Chalaza pattern formation and early integument development are orchestrated by transcription factors *BELL1* (*BEL1*), *NOZZLE/SPOROCYTELESS (NZZ/SPL)* and *SUPERMAN* (*SUP*) {Gaiser et al., 1995; Reiser et al., 1995; Robinson-Beers et al., 1992; Sakai et al., 1995; Schiefthaler et al., 1999; Schneitz et al., 1997; Villanueva et al., 1999; Yang et al., 1999}. The double mutants of *ucn-1* with all the above mutants resulted in additive phenotype suggesting that UCN operate differently to *BEL1, NZZ* and *SUP* during ovule development.

Organized development and inter cellular communication and coordination of epidermal cells in several organs, including ovules, involves the three receptor-like kinases ACR4 and ALE2 {Gifford et al., 2003; Tanaka et al., 2007; Watanabe et al., 2004} and SUB {Chevalier et al., 2005; Kwak et al., 2005}, respectively. Our genetic results, however, indicated that *UCN* function in different signaling pathway than *ACR4*/*ALE2 and SUB*.

4.4.2 *UCN* maintains cellular growth patterns in developing integuments through the negative regulation of *ATS*

Juxtaposition of adaxial and abaxial domains is fundamental to achieve laminar tissue architecture in lateral organs. Disturances in this developmental process can either result in development of variable radially symmetrical lateral organs or ectopic outgrowths {Eshed et al., 2001; Kumaran et al, 2002}. Altering the spatial control of *KAN* gene expression {Eshed et al, 2001; Kerstetter et al., 2001; Hawker and Bowman 2004} results in abaxialisation of lateral organs and cessation of lateral growth. For example, *kan1-2 kan2-1* double mutants develop abaxial outgrowths on rosette leaves {Eshed et al., 2001}. These studies imply that *KAN* genes are negative regulators of growth. Interestingly, the results presented in this study suggest *ATS* to be a positive growth regulator.

4.4.2.1 The localized neoplastic growth in *ucn-1* integuments depends on functional *ATS*

ABERRANT TESTA SHAPE (*ATS*), is an ovule specific KANADI transcription factor and expresses in the abaxial cell layer of inner integument. Defects in *ats* mutants are specific to ovules, which show fused integuments. The cell division aberrations in *ucn-1* integuments coincide with the *ATS* expression domain. Interestingly, ovules of *ucn-1 ats-3* double mutants exhibited *ats*- like integuments that were essentially devoid of *ucn-like* protrusions. This result demonstrates that *ats* is epistatic to *ucn.* Moreover, it strongly suggests that *UCN* and *ATS* act in the same genetic pathway and that *UCN* is a negative regulator of *ATS.* In corroboration to the above data, the activation-tagging line *sk21-D* line, in which *ATS* is expressed at higher levels {Gao et al., 2010} but within its normal expression domain shows ectopic outgrowths on integuments. Taken together the data suggests that negative regulation of *ATS* by *UCN* is mandatory in restraining the aberrant growth during ovule integument development.

However, in *ucn-1 ats-3* double mutants 10 % of the ovules still showed *ucn-1* phenotype. This data implies that there could be still other KANADI genes or other unknown growth regulators in *UCN* mediated growth control are operative in *ucn-1 ats-3* double mutants.

4.4.2.2 UCN suppresses neoplastic growth in ovules through post-transcriptional negative regulation of ATS

In contrast to 45-fold more *ATS* expression in *sk21-D* line, in *ucn-1* mutants; however, *ATS* expression is upregulated by about 15 to 20 percent only. This small increase is likely due to the altered morphology of the tissue. One cannot formally exclude that such minor effects are causative, however, it seems most parsimonious to suggest that *UCN* negatively regulates *ATS* at the posttranscriptional level. The presented evidence suggests a direct interaction at protein level. This notion is further substantiated by the finding that UCN can directly interact with ATS in a living plant cell and ATS phodsphorylation by UCN, in vitro. These results indicate that ATS is the main direct downstream target of UCN in integument growth control. The corn AGC kinase BIF2 and the transcription factor BA1 have also been suggested to interact in the nucleus during axillary meristem initiation {Skirpan et al., 2008}. Till date no protein is known to interact directly with KAN family proteins. For the first time, our work identified a upstream negative regulator of KAN that may modulates the KAN protein activity by differential phosphorylation.

The combined genetic, biochemical and cell biological evidence suggests that UCN suppresses tumor formation in ovules through the direct negative regulation of the KANADI transcription factor ATS. *UCN* acts in a context-dependent fashion as tumor development in other floral tissues still occurs in *ucn ats* double mutants. Thus, *UCN* appears to be a general tumor suppressor that interacts with additional, as yet to be identified factors. Furthermore, the results suggest an additional function to *ATS* in the control of cell proliferation and differentiation in addition to its role in tissue polarity.

4.5 Adaxial-abaxial (ad/ab) tissue polarity is maintained in *ucn-1* mutant

Coordinating growth and communication between adjacent cells is a critical yet poorly understood aspect of tissue development and organ morphogenesis. The antagonistic interaction between the ad factors HD-ZIPIII and the ab factors KANADI is central to the establishment of ad/ab polarity, juxtaposition of these two domains during leaf laminar growth {Eshed et al., 2001}. Members of these gene families are also implied in the regulation of integument polarity {Kelley et al., 2009}. Problems in adaxial-

abaxial patterning frequently result in aberrant outgrowths: for example, abaxial outgrowths develop on rosette leaves on *kan1-2 kan2-1* double mutants. Similar ectopic pig-like structures were developed on both adaxial side of the leaf in *piggyback* (*pgy*) *asymmentrical leaves1* double mutants due to compromise in dorso-ventral patterning {Pinon et al., 2008}. In the ovule, *UCN* functions by controlling two important polarity regulators: *ATS* and *INO*. The KANADI transcription factor ATS is implied in the promotion of abaxial cell fate and laminar outgrowth in integuments {Balasubramanian and Schneitz, 2002; Kelley et al., 2009}. In addition, the YABBY gene family is best known for their role in the specification of abaxial identity in lateral organs such as leaves and flowers {Sarojam et al, 2010}. In accordance with this YABBY gene *INO* was found to be expressed in the abaxial (outer) cell layer of the outer integument {Balasubramanian and Schneitz, 2000; Villanueva et al., 1999}. Thus, a natural hypothesis would be to assume that tumor formation in *ucn* integuments relates to altered adaxial-abaxial tissue polarity. Given the complex role of *KANADI* and other polarity genes in integument development {Eshed et al., 2001; McAbee et al., 2006; Kelley et al., 2009} we cannot completely rule out such a model. However, alterations in outer integument polarity are usually accompanied by obvious changes in the spatial expression of *INO* {Balasubramanian and Schneitz, 2002; Meister et al., 2002}. By contrast, spatial *ATS* and *INO* expression is unaltered in *ucn-1* mutants indicating that *UCN* does not noticeably influence tissue polarity of ovules. This feature was evident by the normal laminar growth of the integuments. To achieve proper organogenesis, pattern formation and morphogenesis has to be intimately coupled; however, mutations in the *UCN* affect morphogenesis but not pattern formation suggest that pattern formation and morphogenesis are two independent processes.

4.6 Distinct AGC kinase family members regulate the neoplastic growth suppression across the animal and plant kingdoms

Whole-genome sequencing studies along with functional studies of a good number of the genes strongly points to independent evolution of multi-cellularity in animals and plants from a unicellular common ancestor. The basic mechanisms of pattern formation and of cell-cell communication in development appear to be independently derived in plants and animals {Meyerowitz, 2002}. Nonetheless, in the overall logic of development in the two lineages there are some surprising similarities.

In this thesis, I showed that UCN is a member of the AGC kinase family. Interestingly, the AGC kinase family includes several members known to play prominent and diverse roles in neoplastic growth regulation in animals {Pearce et al., 2010}. For example, the AGC kinase Warts/LATS is a core element of the Hippo signaling pathway involved in tumor suppression {Halder and Johnson, 2011}. Mutations in *warts*/*LATS* result in tissue overproliferation and tumorigenesis in Drosophila and mouse {Justice et al., 1995; St John et al., 1999; Xu et al., 1995}. Although UCN and Warts/LATS belong to distinct AGC kinase subfamilies and different kingdoms, the available evidence suggests surprising similarities in their modes of action. Commonalities include the observations that UCN and Warts/LATS each function by negatively regulating a main downstream target. This target is a transcription factor whose activity is modulated by physical interaction with the kinase. Results from this study imply that UCN suppresses tumor formation in integuments through the negative posttranscriptional regulation of the transcription factor gene *ATS*, likely through direct modification of ATS in the nucleus. By contrast, Warts and LATS are localized in the cytoplasm and restrict the transcriptional activity of the targets Yorkie and Yap, respectively, through mediating their cytoplasmic retention {Halder and Johnson, 2011}. (Fig. 4.1)

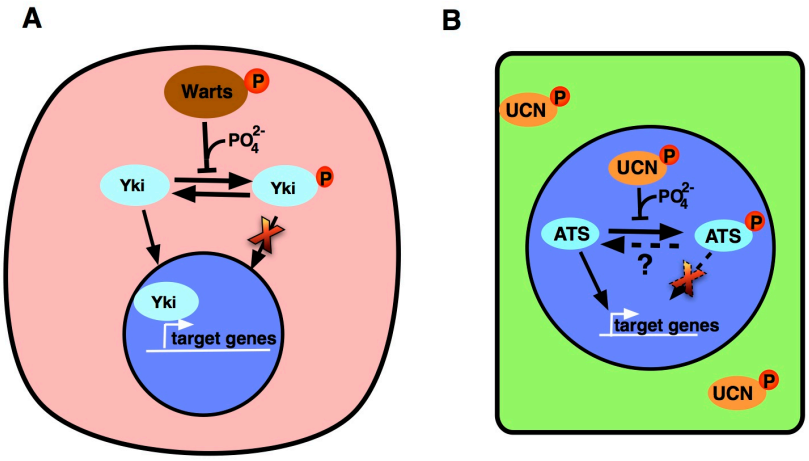

Figure 4.1. Comparative model of Warts and UCN mediated tumor suppression. (A). Drosophila AGC kinase Warts negatively regulating the transcription factor Yki, in the cytoplasm. (B) Arabidopsis AGC kinase UCN negatively regulating transcription factor ATS in the nucleus.

Thus, it will be interesting to explore further the *UCN* mechanism to get novel insight into neoplastic growth suppression in plants and to compare it to the mode of action of animal tumor suppressors, such as Warts and LATS.

5. Conclusion

Tissue morphogenesis relies on the coordination of cellular behavior within a tissue. In animals and humans, it is well described that hereditary gene defects in many components of the underlying signaling processes can spontaneously cause tumorigenesis and cancer. Genes encoding AGC-class kinases play important roles in growth control and include tumor suppressors, such as Warts/LATS, or oncogenes, such as AKT/PKB.

In comparison to animals, plants seem to have evolved very robust mechanisms to maintain tissue architecture of differentiating organs. Most of known plant tumor biology relates to various forms of pathogen-induced tumorigenesis, for example through bacterial, fungal, or viral infections. However, few genetic tumors have been described in plants, mainly in classic literature dealing with inter-species hybrids and poorly understood genetics.

So far, there are no reports known to describing and molecularly studying recessive mutations that lead to real tumor-like outgrowths on plant tissue. Ectopic expression of many core cell cycle regulators failed to result in tumor formation. Even in loss-of-function mutations of RETINOBLASTOMA-RELATED (RBR), an ortholog of human Rb protein, a hallmark tumor suppressor in animals, no tumors are formed. Thus, what plant mechanisms prevent localized disorganization of growth that frequently occurs in animal tumors? Clear evidence for monogenic, bona-fide tumor suppressors in plants is presently lacking from the literature.

In this thesis I present the molecular characterization of the Arabidopsis *UNICORN* (*UCN*) locus. *UCN* functions as a tumor suppressor as plants homozygous for recessive mutations in the *UNICORN* (*UCN*) locus show spontaneous, local disorganized growth of differentiated tissue (ectopic cell proliferation, neoplastic growth analogous to benign tumors in animals) in ovules, stamens, petals, and embryos. The defect is initiated by the aberrant orientation of cell divisions. Neoplastic outgrowths can grow to considerable size relative to the dimension of the affected organ. Eventually, loss of *UCN* activity results in altered expression levels of core cell cycle genes.

Cloning and molecular characterization reveals that *UCN* encodes a functional kinase of the plant specific AGCVIII class. Biochemical, immunological, and cell-biological data indicate that UCN forms a dimer and localizes to the nucleus.

UCN suppresses neoplastic growth in ovules by repressing the KANADI transcription factor ATS, normally involved in adaxial-abaxial polarity in ovule development. This result is based on the genetic observations that *ats* is epistatic to *ucn* and that ectopic expression of *ATS* results in a *ucn*-like phenotype. In addition, the biochemical and cell-biological data demonstrate that UCN can phosphorylate ATS in vitro and that UCN and ATS form a dimer in a living plant cell.

Plant UCN and the well-described animal AGC kinases and tumor suppressors Warts/LATS belong to the same kinase family. They share some similarity in their mode of action i.e., regulation of transcription factor through a direct negative regulation.

6. References

Ahuja MR. (1998). Genetic tumors in *Nicotiana* and other plants. *Q Rev Biol.* **73**, 439-462.

Alonso JM., Stepanova AN., Leisse TJ., Kim CJ., Chen H., Shinn P., Stevenson D.K., Zimmerman J., Barajas P., Cheuk R. et al., (2003). Genome-wide insertional mutagenesis of *Arabidopsis thaliana*. *Science*. **301**, 653-657.

Altschul SF., Gish W., Miller W., Myers EW., and Lipman, DJ. (1990). Basic local alignment search tool. *J. Mol. Biol*. **215**, 403-410.

Anand VK., Bauer C., and Heberlein GT. (1975). Effect of gibberellic acid on crown gall tumor induction in aging primary pinto leaves. *Plant Physiol*. **55**, 1016-1017.

Anthony RG., Henriques R., Helfer A., Mészáros T., Rios G., Testerink C., Munnik T., Deák M., Koncz C., and Bögre L. (2004). A protein kinase target of a PDK1 signalling pathway is involved in root hair growth in Arabidopsis. *EMBO J*. **23**, 572-581.

Armstrong WP. (1995). To be or not to be a gall. *Pacific Horti.* **56**, 39-45.

Arnold K., Bordoli L., Kopp J., and Schwede T. (2006). The SWISS-MODEL workspace: a web-based environment for protein structure homology modeling. *Bioinformatics*. **22**, 195-201.

Ascencio-Ibáñez JT., Sozzani R., Lee TJ., Chu TM., Wolfinger RD., Cella R., and Hanley-Bowdoin L. (2008). Global analysis of Arabidopsis gene expression uncovers a complex array of changes impacting pathogen response and cell cycle during geminivirus infection. *Plant Physiol*. **148**, 436-454.

Baker SC., Robinson-Beers K., Villanueva JM., Gaiser JC., and Gasser CS. (1997). Interactions among genes regulating ovule development in *Arabidopsis thaliana. Genetics*. **145**, 1109-1124.

Baginsky S., and Gruissem W. (2009). The chloroplast kinase network: new insights from large-scale phosphoproteome profiling. *Mol Plant*. **2**, 1141-1153.

Balasubramanian S., and Schneitz K. (2000). *NOZZLE* regulates proximal-distal pattern formation, cell proliferation and early sporogenesis during ovule development in *Arabidopsis thaliana. Development*. **127**, 4227-4238.

Balasubramanian S., and Schneitz K. (2002). *NOZZLE* links proximal-distal and adaxial-abaxial pattern formation during ovule development in *Arabidopsis thaliana. Development*. **129**, 4291-4300.

Bao Y., Hata Y., Ikeda M., and Withanage K. (2011). Mammalian Hippo pathway: from development to cancer and beyond. *J Biochem*. **149**, 361-379.

Baud S., Bellec Y., Miquel M., Bellini C., Caboche M., Lepiniec L., Faure JD., and Rochat C. (2004). *gurke* and *pasticcino3* mutants affected in embryo development are impaired in acetyl-CoA carboxylase. *EMBO Rep*. **5**, 515-520.

Becraft PW., Stinard PS., and McCarty DR. (1996). CRINKLY4: A TNFR-like receptor kinase involved in maize epidermal differentiation. *Science*. **273**, 1406-1409.

Beemster GT., Fiorani F., and Inze, D. (2003). Cell cycle: the key to plant growth control? *Trends Plant Sci.* **8**, 154-158.

Benjamins R., Quint A., Weijers D., Hooykaas P., and Offringa R. (2001). The PINOID protein kinase regulates organ development in Arabidopsis by enhancing polar auxin transport. *Development*. **128**, 4057-4067.

Benkert P., Künzli M., and Schwede T. (2009). QMEAN server for protein model quality estimation. *Nucleic Acids Res*. **37**, W510-4.

Berger, A.H., Knudson, A.G., and Pandolfi, P.P. (2011). A continuum model for tumour suppression. *Nature*. **476**, 163-169.

Bird MD., and Koltai H. (2000). Plant parasitic nematodes: habitats, hormones and horizontally-acquired genes. *J. Plant Growth Regul.* **19**, 183-194.

Blakeslee AF., and Satina S. (1947). Ovular tumors associated with hybrid embryos in Datura. *Science.* **105**, 633.

Bleckmann A., Weidtkamp-Peters S., Seidel CA., and Simon R. (2010). Stem cell signaling in Arabidopsis requires CRN to localize CLV2 to the plasma membrane. *Plant Physiol*. **152**, 166-76.

Bögre L., Ökrész L., Henriques R., and Anthony RG. (2003). Growth signalling pathways in Arabidopsis and the AGC protein kinases. *Trends Plant Sci.* **8**, 424-431.

Box MS., Coustham V., Dean C., and Mylne JS. (2011). Protocol: A simple phenol-based method for 96-well extraction of high quality RNA from Arabidopsis. *Plant Methods.* **7**, 7.

Brambilla V., Battaglia R., Colombo M., Masiero S., Bencivenga S., Kater MM., and Colombo L. (2007). Genetic and molecular interactions between *BELL1* and MADS box factors support ovule development in Arabidopsis. *Plant Cell*. **19**, 2544-2556.

Brefort T., Doehlemann G., Mendoza-Mendoza A., Reissmann S., Djamei A., and Kahmann R. (2009). Ustilago maydis as a Pathogen. *Annu Rev Phytopathol*. **47**, 423-445.

Camehl I., Drzewiecki C., Vadassery J., Shahollari B., Sherameti I., Forzani C., Munnik T., Hirt H., and Oelmüller R. (2011). The OXI1 kinase pathway mediates Piriformospora indica-induced growth promotion in Arabidopsis. *PLoS Pathog*. **7**, e1002051.

Carpten JD., Faber AL., Horn C., Donoho GP., Briggs SL., Robbins CM., Hostetter G., Boguslawski S., et al., (2007). A transforming mutation in the pleckstrin homology domain of AKT1 in cancer. *Nature*. **448**, 439-444.

Chevalier D., Batoux M., Fulton L., Pfister K., Yadav RK., Schellenberg M., and Schneitz, K. (2005). *STRUBBELIG* defines a receptor kinase-mediated signaling pathway regulating organ development in *Arabidopsis*. *Proc. Natl. Acad. Sci. U S A*. **102**, 9074-9079.

Christie JM., Reymond P., Powell GK., Bernasconi P., Raibekas AA., Liscum E., and Briggs WR. (1998). Arabidopsis NPH1: a flavoprotein with the properties of a photoreceptor for phototropism. *Science*. **282**, 1698-1701.

Chung SK., and Parrish RW. (1995). Studies on the promoter of the *Arabidopsis thaliana cdc2a* gene. *FEBS Letters.* **362**, 215-219.

Clark SE., Running MP., and Meyerowitz EM. (1993). *Clavata1*, a regulator of meristem and flower development in *Arabidopsis*. *Development.* **119,** 397-418.

Clark RM., Schweikert G., Toomajian C., Ossowski S., Zeller G., Shinn P., Warthmann N., Hu TT., Fu G., Hinds DA., Chen H., Frazer KA., Huson DH., Schölkopf B., Nordborg M., Rätsch G., Ecker JR., and Weigel D. (2007). Common sequence polymorphisms shaping genetic diversity in *Arabidopsis thaliana*. *Science*. **317**, 338-342.

Clough SJ., and Bent AF. (1998). Floral dip: a simplified method for *Agrobacterium*-mediated transformation of *Arabidopsis thaliana*. *Plant J.* **16,** 735-743.

Colombo L., Battaglia R., and Kater MM. (2008). Arabidopsis ovule development and its evolutionary conservation. *Trends Plant Sci*. **13**, 444-450.

Cooper JA., and MacAuley A. (1988). Potential positive and negative autoregulation of p60c-src by intermolecular autophosphorylation. *Proc Natl Acad Sci U S A*. **85**, 4232-4236.

Couzens AL., Saridakis V., and Scheid MP. (2009). The hydrophobic motif of ROCK2 requires association with the N-terminal extension for kinase activity. *Biochem J.* **419,** 141-148.

Cutler SR., Ehrhardt DW., Griffitts JS., and Somerville CR. (2000). Random GFP::cDNA fusions enable visualization of subcellular structures in cells of Arabidopsis at a high frequency. *Proc Natl Acad Sci U S A.* **97**, 3718-3723.

Czechowski T., Stitt M., Altmann T., Udvardi MK., and Scheible WR. (2005). Genome-wide identification and testing of superior reference genes for transcript normalization in Arabidopsis. *Plant Physiol.* **139,** 5-17.

De Meutter J., Tytgat T., Witters E., Gheysen G., Van Onckelen H., and Gheysen G. (2003). Identification of cytokinins produced by the plant parasitic nematodes *Heterodera schachtii* and *Meloidogyne incognita*. *Mol Plant Pathol*. **4**, 271-277.

Devos S., Vissenberg K., Verbelen J., and Prinsen E. (2005). Infection of Chinese cabbage by *Plasmodiophora brassica* leads to a stimulation of plant growth: impact on cell wall metabolism and hormone balance. *New Phytologist.* **166**, 241-250.

Desvoyes B., Ramirez-Parra E., Xie Q., Chua N. H., and Gutierrez C. (2006). Cell type-specific role of the retinoblastoma/E2F pathway during Arabidopsis leaf development. *Plant Physiol.* **140**, 67–80.

Diévart A., Dalal M., Tax FE., Lacey AD., Huttly A., Li J., and Clark SE. (2003). *CLAVATA1* dominant-negative alleles reveal functional overlap between multiple receptor kinases that regulate meristem and organ development. *Plant Cell*. **15**, 1198-1211.

DeYoung BJ., Bickle KL., Schrage KJ., Muskett P., Patel K., and Clark SE. (2006). The CLAVATA1-related BAM1, BAM2 and BAM3 receptor kinase-like proteins are required for meristem function in Arabidopsis. *Plant J*. **45**, 1-16.

Deyoung BJ., and Clark SE. (2008). BAM receptors regulate stem cell specification and organ development through complex interactions with CLAVATA signaling. *Genetics*. **180**, 895-904.

Dodueva IE., Frolova NV., and Lutova LA. (2007). Plant tumorigenesis: different ways for shifting systemic control of plant cell division and differentiation. *Transgen Plant J*. **1,** 17-38.

Doehlemann G., Wahl R., Horst RJ., Voll LM., Usadel B., Poree F., Stitt M., Pons-Kühnemann J., Sonnewald U., Kahmann R., and Kämper J. (2008). Reprogramming a maize plant: transcriptional and metabolic changes induced by the fungal biotroph Ustilago maydis. *Plant J.* **56**, 181-195.

Doonan JH., and Sablowski R. (2010). Walls around tumours — why plants do not develop cancer. *Nat Rev Cancer*.**10**, 794-802.

Ebel C., Mariconti L., and Gruissem W. (2004). Plant retinoblastoma homologues control nuclear proliferation in the female gametophyte. *Nature*. **429**, 776-780.

Ek-Ramos MJ., Avila J., Cheng C., Martin GB., and Devarenne TP. (2010). The T-loop extension of the tomato protein kinase AvrPto-dependent Pto-interacting protein 3 (Adi3) directs nuclear localization for suppression of plant cell death. *J Biol Chem.* **285**, 17584-17594.

Emery JF., Floyd SK., Alvarez J., Eshed Y., Hawker NP., Izhaki A., Baum SF., and Bowman JL. (2003). Radial patterning of Arabidopsis shoots by class III HD-ZIP and KANADI genes. *Curr Biol.* **13**, 1768-1774.

Eshed Y., Baum SF., Perea JV., and Bowman J. (2001). Establishment of polarity in lateral organs of plants. *Curr Biol.* **11,** 1251-1260.

Eshed Y., Izhaki A., Baum SF., Floyd SK., and Bowman JL. (2004). Asymmetric leaf development and blade expansion in Arabidopsis are mediated by KANADI and YABBY activities. *Development*. **131**, 2997-3006.

Faure JD., Vittorioso P., Santoni V., Fraisier V., Prinsen E., Barlier I., Van Onckelen H., Caboche M., and Bellini C. (1998). The *PASTICCINO* genes of *Arabidopsis*

thaliana are involved in the control of cell division and differentiation. *Development.* **125**, 909-918.

Fernando WGD., Zhang JX., Chen CQ., Remphrey WR., Schurko A., and Klassen GR. (2005). Molecular and morphological characteristics of *Apiosporina morbosa,* the causal agent of black knot in *Prunus* spp. *Can J of Plant Pathol.* **27**, 364-375.

Fernández-Chacón R., Königstorfer A., Gerber SH., García J., Matos MF., Stevens CF., Brose N., Rizo J., Rosenmund C., and Südhof TC. (2001). Synaptotagmin I functions as a calcium regulator of release probability. *Nature*. **410**, 41-49.

Finn R.D., Tate J., Mistry J., Coggill P.C., Sammut S.J., Hotz H.R., Ceric G., Forslund K., Eddy S.R., Sonnhammer, EL. et al., (2008). The Pfam protein families database. *Nucleic Acids Res*. **36**, D281-8.

Fischer MA., Temmerman K., Ercan E., Nickel W., and Seedorf, M. (2009). Binding of plasma membrane lipids recruits the yeast integral membrane protein lst2 to the cortical ER. *Traffic*. **10**, 1084-1097.

Forzani C., Carreri A., de la Fuente van Bentem S., Lecourieux D., Lecourieux F., and Hirt H. (2011). The Arabidopsis protein kinase Pto-interacting 1-4 is a common target of the oxidative signal-inducible 1 and mitogen-activated protein kinases. *FEBS J.* **278**, 1126-1136.

Frank M., Guiv'Arch A., Krupkova E., Lorenz-Meyer I., Chriqui D., and Schmulling T. (2002). *TUMOROUS SHOOT DEVELOPMENT (TSD)* genes are required for coordinated plant shoot development. *Plant J.* **29**, 73- 85.

Freeling M., and Hake S. (1985). Developmental genetics of mutants that specify knotted leaves in maize. *Genetics*. **111**, 617-634.

Friml J., Yang X., Michniewicz M., Weijers D., Quint A., Tietz O., Benjamins R., Ouwerkerk PB., Ljung K., Sandberg G., Hooykaas PJ., Palme K., and Offringa R.

(2004). A PINOID-dependent binary switch in apical-basal PIN polar targeting directs auxin efflux. *Science*. **306**, 862-865.

Galván-Ampudia CS., and Offringa R. (2007). Plant evolution: AGC kinases tell the auxin tale. *Trends Plant Sci.* **12,** 541-547.

Gaiser JC., Robinson-Beers K., and Gasser C.S. (1995). The Arabidopsis *SUPERMAN* gene mediates asymmetric growth of the outer integument of ovules. *Plant Cell*. **7**, 333-345.

Gao P., Li X., Cui D., Wu L., Parkin I., and Gruber MY. (2010). A new dominant *Arabidopsis transparent testa* mutant, *sk21-D*, and modulation of seed flavonoid biosynthesis by KAN4. *Plant Biotechnol J.* **8,** 979-993.

Gelvin SB. (2003). Agrobacterium-mediated plant transformation: the biology behind the "gene-jockeying" tool. *Microbiol Mol Biol Rev.* **67,** 16-37.

Gifford ML., Dean S., and Ingram GC. (2003). The *Arabidopsis ACR4* gene plays a role in cell layer organisation during ovule integument and sepal margin development. *Development*. **130**, 4249-4258.

Gifford ML., Robertson FC., Soares DC., and Ingram GC. (2005). ARABIDOPSIS CRINKLY4 function, internalization, and turnover are dependent on the extracellular crinkly repeat domain. *Plant Cell*. **17**, 1154-1166.

Glickmann E., Gardan L., Jacquet S., Hussain S., Elasri M., Petit A., and Dessaux Y. (1998). Auxin production is a common feature of most pathovars of *Pseudomonas syringae. Mol Plant Microbe In.* **11**, 156-162.

Goldshmidt A., Alvarez JP., Bowman JL., and Eshed Y. (2008). Signals derived from YABBY gene activities in organ primordia regulate growth and partitioning of Arabidopsis shoot apical meristems. *Plant Cell*. **20**, 1217-1230.

Gross-Hardt R., Lenhard M., and Laux T. (2002). *WUSCHEL* signaling functions in interregional communication during Arabidopsis ovule development. *Genes Dev*. **16**, 1129-1138.

Guo Y., and Clark SE. (2010). Membrane distributions of two ligand-binding receptor complexes in the CLAVATA pathway. *Plant Signal Behav*. **5**, 1442-1445.

Haber D., and Harlow E. (1997). Tumour-suppressor genes: evolving definitions in the genomic age. *Nat Genet.* **16**, 320-322.

Haberer G., Erschadi S., and Torres-Ruiz RA. (2002). The Arabidopsis gene *PEPINO/PASTICCINO2* is required for proliferation control of meristematic and non-meristematic cells and encodes a putative anti-phosphatase. *Dev Genes Evol*. **212**, 542-550.

Halder G., and Johnson RL. (2011). Hippo signaling: growth control and beyond. *Development.* **138,** 9-22.

Hamilton CM. (1997). A binary-BAC system for plant transformation with high-molecular-weight DNA. *Gene*. **200**, 107-116.

Hanks SK., Quinn AM., and Hunter T. (1988). The protein kinase family: conserved features and deduced phylogeny of the catalytic domains. *Science*. **241**, 42-52.

Hanks SK., and Quinn AM. (1991). Protein kinase catalytic domain sequence database: identification of conserved features of primary structure and classification of family members. *Methods Enzymol*. **200**, 38-62.

Hanley-Bowdoin L., Settlage SB., and Robertson D. (2004). Reprogramming plant gene expression: a prerequisite to geminivirus DNA replication. *Mol Plant Pathol.* **5**, 149-156.

Harashima H., and Schnittger A. (2010). The integration of cell division, growth, and differentiation. *Curr. Opin. Plant Biol.* **13,** 66–74.

Harrar Y., Bellec Y., Bellini C., and Faure J. (2003). Hormonal control of cell proliferation requires *PASTICCINO* genes. *Plant Physiology* **132,** 1217-1227.

Hawker NP., and Bowman JL. (2004). Roles for Class III HD-Zip and KANADI genes in Arabidopsis root development. *Plant Physiol*. **135***,* 2261-2270.

Hill TA., Broadhvest J., Kuzoff RK., and Gasser CS. (2006). *Arabidopsis SHORT-INTEGUMENTS 2* is a mitochondrial DAR GTPase. *Genetics*. **174**, 707-718.

Hoefle C., Huesmann C., Schultheiss H., Bornke F., Hensel G., Kumlehn J., and Hückelhoven R. (2011). A barley ROP GTPase ACTIVATING PROTEIN associates with microtubules and regulates entry of the barley powdery mildew fungus into leaf epidermal cells. *Plant Cell.* **23,** 2422-2439.

Hunter CT., Hill Kirienko DR., Sylvester AW., Peter GF., McCarty DR., and Koch KE. (2011). Cellulose Synthase-Like D1 is integral to normal cell division, expansion, and leaf development in maize. *Plant Physiol*. doi: http:/ / dx. doi. org/ 10. 1104/ pp. 111. 188466.

Izhaki A., and Bowman JL. (2007). KANADI and class III HD-Zip gene families regulate embryo patterning and modulate auxin flow during embryogenesis in Arabidopsis. *Plant Cell.* **19**, 495-508.

Jenik PD., and Irish VF. (2000). Regulation of cell proliferation patterns by homeotic genes during Arabidopsis floral development. *Development*. **127**, 1267-1276.

Justice RW., Zilian O., Woods DF., Noll M., and Bryant PJ. (1995). The *Drosophila* tumor suppressor gene *warts* encodes a homolog of human myotonic dystrophy kinase and is required for the control of cell shape and proliferation. *Genes Dev* **9,** 534-546.

Kamps MP., Taylor SS., and Sefton BM. (1984). Direct evidence that oncogenic tyrosine kinases and cyclic AMP-dependent protein kinase have homologous ATP-binding sites. *Nature*. **310**, 589-592.

Kelley DR., Skinner DJ., and Gasser CS. (2009). Roles of polarity determinants in ovule development. *Plant J*. **57**, 1054-1064.

Kerstetter RA., Bollman K., Taylor RA., Bomblies K., and Poethig RS. (2001). *KANADI* regulates organ polarity in *Arabidopsis*. *Nature.* **411,** 706-709.

Klucher KM., Chow H., Reiser L., and Fischer RL. (1996). The *AINTEGUMENTA* gene of Arabidopsis required for ovule and female gametophyte development is related to the floral homeotic gene *APETALA2*. *Plant Cell*. **8**, 137-153.

Knighton DR., Cadena DL., Zheng J., Ten Eyck LF., Taylor SS., Sowadski JM., and Gill GN. (1993). Structural features that specify tyrosine kinase activity deduced from homology modeling of the epidermal growth factor receptor. *Proc Natl Acad Sci U S A*. **90**, 5001-5005.

Koncz C., and Schell, J. (1986). The promoter of TL-DNA gene 5 controls the tissue-specific expression of chimaeric genes carried by a nove1 type of Agrobacterium binary vector. *MoI. Gen. Genet.* **204**,383-396.

Kostoff D. (1939). Abnormal mitosis in tobacco plants forming hereditary tumor. *Nature.* **144**, 599.

Krizek BA. (1999). Ectopic expression of *AINTEGUMENTA* in Arabidopsis plants results in increased growth of floral organs. *Dev Genet*. **25**, 224-236.

Krupková E., Immerzeel P., Pauly M., and Schmülling T. (2007). The *TUMOROUS SHOOT DEVELOPMENT2* gene of Arabidopsis encoding a putative methyltransferase is required for cell adhesion and coordinated plant development. *Plant J.* **50**, 735-750.

Krupková E., and Schmülling T. (2009). Developmental consequences of the tumorous shoot development1 mutation, a novel allele of the cellulose-synthesizing *KORRIGAN1* gene. *Plant Mol Biol*. **71**, 641-655.

Kudo H., Uyeda I., and Shikata E. (1991). Viruses in the phytoreovirus genus of the *Reoviridae* family have the same conserved terminal sequences. *J Gen Virol.* **72**, 2857-2866.

Kumaran MK., Bowman JL., and Sundaresan V. (2002). *YABBY* polarity genes mediate the repression of *KNOX* homeobox genes in *Arabidopsis. Plant Cell* **14**, 2761-2770.

Kwak SH., Shen R., and Schiefelbein J. (2005). Positional signaling mediated by a receptor-like kinase in Arabidopsis. *Science*. **307**, 1111-1113.

Larkin MA., Blackshields G., Brown NP., Chenna R., McGettigan PA., McWilliam H., Valentin F., Wallace IM., Wilm A., Lopez R., Thompson JD., Gibson TJ., and Higgins DG. (2007). Clustal W and Clustal X version 2.0. *Bioinformatics*. **23**, 2947-2948.

Lee JH., Kim D-M., Lim YP., and Pai H-S. (2004). The shooty callus induced by suppression of tobacco *CHRK1* receptor-like kinase is a phenocopy of the tobacco genetic tumor. *Plant Cell Rep.* **23**, 397-403.

Léon-Kloosterziel KM., Keijzer CJ., and Koornneef M. (1994). A seed shape mutant of *Arabidopsis* that is affected in integument development. *Plant Cell.* **6,** 385-392.

Lohrig K., Müller B., Davydova J., Leister D., and Wolters DA. (2009). Phosphorylation site mapping of soluble proteins: bioinformatical filtering reveals potential plastidic phosphoproteins in Arabidopsis thaliana. *Planta*. **229**, 1123-1134.

Malumbres M., AND Barbacid M. (2001). To cycle or not to cycle: a critical decision in cancer. *Nat Rev Cancer.* **1**, 222-231.

Martienssen, RA. (1998). Functional genomics: probing plant gene function and expression with transposons. *Proc Natl Acad Sci U S A*. **95**, 2021-2026.

Martin FW. (1966). Frosty spot. A developmental disturbance of the tomato leaf. Ann. Bot. (London) (N.S.) **30**, 701-709.

McAbee JM., Hill TA., Skinner DJ., Izhaki A., Hauser BA., Meister RJ., Venugopala Reddy G., Meyerowitz EM., Bowman JL., and Gasser CS. (2006). *ABERRANT TESTA SHAPE* encodes a KANADI family member, linking polarity determination to separation and growth of Arabidopsis ovule integuments. *Plant J.* **46:** 522-531.

McCallum CM., Comai L., Greene EA., and Henikoff S. (2000). Targeting induced local lesions IN genomes (TILLING) for plant functional genomics. *Plant Physiol*. **123**, 439-42.

Meister RJ., Kotow LM., and Gasser CS. (2002). *SUPERMAN* attenuates positive *INNER NO OUTER* autoregulation to maintain polar development of Arabidopsis ovule outer integuments. *Development*. **129**, 4281-4289.

Meister RJ., Williams LA., Monfared MM., Gallagher TL., Kraft EA., Nelson CG., and Gasser CS. (2004). Definition and interactions of a positive regulatory element of the Arabidopsis *INNER NO OUTER* promoter. *Plant J*. **37**, 426-438.

Melo F., and Feytmans E. (1998). Assessing protein structures with a non-local atomic interaction energy. *J Mol Biol*. **277**, 1141-1152.

Menges M., de Jager S.M., Gruissem W., and Murray J.A. (2005). Global analysis of the core cell cycle regulators of Arabidopsis identifies novel genes, reveals multiple and highly specific profiles of expression and provides a coherent model for plant cell cycle control. *Plant J*. **41**, 546-566.

Meyerowitz EM. (2002). Plants compared to animals: the broadest comparative study of development. *Science*. **295**, 1482-1485.

Michniewicz M., Zago MK., Abas L., Weijers D., Schweighofer A., Meskiene I., Heisler MG., Ohno C., Zhang J., Huang F., Schwab R., Weigel D., Meyerowitz EM., Luschnig C., Offringa R., and Friml J. (2007). Antagonistic regulation of PIN

phosphorylation by PP2A and PINOID directs auxin flux. *Cell*. **130**, 1044-1056.

Mizukami Y., and Fischer RL. (2000). Plant organ size control: *AINTEGUMENTA* regulates growth and cell numbers during organogenesis. *Proc Natl Acad Sci U S A*. **97**, 942-947.

Mora A., Komander D., van Aalten DM., and Alessi DR. (2004). PDK1, the master regulator of AGC kinase signal transduction. *Semin Cell Dev Biol*. **15**, 161-170.

Morris R. (1986). Genetic specifying auxin and cytokinin biosynthesis in phyto-pathogens. *Annu Rev Plant Physiol.* **37**, 509-538.

Motose H., Tominaga R., Wada T., Sugiyama M., and Watanabe Y. (2008). A NIMA-related protein kinase suppresses ectopic outgrowth of epidermal cells through its kinase activity and the association with microtubules. *Plant J*. **54**, 829-844.

Mouille G., Ralet MC., Cavelier C., Eland C., Effroy D., Hématy K., McCartney L., Truong HN., Gaudon V., Thibault JF., Marchant A., and Höfte H. (2007). Homogalacturonan synthesis in Arabidopsis thaliana requires a Golgi-localized protein with a putative methyltransferase domain. *Plant J*. **50**, 605-614.

Müller R., Bleckmann A., and Simon R. (2008). The receptor kinase CORYNE of Arabidopsis transmits the stem cell-limiting signal CLAVATA3 independently of CLAVATA1. *Plant Cell*. **20**, 934-946.

Nagar S., Pedersen TJ., Carrick KM., Hanley-Bowdoin L., and Robertson. (1995). A geminivirus induces expression of a host DNA synthesis protein in terminally differentiated plant cells. *Plant Cell*. **7**, 705-719.

Nicol F., His I., Jauneau A., Vernhettes S., Canut H., and Höfte H. (1998). A plasma membrane-bound putative endo-1,4-beta-D-glucanase is required for normal wall assembly and cell elongation in Arabidopsis. *EMBO J*. **17**, 5563-5576.

Nuttall VW., and Lyall LH. (1964). Inheritance of neoplastic pods in the pea. *J Hered.*

55, 184-186.

Oyama T., Shimura Y., and Okada K. (2002). The IRE gene encodes a protein kinase homologue and modulates root hair growth in Arabidopsis. *Plant J*. **30**, 289-299.

Pearce LR., Komander D., and Alessi DR. (2010). The nuts and bolts of AGC protein kinases. *Nat Rev Mol Cell Biol.* **11**, 9-22.

Pekker I., Alvarez JP., and Eshed Y. (2005). Auxin response factors mediate Arabidopsis organ asymmetry via modulation of KANADI activity. *Plant Cell*. **17**, 2899-2910.

Pettersen EF., Goddard TD., Huang CC., Couch GS., Greenblatt DM., Meng EC., and Ferrin TE. (2004). UCSF Chimera - a visualization system for exploratory research and analysis. *J Comput Chem*. **25**, 1605-1612.

Peterson RT., and Schreiber SL. (1999). Kinase phosphorylation: Keeping it all in the family. *Curr Biol*. **9**, R521-524.

Petersen LN., Ingle RA., Knight MR., and Denby KJ. (2009). OXI1 protein kinase is required for plant immunity against Pseudomonas syringae in Arabidopsis. *J Exp Bot*. **60**, 3727-3735.

Pillitteri LJ., Bemis SM., Shpak ED., and Torii KU. (2007). Haploinsufficiency after successive loss of signaling reveals a role for ERECTA-family genes in Arabidopsis ovule development. *Development*. **134**, 3099-3109.

Pinon V., Etchells JP., Rossignol P., Collier SA., Arroyo JM., Martienssen RA., and Byrne ME. (2008). Three *PIGGYBACK* genes that specifically influence leaf patterning encode ribosomal proteins. *Development*. **135**, 1315-1324.

Qian W., Liao BY., Chang AY., and Zhang J. (2010). Maintenance of duplicate genes and their functional redundancy by reduced expression. *Trends Genet*. **26**, 425-430.

Reiland S., Messerli G., Baerenfaller K., Gerrits B., Endler A., Grossmann J., Gruissem W., and Baginsky S. (2009). Large-scale Arabidopsis phosphoproteome profiling reveals novel chloroplast kinase substrates and phosphorylation networks. *Plant Physiol*. **150**, 889-903.

Reiser L., Modrusan Z., Margossian L., Samach A., Ohad N., Haughn GW., and Fischer RL. (1995). The *BELL1* gene encodes a homeodomain protein involved in pattern formation in the Arabidopsis ovule primordium. *Cell*. **83**, 735-742.

Remington DL., Vision TJ., Guilfoyle TJ., and Reed JW. (2004). Contrasting modes of diversification in the Aux/IAA and ARF gene families. *Plant Physiol*. **135**, 1738-1752.

Rentel MC., Lecourieux D., Ouaked F., Usher SL., Petersen L., Okamoto H., Knight H., Peck SC., Grierson CS., Hirt H., and Knight MR. (2004). OXI1 kinase is necessary for oxidative burst-mediated signalling in Arabidopsis. *Nature.* **427**, 858-861.

Riou-Khamlichi C., Huntley R., Jacqmard A., and Murray JA. (1999). Cytokinin activation of Arabidopsis cell division through a D-type cyclin. *Science*. **83**, 1541-1544.

Robert HS., and Offringa R. (2008). Regulation of auxin transport polarity by AGC kinases. *Curr Opin Plant Biol*. **11**, 495-502.

Robinson-Beers K., Pruitt RE., and Gasser CS. (1992). Ovule development in wild-type Arabidopsis and two female-sterile mutants. *Plant Cell*. **4**, 1237-1249.

Roudier F., Fedorova E., Lebris M., Lecomte P., Györgyey J., Vaubert D., Horvath G., Abad P., Kondorosi A., and Kondorosi E. (2003). The Medicago species A2-type cyclin is auxin regulated and involved in meristem formation but dispensable for endoreduplication-associated developmental programs. *Plant Physiol.* **131**, 1091-1103.

Roudier F., Gissot L., Beaudoin F., Haslam R., Michaelson L., Marion J., Molino D., Lima A., Bach L., Morin H., Tellier F., Palauqui JC., Bellec Y., et al (2010). Very-long-chain fatty acids are involved in polar auxin transport and developmental patterning in Arabidopsis. *Plant Cell*. **22**, 364-375.

Reynolds JO, Eisses JF, Sylvester AW. (1998). Balancing division and expansion during maize leaf morphogenesis: analysis of the mutant, *warty-1*. *Development*. **125**, 259-68.

Salisbury FB., and Ross CW. (1985). Plant physiology. Third edition. Wadsworth Publishing Co., Belmont, California.

Sakai H., Medrano LJ., and Meyerowitz EM. (1995). Role of *SUPERMAN* in maintaining Arabidopsis floral whorl boundaries. *Nature*. **378**, 199-203.

Sakai T., Kagawa T., Kasahara M., Swartz TE., Christie JM., Briggs WR., Wada M., and Okada K. (2001). Arabidopsis nph1 and npl1: blue light receptors that mediate both phototropism and chloroplast relocation. *Proc Natl Acad Sci U S A.* **98**, 6969-6974.

Sambrook J., EF Fritsch., and T Maniatis. (1989). *Molecular cloning*. Cold Spring Harbor Laboratory Press, Plainview, NY.

Santner AA., and Watson JC. (2006). The WAG1 and WAG2 protein kinases negatively regulate root waving in Arabidopsis. *Plant J*. **45**, 752-64.

Sarojam R., Sappl PG., Goldshmidt A., Efroni I., Floyd SK., Eshed Y., and Bowman JL. (2010). Differentiating Arabidopsis shoots from leaves by combined YABBY activities. *Plant Cell*. **22**, 2113-2130.

Schiefthaler U., Balasubramanian S., Sieber P., Chevalier D., Wisman E., and Schneitz K. (1999). Molecular analysis of *NOZZLE*, a gene involved in pattern formation and early sporogenesis during sex organ development in *Arabidopsis thaliana*. *Proc. Natl. Acad. Sci. U S A*. **96**, 11664-11669.

Schliebner I., Pribil M., Zühlke J., Dietzmann A., and Leister D. (2008). A Survey of Chloroplast Protein Kinases and Phosphatases in *Arabidopsis thaliana*. *Curr Genomics*. **9**, 184-190.

Schneitz K., Hülskamp M., Kopczak SD., and Pruitt RE. (1997). Dissection of sexual organ ontogenesis: a genetic analysis of ovule development in *Arabidopsis thaliana*. *Development.* **124**, 1367-1376.

Schneitz K., Hulskamp M., and Pruitt RE. (1995). Wild-type ovule development in *Arabidopsis thaliana*: a light microscope study of cleared whole-mount tissue. *Plant J.* **7,** 731-749.

Schatlowski N., Stahl Y., Hohenstatt ML., Goodrich J., and Schubert D. (2010). The CURLY LEAF interacting protein BLISTER controls expression of polycomb-group target genes and cellular differentiation of Arabidopsis thaliana. *Plant Cell*. **22**, 2291-2305.

Sessions A., Burke E., Presting G., Aux G., McElver J., Patton D., Dietrich B., Ho P., Bacwaden J., Ko C. et al. (2002). A high-throughput Arabidopsis reverse genetics system. *Plant Cell*. **14**, 2985-2994.

Sharp WR., and Gunckel JE. (1969). Physiological comparisons of pith callus with crown-gall and genetic tumors of Nicotiana glauca, N. langsdorffii, and N. glauca-langsdorffii grown in vitro. I. Tumor induction and proliferation. *Plant Physiol.* **44**, 1069-1072.

Sherr CJ. (2004). Principles of tumor suppression. *Cell.* **116**, 235-246.

Shih MC., Heinrich P., and Goodmann HM. (1991). Cloning and chromosomal mapping of nuclear genes encoding chloroplast and cytosolic glyceraldehyde-3-phosphate dehydrogenase from *Arabidopsis thaliana*. *Gene.* **104,** 133-138.

Shin OH., Rhee JS., Tang J., Sugita S., Rosenmund C., and Südhof TC. (2003). Sr2+ binding to the Ca2+ binding site of the synaptotagmin 1 C2B domain triggers fast exocytosis without stimulating SNARE interactions. *Neuron*. **37**, 99-108.

Sieber P., Gheyeselinck J., Gross-Hardt R., Laux T., Grossniklaus U., and Schneitz K. (2004). Pattern formation during early ovule development in *Arabidopsis thaliana*. *Dev Biol.* **273**, 321-334.

Sieberer T., Hauser MT., Seifert GJ., and Luschnig C. (2003). PROPORZ1, a putative Arabidopsis transcriptional adaptor protein, mediates auxin and cytokinin signals in the control of cell proliferation. *Curr Biol.* **13**, 837-842.

Sieburth LE., and Meyerowitz EM. (1997). Molecular dissection of the AGAMOUS control region shows that cis elements for spatial regulation are located intragenically. *Plant Cell.* **9**, 355-365.

Sijacic P., Wang W., and Liu Z. (2011). Recessive antimorphic alleles overcome functionally redundant loci to reveal TSO1 function in Arabidopsis flowers and meristems. *PLoS Genet*. **7**: e1002352.

Skibbe DS., Doehlemann G., Fernandes J., and Walbot V. (2010). Maize tumors caused by *Ustilago maydis* require organ-specific genes in host and pathogen. *Science.* **328**, 89–92.

Skinner DJ., Hill TA., and Gasser CS. (2004). Regulation of ovule development. *Plant Cell*. **16,** Suppl: S32-45.

Skinner DJ., Baker SC., Meister RJ., Broadhvest J., Schneitz K., and Gasser CS. (2001). The Arabidopsis *HUELLENLOS* gene, which is essential for normal ovule development, encodes a mitochondrial ribosomal protein. *Plant Cell*. **13**, 2719-2730.

Skirpan A., Wu X., and McSteen P. (2008). Genetic and physical interaction suggest that BARREN STALK 1 is a target of BARREN INFLORESCENCE2 in maize inflorescence development. *Plant J.* **55,** 787-797.

Smith LG., Greene B., Veit B., and Hake S. (1992). A dominant mutation in the maize homeobox gene, *Knotted-1*, causes its ectopic expression in leaf cells with altered fates. Development. **116**, 21-30.

Smith LG., Hake S., and Sylvester AW. (1996). The *tangled-1* mutation alters cell division orientations throughout maize leaf development without altering leaf shape. Development. **122**, 481-489.

Smith LM., Bomblies K., and Weigel D. (2011). Complex evolutionary events at a tandem cluster of *Arabidopsis thaliana* genes resulting in a single-locus genetic incompatibility. *PLoS Genet.* **7**, e1002164.

Smyth DR., Bowman JL., and Meyerowitz EM. (1990). Early flower development in Arabidopsis. *Plant Cell*. **2**, 755-767.

St John MA., Tao W., Fei X., Fukumoto R., Carcangiu ML., Brownstein DG., Parlow AF., McGrath J., and Xu T. (1999). Mice deficient of *Lats1* develop soft-tissue sarcomas, ovarian tumours and pituitary dysfunction. *Nat Genet.* **21,** 182-186.

Strader LC., Ritchie S., Soule JD., McGinnis KM., and Steber CM. (2004). Recessive-interfering mutations in the gibberellin signaling gene *SLEEPY1* are rescued by overexpression of its homologue, *SNEEZY*. *Proc Natl Acad Sci U S A.* **101**, 12771-12776.

Streissle G., and Maramorosch K. (1963). Reovirus and wound-tumor virus: serological cross reactivity. *Science.* **140**, 996-997.

Sugiyama N., Nakagami H., Mochida K., Daudi A., Tomita M., Shirasu K., and Ishihama Y. (2008). Large-scale phosphorylation mapping reveals the extent of tyrosine phosphorylation in Arabidopsis. *Mol Syst Biol*. **4**, 193.

Sundaresan V., Springer P., Volpe T., Haward S., Jones JD., Dean C., Ma H., and Martienssen R. (1995). Patterns of gene action in plant development revealed by

enhancer trap and gene trap transposable elements. *Genes Dev*. **9**, 1797-1810.

Tamura K., Dudley J., Nei M., and Kumar S. (2007). MEGA4: Molecular Evolutionary Genetics Analysis (MEGA) software version 4.0. *Mol Biol Evol*. **24**, 1596-1599.

Tanaka H., Watanabe M., Watanabe D., Tanaka T., Machida C., and Machida Y. (2002). ACR4, a putative receptor kinase gene of Arabidopsis thaliana, that is expressed in the outer cell layers of embryos and plants, is involved in proper embryogenesis. *Plant Cell Physiol*. **43**, 419-428.

Tanaka H., Dhonukshe P., Brewer PB., and Friml J. (2006). Spatiotemporal asymmetric auxin distribution: a means to coordinate plant development. *Cell Mol Life Sci*. **63**, 2738-2754.

Tanaka H., Watanabe M., Sasabe M., Hiroe T., Tanaka T., Tsukaya H., Ikezaki M., Machida C., and Machida Y. (2007). Novel receptor-like kinase ALE2 controls shoot development by specifying epidermis in Arabidopsis. *Development*. **134**, 1643-1652.

Tao W., Zhang S., Turenchalk GS., Stewart RA., St John MA., Chen W., and Xu T. (1999). Human homologue of the Drosophila melanogaster lats tumour suppressor modulates CDC2 activity. *Nat Genet*. **21**, 177-181.

Tavares S., Inácio J., Fonseca A., and Oliveira C. (2004). Direct detection of *Taphrina deformans* on peach trees using molecular methods. *Eur J Plant Pathol.* **110**, 973-982

Testerink C., and Munnik T. (2005). Phosphatidic acid: a multifunctional stress signaling lipid in plants. *Trends Plant Sci*. **10**, 368-375.

Thompson JD., Higgins DG., and Gibson TJ. (1994). CLUSTAL W: improving the sensitivity of progressive multiple sequence alignment through sequence weighting, position-specific gap penalties and weight matrix choice. *Nucleic Acids Res*. **22**, 4673-4680.

Till BJ., Reynolds SH., Greene EA., Codomo CA., Enns LC., Johnson JE., Burtner C., Odden AR., Young K., Taylor NE, et al. 2003. Large-scale discovery of induced point mutations with high-throughput TILLING. *Genome Res.* **13,** 524-530.

Toker A., and Newton AC. (2000). Cellular signaling: pivoting around PDK-1. *Cell.* **103**, 185-188.

Torii KU., Mitsukawa N., Oosumi T., Matsuura Y., Yokoyama R., Whittier RF., and Komeda Y. (1996). The Arabidopsis ERECTA gene encodes a putative receptor protein kinase with extracellular leucine-rich repeats. *Plant Cell*. **8**, 735-746.

Torres-Ruiz RA., and Jürgens G. (1994). Mutations in the *FASS* gene uncouple pattern formation and morphogenesis in *Arabidopsis* development. *Development.* **120,** 2967-2978.

Torres-Ruiz RA., Lohner A., and Jürgens G. (1996). The GURKE gene is required for normal organization of the apical region in the Arabidopsis embryo. *Plant J*. **10**, 1005-1016.

Truernit E., and Haseloff J. (2008). *Arabidopsis thaliana* outer ovule integument morphogenesis: ectopic expression of *KNAT1* reveals a compensation mechanism. *BMC Plant Biol.* **8**, 35.

Ulmasov T., Hagen G., and Guilfoyle TJ. (1999). Dimerization and DNA binding of auxin response factors. *Plant J*. **19**, 309-319.

van den Bogaart G., Meyenberg K., Risselada HJ., Amin H., Willig KI., Hubrich BE., Dier M., Hell SW., Grubmüller H., Diederichsen U., and Jahn R. (2011). Membrane protein sequestering by ionic protein-lipid interactions. *Nature*. **479**, 552-555.

Vandeputte O., Oden S., Mol A., Vereecke D., Goethals K., El Jaziri M., and Prinsen E. (2005). Biosynthesis of auxin by the gram-positive phytopathogen *Rhodococcus*

fascians is controlled by compounds specific to infected plant tissues. *Appl. Environ. Microbiol.* **71**, 1169-1177.

Varotto C., Pesaresi P., Meurer J., Oelmuller R., Steiner-Lange S., Salamini F., and Leister D. (2000). Disruption of the Arabidopsis photosystem I gene psaE1 affects photosynthesis and impairs growth. *Plant J.* **22**, 115-124.

Villanueva JM., Broadhvest J., Hauser BA., Meister R.J., Schneitz K., and Gasser CS. (1999). *INNER NO OUTER* regulates abaxial/adaxial patterning in *Arabidopsis* ovules. *Genes Dev*. **13**, 3160-3169.

Visvader JE. (2011). Cells of origin in cancer. *Nature* **469**, 314-322.

Vivanco I., and Sawyers CL. (2002). The phosphatidylinositol 3-Kinase AKT pathway in human cancer. *Nat Rev Cancer*. **2**, 489-501.

Völker A., Stierhof YD., and Jürgens G. (2001). Cell cycle-independent expression of the *Arabidopsis* cytokinesis-specific syntaxin KNOLLE results in mistargeting to the plasma membrane and is not sufficient for cytokinesis. *J Cell Sci.* **114**, 3001-3012.

Wachsman G., Heidstra R., and Scheres B. (2011). Distinct cell-autonomous functions of *RETINOBLASTOMA-RELATED* in Arabidopsis stem cells revealed by the brother of brainbow clonal analysis system. *Plant Cell*. **23**, 2581-2591.

Walter M., Chaban C., Schutze K., Batistic O., Weckermann K., Nake C., Blazevic D., Grefen C., Schumacher K., Oecking C, et al. (2004). Visualization of protein interactions in living plant cells using bimolecular fluorescence complementation. *Plant J.* **40**, 428-438.

Watanabe M., Tanaka H., Watanabe D., Machida C., and Machida Y. (2004). The ACR4 receptor-like kinase is required for surface formation of epidermis-related tissues in *Arabidopsis thaliana*. *Plant J.* **39**, 298-308.

Weinberg RA. (2006). The biology of cancer. Garland Science, New York, NY.

Xu T., Wang W., Zhang S., Stewart RA., and Yu W. (1995). Identifying tumor suppressors in genetic mosaics: the *Drosophila lats* gene encodes a putative protein kinase. *Development* **121**, 1053-1063.

Xu L., Xu Y., Dong A., Sun Y., Pi L., Xu Y., and Huang H. (2003). Novel *as1* and *as2* defects in leaf adaxial-abaxial polarity reveal the requirement for *ASYMMETRIC LEAVES1* and *2* and ERECTA functions in specifying leaf adaxial identity. *Development*. **130**, 4097-4107.

Yang WC., Ye D., Xu J., and Sundaresan V. (1999). The *SPOROCYTELESS* gene of Arabidopsis is required for initiation of sporogenesis and encodes a novel nuclear protein. *Genes Dev*. **13**, 2108-2117.

Yoo SD., Cho YH., and Sheen J. (2007). Arabidopsis mesophyll protoplasts: a versatile cell system for transient gene expression analysis. *Nat Protoc.* **2**, 1565-1572.

Yu QB., Li G., Wang G., Sun JC., Wang PC., Wang C., Mi HL., Ma WM., Cui J., Cui YL., Chong K., Li YX., Li YH., Zhao Z., Shi TL., and Yang ZN. (2008). Construction of a chloroplast protein interaction network and functional mining of photosynthetic proteins in Arabidopsis thaliana. *Cell Res*. **18**, 1007-1019.

Zegzouti H., Li W., Lorenz TC., Xie M., Payne CT., Smith K., Glenny S., Payne GS., and Christensen SK. (2006a). Structural and functional insights into the regulation of Arabidopsis AGCVIIIa kinases. *J Biol Chem*. **281**, 35520-35530.

Zegzouti H., Anthony RG., Jahchan N., Bögre L., and Christensen SK. (2006b). Phosphorylation and activation of PINOID by the phospholipid signaling kinase 3-phosphoinositide-dependent protein kinase 1 (PDK1) in Arabidopsis. *Proc Natl Acad Sci U S A*. **103**, 6404-6409.

Zhang Y., He J., and McCormick S. (2009a). Two Arabidopsis AGC kinases are critical for the polarized growth of pollen tubes. *Plant J*. **58**, 474-484.

Zhang Y., and McCormick S. (2009b). AGCVIII kinases: at the crossroads of cellular signaling. *Trends Plant Sci.* **14**, 689-695.

Zhou H., and Zhou Y. (2002b). Distance-scaled, finite ideal-gas reference state improves structure-derived potentials of mean force for structure selection and stability prediction. *Protein Sci*. **11**, 2714-2726.

Zourelidou M., Müller I., Willige BC., Nill C., Jikumaru Y., Li H., and Schwechheimer C. (2009). The polarly localized D6 PROTEIN KINASE is required for efficient auxin transport in *Arabidopsis thaliana*. *Development*. **136**, 627-636.

7. Supplementary data

Supplemental Table 7.1. Summary of *ucn and ucnl* alleles

Allele	Mutagen	Mutation#	Amino acid change/transcript	Background	Reference
ucn-1	EMS	C>T, 44345	G165S	L*er*	this study Schneitz et. al. 1997
ucn-2	T-DNA SALK_002381	44218/LB	L209--*	Col	this study
ucn-3	T-DNA SALK_056694	44942/LB	RNA+	Col	this study
ucn-4	T-DNA SALK_084711	44881/LB	RNA+	Col	this study
ucn-5	T-DNA SALK_084708	44869/LB	RNA+	Col	this study
ucn-6	T-DNA SALK_143744	LB/43554	RNA+	Col	this study
ucn-7	EMS TILLING	G>A, 44713	S42F	Col *er-105*	this study
ucn-8	EMS TILLING	C>T, 44029	G270E	Col *er-105*	this study
ucn-9	EMS TILLING	C>T, 43880	D320N	Col *er-105*	this study
ucnl-1	T-DNA SAIL_238_A09	46938/LB	RNA+	Col	this study

ucnl-2	T-DNA GT931.DS5	46818/LB	RNA+	L*er*	this study
ucnl-3	T-DNA SALK_117406	46808/LB	M1--*	Col	this study
ucnl-4	T-DNA SALK_066654	LB/46780	S10--*	Col	this study
ucnl-5	T-DNA SALK_024621	46465/LB	L116-- *	Col	this study

[#]the coordinates refer to the BAC (F23H24 and MOE17) sequence and relate to the ATG of *UCN* (At1g51170) - 44847 bp and UCNL(At3g20830) - 46813 bp.

--*premature stop preceded by artificial sequence of amino acids of variable length (*ucn-2*: ND; *ucnl-3*: 2 aa; *ucnl-4*: ND, ucnl-5:10 aa).

Abbreviations: LB, Left border of T-DNA insertion; N.D., not determined.

Supplemental Table 7.2. List of primers used in this study.

Primer Name	**Sequence (5' to 3')**
UCN (gen KpnI)_F	ATATAGGTACCATAACATCATAAATTTGGAGTTATTCG
UCN (gen PstI)_R	ATATACTGCAGTGTGTGCATTACAGATT
At1g51160 (KpnI)_F	ATATAGGTACCGTTCTTGTTAAGTACTATGTTTACTCG
At1g51160 (PstI)_R	ATATACTGCAGTCCACGCGTGGGAGAAT
At1g51150 (KpnI)_F	ATATAGGTACCGAATTCAGGAAGCTGTT
At1g51150 (BamHI)_R	ATATAGGATCCTGCTTCCGTCGTCTCCG
UCN (T-DNA_gt)_F	CGTAATCATCAAGTACCATGC
UCN (T-DNA_gt)_R	GGAGTTATTCGAGATGCA
UCN (Till)_F	AGGGACACGAGGAGACATAAACGCAAC
UCN (Till)_R	CACGCGTGGATCAGAAATCAACAAAC
UCNL (T-DNA_gt)_F	CACCTCCGTTAACAAATCCCACC
UCNL (T-DNA_gt)_R	ACTTAATATCATTCTTAAAGTATCGCAAATTC
UCN (pGEX_XmaI)_F	ATGCATCCCGGGATGGAGACAAGACCATCATCATCATC
UCN (pGEX_NotI)_R	ATATATGCGGCCGCTCAGAAATCAACAAACGGATTGTTTTC
UCN (K55E)_F	CTTCTCCCTTTGCTTTAGAACTCGTCGACAAATC

UCN (K55E)_R	GATTTGTCGACGAGTTCTAAAGCAAAGGGAGAAG
UCN (KpnI)_F	ATAGGTACCATGGAGACAAGACCATCATCATCATC
UCN (HindIII)_R	ATAAAGCTTTCAGAAATCAACAAACG
ATS (pGEX_BamHI)_F	ATATATGGATCCATGATGATGTTAGAGTCAAG
ATS (pGEX XhoI)_R	ATCTATCTCGAGTTAGCACTTGAGAAGGG
UCN (BiFC_AscI)_F	ATAGATGGCGCGCCATGGAGACAAGACCATCATCATC
UCN (BiFC_Xma)_R	ATATATCCCGGGGAAATCAACAAACG
ATS (BiFC_AscI)_F	ATAGATGGCGCGCCATGATGATGTTAGAGTCAAGAA
ATS (BiFC_Xma)_R	ATATATCCCGGGGCACTTGAGAAGGGTTAAATCACT
ATSsense_831_F	TAATACGACTCACTATAGGG ATGATGATGTTAGAGTCAAGA
ATSsense_831_R	TTAGCACTTGAGAAGGGTTAA
ATSas_831_F	ATGATGATGTTAGAGTCAAGA
ATSas_831_R	TAATACGACTCACTATAGGG TTAGCACTTGAGAAGGGTTAA
UCN (RT)_F	TCTTCCTCGTCCACGACTCTG
UCN (RT)_R	GCTAAGAGTTTTGGGAGAAATGG
UCNL (RT)_F	ATGGAGCCATCACCGTCG
UCNL (RT)_R	GGGACGAGCTTGACCGC
GAPC (RT)_F	CACTTGAAGGGTGGTGCCAAG
GAPC (RT)_R	CCTGTTGTCGCCAACGAAGTC
UBC21 (qRT)_F	TCCTCTTAACTGCGACTCAGG
UBC21 (qRT)_R	GCGAGGCGTGTATACATTTG
At4g33380 (qRT)_F	TGAAGGAGAGGAAGAGCCTGAGGAA
At4g33380 (qRT)_R	CCCCATCTCACTGCAGCACCAC
At2g28390 (qRT)_F	AGATTGCAGGGTACGCCTTGAGG
At2g28390 (qRT)_R	ACACGCATTCCACCTTCCGCG
At5g46630 (qRT)_F	CCAAATGGAATTTCAGGTGCCAATG
At5g46630 (qRT)_R	CAATGCGTACCTTGAGAAAACGAAC
UCN (qRT)_F	GCCGTGCAAGGTGGGAAATTC
UCN (qRT)_R	AAGCTAAGAGTTTTGGGAGAAATGGG

UCNL (qRT)_F	CCATCACCGTCGTCCCCACCAT
UCNL (qRT)_R	CGCCTTTACCGAGGATTTTGAGAGC
INO (qRT)_F	GCTCCCCAACATGACGACAACA
INO (qRT)_R	GCTTGTAAACGGTACACTCACCAGCA
ATS (qRT)_F	GGATCACCAGGAGAAGGAAAGGT
ATS (qRT)_R	GCACAGATGATGAGTTTGGCGA
RBR1 (qRT)_F	CGCCGTCAAGGGAGAATAGGG
RBR1 (qRT)_R	AGCAGCGGCTTTACGGCAGG
CYCD3;1 (qRT)_F	CCTCCTCTCTGTAATCTCCGATTCA
CYCD3;1 (qRT)_R	ATAATTCGCATCATGGTAGCTGC
CYCD3;2 (qRT)_F	TGTCTCAGCTTGTTGCTGTGGCT
CYCD3;2 (qRT)_R	TGCTTCTTCCACTTGGAGGTCT
CYCD3;3 (qRT)_F	ACTCAAAGTTGATTCGGAGAAGGT
CYCD3;3 (qRT)_R	GGACTAGCGGGTTGTTGCAT
CYCD2;1 (qRT)_F	GACAAGGATTGGGCTGCTCAGT
CYCD2;1 (qRT)_R	ACAAACTTGGGATCTTCCACCTGTA
KRP1 (qRT)_F	TCGTCGTCTTGTAGTGGGAGCAAT
KRP1 (qRT)_R	TCTTCCTCTTCGTACCCCGTCG
KRP2 (qRT)_F	TCGTCGGTTTCGTGTTGTTCTACA
KRP2 (qRT)_R	GATCGTCACCGTTATTTTCCTCAA
KRP3 (qRT)_F	ACAGAGGCTATTCATGGAGAAGTACAAC
KRP3 (qRT)_R	ACCCATTCGTAACGTCCGCTG
KRP4 (qRT)_F	ACACACTCAAAGCTTCAACAGGAC
KRP4 (qRT)_R	AAGCTTTGTAGACGATCCCGG
KRP6 (qRT)_F	CACCAGCAATTTCAGAAAAGAGACG
KRP6 (qRT)_R	GGAGTCTTCCTCACCCCCGG
SIM (qRT)_F	GGCTGCACCACTCCCACTTCT
SIM (qRT)_R	ACGGTGTGGAAGGTGGACGG
SMR1 (qRT)_F	CGCCGTCGTAGACTCTCCACCT
SMR1 (qRT)_R	CATCAGAGCCGCCGTAGCCGA
CCS52A2 (qRT)_F	TGTGGTTACTGGTGTTAGCCCT
CCS52A2 (qRT)_R	GCCGGCGCATCCAATACCTTA

IV. Acknowledgments

First and foremost, I am profoundly indebted to my thesis supervisor, Prof. Dr. Kay Schneitz for his encouragement, inspirational discussions, and thoughtful guidance. I want to express my deeply heart-felt thanks to him for all his contributions of time, ideas, and funding to make my Ph.D. experience stimulating and productive.

Prof. Ramon A. Torres Ruiz and Dr. Farhah Assaad deserves a special mention for their interest in my work and cherishing my 'eureka' moments, fruitful discussions and encouragement during my Ph.D. stay at Weihenstephan.

I owe my gratitude to Maxi and Charlotte for their research assistantship. I would like to thank my dear friends Hari and Bjoern for their time, interest in my work, helpful comments, and thoughtful discussions.

It is a pleasure to thank the master and bachelor students and visiting scholar who worked with me. The list includes Andreas, Charlotte, Daniel, Dorothee, Hong, Katharina, Lukas, Marcel, Priya, Sarah, and Silvia. It was pleasure teaching and guiding them.

I am thankful to many of my past and preset colleagues: Banu, Carina, Christine, Lynette, Karen, Martine, Maxi, Prasad, Ram, and Tom for creating a harmonious and enjoyable work environment in the lab and fun-filled coffee and cake breaks.

I am grateful to our group's administrative secretory Beate Seeliger, who was always ready to help in dealing with the bureaucratic matters.

My time in Freising/Munich was made enjoyable and enriched in large part due to many friends like Ajay, Bhargavi, Bjoern, Hari, Hema, Indu, Irmi, Madhavi, Prasad, Ram, Rama, Sasi, Shiva, Suku and Vijay. Rama needs a special mention for keeping me on spiritual track. I cherished the time with Ram and Vijay in Freising in my first year of my Ph.D. studies.

I owe a special debt to my friends Hari and Bhargavi for their friendship and hosting me over weekends as I wrote this thesis. I enjoyed my time with them, and they made me feel at home.

I specially thank my three Master musketeers Prasad, Srinu and Suresh for their friendship and support throughout these years.

Most importantly, I would like to thank my parents and my dearest brother Vasu, sis-in-law Kavitha, nephews, uncle and granny for their unconditional love, endless support, and encouragement during my doctoral time and in all pursuits.

Last but not the least, I would like to acknowledge my experimental model organism - *Arabidopsis thaliana* and my favorite gene *UNICORN* for being instrumental in expanding my scientific knowledge.